Methylmercury in Seawater and Its Bioaccumulation in Marine Food Webs of the Canadian Arctic

By

Kang Wang

A thesis submitted to the Faculty of Graduate Studies of

The University of Manitoba

in partial fulfillment of the degree of

Doctor of Philosophy

Department of Environment and Geography

University of Manitoba

Abstract

Mercury (Hg) is a major contaminant in the Arctic marine ecosystem, with concentrations in marine mammals and Indigenous Peoples frequently exceeding safety thresholds. The key step of Hg bioaccumulation is Hg methylation in the ocean, as the resulting monomethylmercury (MMHg) biomagnifies in the marine food webs. However, little is known about the sources and dynamics of seawater MMHg in the Arctic. In this research, high vertical resolution profiles of total Hg and methylated Hg (MeHg, sum of MMHg and dimethylmercury) were measured, for the first time, in seawater across the Canadian Arctic from the Canada Basin in the west, through the Canadian Arctic Archipelago, to Baffin Bay in the east and reaching Labrador Sea in the North Atlantic Ocean. Whereas total Hg concentrations are lower in the western Canadian Arctic, MeHg is enriched at shallow depths and its peak concentration decreases from west to east. Biological uptake of this subsurface MeHg and subsequent biomagnification can readily explain the regional gradients of biotic Hg in the Canadian Arctic. Seawater MeHg concentrations show significant correlations with nutrients and apparent oxygen utilization, but this does not necessarily support that MeHg is produced in-situ in the water column; instead, further analysis with water masses and N* reveals that the subsurface MeHg is likely originated from the Chukchi Sea sediments and advected within the Upper Halocline Water to the Canadian Arctic. The long-distance transport implies that MeHg in Arctic seawater must have a half-life much longer than previously determined from the seawater incubation approach, which is problematic in estimating Hg methylation and demethylation rates in seawater. Incubation studies with an Arctic copepod (*Calanus hyperboreus*) show that the microenvironments in copepod guts and

fecal pellets are unlikely hotspots for Hg methylation, and that the copepod preferentially bioaccumulates MMHg over inorganic Hg and the main uptake pathway is trophic transfer. This study underlines the importance of seawater MeHg in controlling Hg bioaccumulation in Arctic marine food webs, and calls for more studies on processes that produce and maintain the subsurface seawater MeHg enrichment to better understand the exposure of MeHg to the Arctic ecosystem and Indigenous Peoples.

Acknowledgements

Foremost, I express my sincere gratitude to my supervisor Dr. Feiyue Wang for providing the opportunity to do this research. He has been supporting me throughout my PhD study with his knowledge, enthusiasm, inspiration, patience and encouragement. All these are invaluable to me, and I simply could not wish for a better supervisor and mentor.

I would like to thank my committee member, Drs. Robbie Macdonald, Zou Zou Kuzyk and Gary Stern, for their guidance and support throughout my research. Especially, I am grateful to Dr. Robbie Macdonald for his immense knowledge, insightful advice and great sensitivity in grasping essence of scientific questions. A big thank you to Dr. Kathleen Munson, for all the guidance and assistance she has given me in carrying out the research project.

Special thanks to Debbie Armstrong, for her time spent training me on instruments, support for field trips, and assistance in lab work throughout my PhD study. I also thank my lab mates Amanda Chalk, Sarah Beattie, Wen Xu, Ashley Elliott, Dan Zhu and Jiang Liu for helping with field sampling and lab work.

Thank you to the collaborators, Alexis Beaupré-Laperrière and Dr. Alfonso Mucci of McGill University for their help in water mass analysis, and Drs. Peter Stief and Ronnie Glud of the Southern Denmark University for their help in the copepod incubation study. Thank you to Dr. Carl Lamborg of the University of California Santa Cruz for providing the stock solution of isotopically enriched monomethylmercury. Thank you to Dr. Robert Letcher of the Environment and Climate Change Canada for providing a digital version of polar bear Hg data. Thank you to all the GEOTRACES

participants, especially the members of the rosette sampling team. Thank you to the captains and crew of the CCGS Amundsen for their hard work and supports during the scientific cruises. I also thank the scientists and staff for the help and supports during the research campaign at the Disco Bay Arctic Station affiliated with the University of Copenhagen.

Finally, this study was made possible by financial support from the University of Manitoba, Natural Science and Engineering Research Council of Canada, ArcticNet, the Canadian Arctic GEOTRACES program, and the Canada Research Chairs Program.

Dedications

This thesis is dedicated to my parents, Fushan Wang and Fengyu Guo, my wife Linlin Zhang, and our daughter Shiqi Winnie Wang. Their never-ending love and support and great sacrifices made this, and all of my accomplishments, possible.

Table of Contents

List of Tables

List of Figures

List of Acronyms

AMDE – Atmospheric Mercury Depletion Event

AOU – Apparent Oxygen Utilization

ATW – Atlantic Water

BAF – Bioaccumulation Factor

BBAW – Baffin Bay Arctic Water

BBDW – Baffin Bay Deep Water

BCF – Bioconcentration Factor

BAF – Biomagnification Factor

CA – Canadian Arctic

CAA – Canadian Arctic Archipelago

CBDW – Canada Basin Deep Water

CCGS – Canadian Coast Guard Ship

CRM – Certified Reference Material

CTD – Conductivity Temperature Depth (Pressure)

CVAFS – Cold Vapor Atomic Fluorescence Spectroscopy

DIC – Dissolved Inorganic Carbon

DL – Detection Limit

DMHg – Dimethylmercury

DO – Dissolved Oxygen

GEM – Gaseous Elemental Mercury

Hg – Mercury

Hg(0) – Elemental Mercury

Hg^{2+} – Mercuric Ion

Hg(II) – Divalent Mercury

ICM-MS – Inductively-Coupled Plasma Mass Spectrometer

IUPAC – International Union of Pure and Applied Chemistry

LLOQ – Lower Limit of Quantification

MeHg – Methylmercury, or methylated mercury

MMHg – Monomethylmercury

MW – Meteoric Water, or Mackenzie River Water

N-ATW – Northern (Arctic) Atlantic Water

OM – Organic Matter

OMP – Optimum Multiparameter

PILMS – Portable *In-situ* Laboratory for Mercury Speciation

PML – Polar Mixed Layer

POM – Particulate Organic Matter

S-ATW – Sothern (Labrador Sea) Atlantic Water

SCM – Subsurface Chlorophyll Maximum

SIM – Sea-Ice Melt

SRP – Soluble Reactive Phosphorus

TA – Total Alkalinity

THg – Total Mercury

UCTEL – Ultra Clean Trace Elements Laboratory

UHW – Upper Halocline Water

Use of Copyrighted Material

Chapter 2 of this thesis is reproduced with minor modifications from Wang et al. (2018), Subsurface seawater methylmercury maximum explains biotic mercury concentrations in the Canadian Arctic. *Scientific Reports,* 8(1), 14465. https://doi.org/10.1038/s41598-018-32760-0.

Contribution of Authors to Thesis Chapters

Chapter 2

I was part of the team (Feiyue Wang, Kang Wang and Kathleen M. Munson) that designed this project and sampling plan. I collected and analyzed the samples with assistance from Kathleen M. Munson. I and Feiyue Wang led the writing of the manuscript, with major contributions and support from Kathleen M. Munson, Robie W. Macdonald and Alfonso Mucci. All authors (Kang Wang, Feiyue Wang, Kathleen M. Munson, Robie W. Macdonald, Alexis Beaupré-Laperrière and Alfonso Mucci) interpreted data.

Chapter 3

I was part of the team (Feiyue Wang, Kang Wang and Kathleen M. Munson) that designed this project and interpreted the data. I conducted the incubation experiments and collected the samples. I analyzed the samples with assistance from Kathleen M. Munson and Debbie Armstrong. I wrote the bulk part of the manuscript, with major contributions and support from Feiyue Wang and Kathleen M. Munson.

Chapter 4

I was part of the team (Feiyue Wang, Kang Wang and Kathleen M. Munson) that designed this project and sampling plan. I collected and analyzed the samples with assistance from Kathleen M. Munson. I wrote the bulk part of the manuscript, with major contributions and support from Feiyue Wang, Kathleen M. Munson, Robie W.

Macdonald and Alfonso Mucci. Alexis Beaupré-Laperrière and Alfonso Mucci analyzed the regional water masses. Kang Wang, Feiyue Wang, Kathleen M. Munson, Robie W. Macdonald, Alexis Beaupré-Laperrière and Alfonso Mucci interpreted data.

Chapter 5

I was part of the team (Feiyue Wang, Kang Wang, Ronnie Glud and Peter Stief) that initiated this project and designed the incubation experiments. I conducted the incubation experiments, collected and analyzed the samples, with assistance from Peter Stief. Feiyue Wang and I interpreted the data. I wrote the bulk part of the manuscript, with major contributions and support from Feiyue Wang and Kathleen M. Munson.

Chapter 1: Introduction

Mercury (Hg) is a contaminant of major concern in the Arctic marine ecosystem, because of its high toxicity and bioaccumulation in the food web (AMAP, 2011, 2018). Monitoring data in the past four decades show that Hg concentrations in Arctic marine mammals are elevated and frequently exceed toxicity thresholds (AMAP, 2011; Dietz et al., 2013). This has raised major concerns over the health of marine mammals and Indigenous Peoples who consume the tissues of these animals (AMAP, 2009). Among different Hg species, it is mainly monomethylmercury (MMHg), rather than inorganic Hg, that mainly bioaccumulates and biomagnifies in the food web and causes toxic effects in top predators (Ruus et al., 2015). Because the ocean is the principal source of MMHg in apex predators (Atwell et al., 1998; Schartup et al., 2017), it is of great importance to understand how Hg is distributed, methylated and bioaccumulated in the Arctic marine environment.

1.1 Background and Knowledge Gap

1.1.1 Mercury in the Arctic

With little industrial activity, the Arctic was thought to be one of the last pristine regions on Earth. However, monitoring since the 1970s shows that Hg concentrations are elevated in marine mammals and Indigenous Peoples in the Arctic (AMAP, 2009). The high Hg levels in Arctic biota have been attributed to bioaccumulation of MMHg in the food web (Koeman et al., 1975; Smith and Armstrong, 1975), but it remains unclear whether the Arctic biotic Hg originated from anthropogenic sources (Eaton and Farant,

1982). In the late 1980s and early 1990s, long-range transport of atmospheric Hg from anthropogenic and natural emissions in the temperate regions and its deposition were postulated to be an important source of Hg in the Arctic (Pacyna and Keeler, 1995; Petersen and Munthe, 1995). The atmospheric Hg deposition is greatly enhanced in springtime during atmospheric mercury depletion events (AMDEs), which were discovered at Alert in the Canadian High Arctic in the mid-1990s (Schroeder et al., 1998). Since then, the Arctic has been considered a sink of global atmospheric Hg, and its deposition has been thought to eventually result in elevated Hg concentrations in Arctic biota (Ariya et al., 2004). However, detailed studies show that AMDEs mainly occur in coastal regions and most of the deposited Hg is soon re-emitted back to the air (Douglas et al., 2012; Johnson et al., 2008). Therefore, AMDEs contribute much less net deposition of atmospheric Hg than previously estimated (Dastoor and Durnford, 2014). In the past decade, both field observations (Emmerton et al., 2013; Leitch et al., 2007; Schuster et al., 2011) and modeling results (Fisher et al., 2012; Soerensen et al., 2016; Zhang et al., 2015) show that rivers are transporting large amounts of Hg to the Arctic Ocean, and the total contribution may exceed that of atmospheric deposition (Dastoor and Durnford, 2014; Fisher et al., 2012; Soerensen et al., 2016; Zhang et al., 2015). According to recent studies, riverine Hg inputs to the Arctic Ocean can be enhanced by tundra uptake of atmospheric Hg(0) (Obrist et al., 2017) and Hg release during permafrost thawing (Schuster et al., 2018). While extensive studies have been conducted on Hg in the atmosphere, biota and terrestrial systems, much less is known about the distribution and dynamics of Hg species in the Arctic seawater, which play crucial roles in the uptake of Hg to biota (Macdonald and Loseto, 2010; Macdonald et al., 2008).

Since the onset of the biotic Hg monitoring program in the Arctic, accumulated data show regional differences in biotic Hg concentrations in the Canadian Arctic. In the western Canadian Arctic, biotic Hg concentrations are higher than those from the eastern regions (AMAP, 2011; Braune et al., 2014; Brown et al., 2018). This longitudinal gradient is not limited to top predators such as polar bears and ringed seals (Brown et al., 2016; Routti et al., 2011), but extends to biota at lower trophic levels such as zooplankton (Pomerleau et al., 2016). This west-to-east gradient has been a major mystery in the Arctic Hg cycle, and several hypotheses have been postulated to explain the spatial trends. Some hypotheses have linked the regional variations in top predator Hg concentrations to feeding behavior and dietary preference (Brown et al., 2016; Horton et al., 2009; St. Louis et al., 2011), but observed longitudinal gradients persist after adjustments are made to account for trophic position (Brown et al., 2018). Other hypotheses attributed higher biotic Hg levels in the western Canadian Arctic to elevated inputs of inorganic Hg to these regions. These inputs include (1) atmospheric deposition of anthropogenic Hg from Asian sources (AMAP, 2005; Brown et al., 2018), which is enhanced locally by AMDEs during polar sunrise (Schroeder et al., 1998); (2) riverine Hg input from the Mackenzie River (Fisher et al., 2012; Leitch et al., 2007), which may be enhanced by a naturally high geological background of Hg (Riget et al., 2005; Wagemann et al., 1996), tundra uptake of atmospheric Hg(0) (Orbrist et al., 2017) and Hg release from permafrost thawing (Schuster et al., 2018). However, these inorganic Hg-based hypotheses do not consider the fact that it is MMHg, not inorganic Hg, that accumulates and biomagnifies in the marine food webs (AMAP, 2011). Although regional differences in seawater MeHg concentrations and the subsequent bioaccumulation has been proposed

as possible factors for the regional differences in polar bear hair Hg concentrations between the Beaufort Sea and Hudson Bay (St. Louis et al., 2011), high-resolution (vertical and horizontal) water column MeHg concentration data were not available at that time to support this hypothesis.

1.1.2 Seawater Mercury Distribution

The major source of Hg to the global ocean is atmospheric deposition (Mason et al., 2012). This was thought to be the case for the Arctic Ocean also (Ariya et al., 2004); however, recent studies suggest that rivers may transport larger amounts of Hg to the Arctic Ocean than atmospheric deposition (Dastoor and Durnford, 2014; Fisher et al., 2012; Soerensen et al., 2016; Zhang et al., 2015). The major sink for Hg in the surface ocean is evasion to the atmosphere, whereas the primary sink for seawater Hg is scavenging by particles and eventual burial in sediments (Mason et al., 1998).

In the open ocean water, total Hg (Hg_T) concentration is typically in the pM range, and its vertical distribution usually exhibits a transient-type pattern, with a surface enrichment because of atmospheric deposition, lower values in the upper ocean due to particle scavenging, and higher concentrations at depth due to release during organic matter (OM) remineralization (Fitzgerald et al., 2007; Mason et al., 2012). In seawater, Hg_T is mainly present as inorganic Hg(II) and Hg(0), although at certain depths the concentrations of methylated Hg (MeHg, sum of MMHg and dimethylmercury (DMHg)) may reach more than 50% of Hg_T (Cossa et al., 2011; Hammerschmidt and Bowman, 2012; Mason et al., 2012; Wang et al., 2012). In marine waters, DMHg and MMHg may inter-convert (Fitzgerald et al., 2007; Mason and Fitzgerald, 1993; Lehnherr et al., 2011),

and the two species are often not differentiated in marine Hg data sets but reported in sum as MeHg (Cossa et al., 2009, 2011; Mason et al., 2012; Sunderland et al., 2009). In the world ocean, MeHg concentration is typically low in the surface water, increases to a peak value at a subsurface layer, and gradually decreases in deeper waters (Bowman et al., 2016; Cossa et al., 2009; Mason and Fitzgerald, 1990; Munson et al., 2015; Sunderland et al., 2009). The surface depletion of MeHg can be explained by photo-demethylation or microbial decomposition, and the decreasing concentrations in deep waters may result from demethylation of MeHg as the resident water ages (Cossa et al., 2009; Sunderland et al., 2009). The subsurface enrichment at depths with high nutrients and low dissolved oxygen (DO) has been attributed to microbial production of MeHg associated with OM remineralization, although the mechanisms are not clear (Mason et al., 2012).

In the Arctic, measurements of Hg species at high spatial resolutions are scarce, due to analytical and logistical constraints. To date, there are only two Hg species data sets with high vertical resolutions in the Arctic, one measured in the Beaufort Sea (Wang et al., 2012) and the other in the central Arctic Ocean (Heimbürger et al., 2015). In both studies, Hg_T concentrations showed the transient-type distribution as typically observed in other oceans. In the Arctic, the vertical distribution of seawater MeHg also followed the general distribution pattern as observed in other oceans, with the exception that the peak value occurs at much shallower water depths.

1.1.3 Mercury Methylation in Marine Environment

Our mechanistic understanding of Hg methylation in the aquatic environment is largely based on studies in freshwater and coastal systems (Obrist et al., 2018). Although abiotic methylation is observed in lab-based studies, Hg methylation in the aquatic environment is primarily a process meditated by anaerobic microbes (Ulrich et al., 2001) Some species of sulfate- and iron-reducing bacteria are identified as Hg methylators (Compeau and Bartha, 1985; Kerin et al., 2006), with corrinoid proteins being suspected to be involved in the methylation pathways (Choi et al., 1994; Ekstrom and Morel, 2007). Recently, Parks et al. (2013) identified the genes (*hgcA* and *hgcB*) and their encoding proteins as being responsible for Hg methylation, which for the first time revealed the detailed mechanisms of Hg methylation by anaerobic bacteria and archaea. The *hgcA* gene encodes a putative corrinoid protein (HgcA) capable of transferring a methyl group to inorganic Hg(II); the *hgcB* gene encodes a 2[4Fe-4S] ferredoxin (HgcB) that reduces HgcA to a state that enables it to receive a new methyl group (Parks et al., 2013).

Where and how MeHg is formed in the ocean, however, remain a subject of debate. Some studies proposed that marine MeHg is mainly supported by its production in anoxic coastal sediments, where Hg methylators are known to be present, with its subsequent release to the overlying seawater (Hammerschmidt and Fitzgerald, 2006; Kraepiel et al., 2003). However, if MeHg in seawater has a life time as short as suggested by Lehnherr et al. (2011), the MeHg produced from coastal sediments can hardly make its way to the open ocean (Cossa et al., 2017). Here, it should be noted that the loss rates of marine MeHg estimated from incubation studies (Lehnherr et al., 2011; Monperrus et al., 2007; Whalin et al., 2007) are several orders of magnitude higher than those

estimated based on Hg and MeHg profiles in the seawater (Mason et al., 1995b; Mason and Fitzgerald, 1993). MeHg production in anoxic deep-sea sediments, although not well documented, could act as a possible source of MeHg in the open ocean (Kraepiel et al., 2003). However, this source cannot explain the observed MeHg profiles, which exhibit maxima in subsurface waters and decreasing concentrations in deeper waters (Cossa et al., 2009; Heimbürger et al., 2015; Mason and Fitzgerald, 1990; Munson et al., 2015; Sunderland et al., 2009).

Currently, the prevailing hypothesis for seawater MeHg is that it mainly originates from in-situ methylation of inorganic Hg(II) in the water column (Cossa et al., 2009; Heimbürger et al., 2015; Mason and Fitzgerald, 1990; Sunderland et al., 2009). In almost all the studies in the world's oceans, MeHg always peaks in the subsurface layer where DO is low and nutrients are high. This distribution pattern supports the hypothesis of in-situ production, and the correlation between MeHg and remineralization proxies such as apparent oxygen utilization (AOU) indicates an association between water column Hg methylation and OM remineralization (Cossa et al., 2009, 2011; Sunderland et al., 2009). In addition, incubation studies have shown the occurrence of Hg methylation in seawater (Lehnherr et al., 2011; Monperrus et al., 2007).

One major problem with the water column Hg methylation hypothesis is that, although DO is low in waters where MeHg enriches (Mason et al., 2012), anoxic conditions are not reached except in the Black Sea (Lamborg et al., 2008); as such, the known anaerobic Hg methylators (i.e., those possess *hgcA* and *hgcB* genes) are unlikely to thrive and produce MeHg in these waters. However, anoxic microenvironments (e.g., copepod guts and fecal pellets) are known to be present in the oxic ambient seawater

(Alldredge and Cohen, 1987; Tang et al., 2011), so there is a possibility that Hg methylation takes place in such anoxic microenvironments. Another possibility is that some aerobic marine microbes may also be capable of methylating Hg, as suggested by the recent finding of *hgcA*- and *hgcB*- like genes in the aerobic microbe *Nitrospina* (Gionfriddo et al., 2016). Finally, abiotic Hg methylation in seawater (Celo et al., 2006) cannot be ruled out, although its contribution in the ambient seawater has never been quantified.

1.1.4 Mercury: from Seawater to Biota

Humans are exposed to Hg primarily via consumption of marine animals and in the form of MMHg (Mason et al., 2012; Sunderland, 2007). Marine animals accumulate MMHg from their prey and ultimately from seawater (Schartup et al., 2017). MMHg concentrations in seawater are typically very low and rarely exceed 0.5 pM (Bowman et al., 2015; Cossa et al., 2009, 2011; Mason and Fitzgerald, 1990; Munson et al., 2015; Wang et al., 2012). Bioaccumulation of MMHg in the food webs includes both bioconcentration from seawater and biomagnification through trophic transfer. Marine phytoplankton is known to bioconcentrate MMHg from seawater (Mason et al., 1996), and zooplankton accumulates it directly from seawater and through grazing phytoplankton (Lee and Fisher, 2017; Pućko et al., 2014). In addition to seawater bioconcentration and trophic transfer, an Arctic copepod (*Calanus hyperboreus*) may bioaccumulate MMHg from the potential Hg methylation in its anoxic guts (Pućko et al., 2014). The greatest degree of bioaccumulation occurs from seawater to phytoplankton at the base of marine food web. In marine phytoplankton, the bioaccumulation factors

(BAFs) of total Hg (Hg_T) and MMHg range from $10^{2.5}$ to $10^{5.0}$ and from $10^{2.6}$ to $10^{5.9}$, respectively (Gosnell et al., 2017; Schartup et al., 2017). In the subsequent bioaccumulation process, MMHg concentrations further increase 2–10 times per increasing trophic level, whereas no further biomagnification is observed for inorganic Hg (Hammerschmidt et al., 2013; Lee and Fisher, 2017; Mason et al., 2012). The preferential bioaccumulation of MMHg over inorganic Hg (Wang and Wong, 2003; Watras and Bloom, 1992) is partly due to the different distribution patterns of Hg species in phytoplankton cells and to the feeding characteristics of zooplankton (Mason et al., 1995a; Reinfelder and Fisher, 1991). In marine phytoplankton cells, MMHg mainly resides in cytoplasm, whereas inorganic Hg is mostly bound to the membrane (Mason et al., 1996). When grazing phytoplankton, zooplankton typically digests cytoplasm, but defecates membrane materials (Mason et al., 1995a; Reinfelder and Fisher, 1991). Zooplankton is also very important in the bioaccumulation process, as it builds up MMHg from seawater and phytoplankton, and transfers MMHg to marine animals at higher trophic levels (Lee and Fisher, 2017; Schartup et al., 2017). In the high trophic level animals, MMHg concentrations can be over 10^6 times higher than those in seawater. For instance, MMHg concentration reaches ~200 μg/kg in Arctic cod (Loseto et al., 2008; Stern and Macdonald, 2005), 100–1000 μg/kg in the muscle of adult ringed seals (Brown et al., 2016), and 500–1800 μg/kg in the muscle of beluga (Gaden and Stern, 2010). Despite their importance, bioconcentration and biomagnification of MMHg at the base of the marine food web has been little studied (Schartup et al., 2017), especially in the Arctic (Foster et al., 2012; Pućko et al., 2014).

1.1.5 Tracing Mercury Transformation with Isotopic Methods

One of the most powerful tools to probe Hg species transformation processes in the environment is the use of stable Hg isotopes (Bergquist and Blum, 2007; Hintelmann et al., 2000). Generally, two types of isotopic methods are used in such studies: Hg isotope fractionation and isotopically labeled Hg addition. The use of Hg isotope fractionation largely depends on accurately and fully characterizing the very small extent of Hg isotope fractionation during species conversions in controlled experiments (Kritee et al., 2013), which has only recently become possible. On the other hand, the isotopic labeling Hg additions have been widely used in the studies of Hg transformation in the environment.

When using isotope addition methods to trace Hg transformations, it is assumed that the added isotopically enriched Hg species behave the same as those originally present in the environment. The method typically involves the following steps. Firstly, one or more isotopically labeled Hg species (with known isotopic ratios) are added to the environmental medium to be studied (e.g., seawater, sediments). Then the medium is incubated for a certain period of time, under specific conditions. The incubations are stopped at a certain time to collect the Hg samples for the measurements of concentrations and isotope compositions in different Hg species, so the Hg transformations can be quantified (Hintelmann et al., 1995; Hintelmann and Ogrinc, 2003).

1.2 Research Hypotheses

To fill critical knowledge gaps and improve our understanding of the Hg biogeochemistry in the Arctic marine system, the objectives of this thesis study were to address the following research hypotheses:

1) Distribution of Hg species (i.e., Hg_T, MeHg) in seawater explains the biotic Hg spatial gradients in the Canadian Arctic;
2) The rates of Hg methylation and demethylation in seawater can be determined by the seawater incubation approach;
3) The Canadian Arctic seawater MeHg originates from in-situ production in the water column;
4) The Arctic marine copepod (*Calanus hyperboreus*) bioaccumulates Hg species through seawater bioconcentration and trophic transfer;
5) Anoxic microenvironments in the guts and/or fecal pellets of *C. hyperboreus* are hotspots for Hg methylation in oxic ambient seawater.

1.3 Dissertation Organization

This dissertation is organized in a "sandwich" style with an introduction chapter (this chapter), four manuscript-ready "results" chapters, and a conclusion chapter.

Chapter 2 presents the distribution of Hg_T and MeHg in seawater along a transect from the Canada Basin in the west, through the Canadian Arctic Archipelago, to Baffin Bay and the Labrador Sea in the east. The results show that the longitudinal gradients of MeHg concentrations in subsurface seawater readily explain the spatial trend of

biological Hg levels in the Canadian Arctic. This chapter has been published in Scientific Reports.

Chapter 3 presents results of Hg isotope addition incubations of seawater from the Canadian Arctic. This method has been commonly used in the literature for rate determinations of methylation and demethylation in seawater. The results presented here show that major problems exist with the method, including unexplainable Hg reaction kinetics and time zero methylation and demethylation, thus casting doubt on published rate constants based on incubation studies and calling for the development of new approaches for such studies.

Chapter 4 discusses the major source(s) of seawater MeHg in the Canadian Arctic. The significant correlations between MeHg and nutrients and AOU appear to suggest an in-situ production of MeHg in the water column associated with OM remineralization. However, further analysis of water masses and N*, a denitrification tracer, reveals that the MeHg enrichment is likely originated from the anaerobic Chukchi Seas sediments, and transported to the Canadian Arctic within the Upper Halocline Water.

Chapter 5 studies the Hg bioaccumulation in an Arctic marine copepod, *Calanus hyperboreus*, and tests the hypothesis of Hg methylation enhancement in anoxic copepod guts and fecal pellets, based on a series of incubation experiments using an addition of inorganic ^{202}Hg(II). Results show that the copepod preferentially bioaccumulates MMHg over inorganic Hg, and the uptake is primarily via trophic transfer. Production of MMHg is not enhanced in the copepod guts or fecal pellets, suggesting that these microenvironments are unlikely hotspots for Hg methylation. The results also suggest that marine algae may inhibit Hg methylation in seawater.

Chapter 6 presents the major conclusions from the study, reviews the limitations, and provides perspectives of future research directions toward a better understanding of Hg biogeochemistry in the Arctic marine system.

Appendix provides details and examples for Hg methylation and demethylation quantification, which were used in Chapters 3 and 5.

References

Alldredge, A.L., and Cohen, Y. (1987). Can microscale chemical patches persist in the sea? Microelectrode study of marine snow, fecal pellets. Science 235, 689-691.

AMAP (2005). AMAP Assessment 2002: Heavy Metals in the Arctic. Arctic Monitoring and Assessment Program: Oslo.

AMAP (2009). AMAP Assessment 2009: Human health in the Arctic. Arctic Monitoring and Assessment Program: Oslo.

AMAP (2011). AMAP Assessment 2011: Mercury in the Arctic. Arctic Monitoring and Assessment Program: Oslo.

AMAP (2018). AMAP Assessment 2018: Biological effects of contaminants on Arctic wildlife and fish. Mercury in the Arctic. Arctic Monitoring and Assessment Program: Tromsø.

Ariya, P.A., Dastoor, A.P., Amyot, M., Schroeder, W.H., Barrie, L., Anlauf, K., Raofie, F., Ryzhkov, A., Davignon, D., and Lalonde, J. (2004). The Arctic: a sink for mercury. Tellus B 56, 397-403.

Atwell, L., Hobson, K.A., and Welch, H.E. (1998). Biomagnification and bioaccumulation of mercury in an arctic marine food web: insights from stable nitrogen isotope analysis. Canadian Journal of Fisheries and Aquatic Sciences 55, 1114-1121.

Bergquist, B.A., and Blum, J.D. (2007). Mass-dependent and-independent fractionation of Hg isotopes by photoreduction in aquatic systems. Science 318, 417-420.

Bowman, K.L., Hammerschmidt, C.R., Lamborg, C.H., and Swarr, G. (2015). Mercury in the north Atlantic ocean: The US GEOTRACES zonal and meridional sections. Deep Sea Research Part II: Topical Studies in Oceanography 116, 251-261.

Bowman, K.L., Hammerschmidt, C.R., Lamborg, C.H., Swarr, G.J., and Agather, A.M. (2016). Distribution of mercury species across a zonal section of the eastern tropical South Pacific Ocean (US GEOTRACES GP16). Marine Chemistry 186, 156-166.

Braune, B., Chételat, J., Amyot, M., Brown, T., Claydon, M., Evans, M., Fisk, A., Gaden, A., Girard, C., and Hare, A. (2014). Mercury in the marine environment of the Canadian Arctic: Review of recent findings. Science of The Total Environment 509-510, 67-90.

Brown, T.M., Fisk, A.T., Wang, X., Ferguson, S.H., Young, B.G., Reimer, K.J., and Muir, D.C. (2016). Mercury and cadmium in ringed seals in the Canadian Arctic: Influence of location and diet. Science of the Total Environment 545, 503-511.

Brown, T.M., Macdonald, R.W., Muir, D.C., and Letcher, R.J. (2018). The distribution and trends of persistent organic pollutants and mercury in marine mammals from Canada's Eastern Arctic. Science of The Total Environment 618, 500-517.

Celo, V., Lean, D.R., and Scott, S.L. (2006). Abiotic methylation of mercury in the aquatic environment. Science of the Total Environment 368, 126-137.

Choi, S.-C., Chase, T., and Bartha, R. (1994). Metabolic pathways leading to mercury methylation in Desulfovibrio desulfuricans LS. Applied and Environmental Microbiology 60, 4072-4077.

Compeau, G., and Bartha, R. (1985). Sulfate-reducing bacteria: principal methylators of mercury in anoxic estuarine sediment. Applied and Environmental Microbiology 50, 498-502.

Cossa, D., Averty, B., and Pirrone, N. (2009). The origin of methylmercury in open Mediterranean waters. Limnology and Oceanography 54, 837-844.

Cossa, D., de Madron, X.D., Schäfer, J., Lanceleur, L., Guédron, S., Buscail, R., Thomas, B., Castelle, S., and Naudin, J.-J. (2017). The open sea as the main source of methylmercury in the water column of the Gulf of Lions (Northwestern Mediterranean margin). Geochimica et Cosmochimica Acta 199, 222-237.

Cossa, D., Heimbürger, L.-E., Lannuzel, D., Rintoul, S.R., Butler, E.C., Bowie, A.R., Averty, B., Watson, R.J., and Remenyi, T. (2011). Mercury in the Southern Ocean. Geochimica et Cosmochimica Acta 75, 4037-4052.

Dastoor, A.P., and Durnford, D.A. (2014). Arctic ocean: is it a sink or a source of atmospheric mercury? Environmental Science & Technology 48, 1707-1717.

Dietz, R., Sonne, C., Basu, N., Braune, B., O'Hara, T., Letcher, R.J., Scheuhammer, T., Andersen, M., Andreasen, C., and Andriashek, D. (2013). What are the toxicological effects of mercury in Arctic biota? Science of the Total Environment 443, 775-790.

Ding, L.-Y., He, N.-N., Yang, S., Zhang, L.-J., Liang, P., Wu, S.-C., Wong, M.H., and Tao, H.-C. (2019). Inhibitory effects of Skeletonema costatum on mercury methylation by Geobacter sulfurreducens PCA. Chemosphere 216, 179-185.

Douglas, T.A., Loseto, L.L., Macdonald, R.W., Outridge, P., Dommergue, A., Poulain, A., Amyot, M., Barkay, T., Berg, T., and Chételat, J. (2012). The fate of mercury in Arctic terrestrial and aquatic ecosystems, a review. Environmental Chemistry 9, 321-355.

Eaton, R., and Farant, J. (1982). The polar bear as a biological indicator of the environmental mercury burden. Arctic 35, 422-425.

Ekstrom, E.B., and Morel, F.M. (2007). Cobalt limitation of growth and mercury methylation in sulfate-reducing bacteria. Environmental Science & Technology 42, 93-99.

Emmerton, C.A., Graydon, J.A., Gareis, J.A., St. Louis, V.L., Lesack, L.F., Banack, J.K., Hicks, F., and Nafziger, J. (2013). Mercury export to the Arctic Ocean from the Mackenzie River, Canada. Environmental Science & Technology 47, 7644-7654.

Fisher, J.A., Jacob, D.J., Soerensen, A.L., Amos, H.M., Steffen, A., and Sunderland, E.M. (2012). Riverine source of Arctic Ocean mercury inferred from atmospheric observations. Nature Geoscience 5, 499-504.

Fitzgerald, W.F., Lamborg, C.H., and Hammerschmidt, C.R. (2007). Marine biogeochemical cycling of mercury. Chemical Reviews 107, 641-662.

Foster, K.L., Stern, G.A., Pazerniuk, M.A., Hickie, B., Walkusz, W., Wang, F., and Macdonald, R.W. (2012). Mercury biomagnification in marine zooplankton food webs in Hudson Bay. Environmental Science & Technology 46, 12952-12959.

Gaden, A., and Stern, G. (2010). Temporal Trends in Beluga, narwhal and walrus mercury levels: links to climate chage. In A Little Less Arctic: Top Predators in the World's Largest Northern Island Sea, Hudson Bay (Springer), pp. 197 - 216.

Gionfriddo, C.M., Tate, M.T., Wick, R.R., Schultz, M.B., Zemla, A., Thelen, M.P., Schofield, R., Krabbenhoft, D.P., Holt, K.E., and Moreau, J.W. (2016). Microbial mercury methylation in Antarctic sea ice. Nature microbiology 1, 16127.

Gosnell, K.J., Balcom, P.H., Tobias, C.R., Gilhooly, W.P., and Mason, R.P. (2017). Spatial and temporal trophic transfer dynamics of mercury and methylmercury into zooplankton and phytoplankton of Long Island Sound. Limnology and Oceanography 62, 1122-1138.

Hammerschmidt, C.R., and Bowman, K.L. (2012). Vertical methylmercury distribution in the subtropical North Pacific Ocean. Marine Chemistry 132, 77-82.

Hammerschmidt, C.R., Finiguerra, M.B., Weller, R.L., and Fitzgerald, W.F. (2013). Methylmercury accumulation in plankton on the continental margin of the Northwest Atlantic Ocean. Environmental Science & Technology 47, 3671-3677.

Hammerschmidt, C.R., and Fitzgerald, W.F. (2006). Methylmercury cycling in sediments on the continental shelf of southern New England. Geochimica et Cosmochimica Acta 70, 918-930.

Heimbürger, L.-E., Sonke, J.E., Cossa, D., Point, D., Lagane, C., Laffont, L., Galfond, B.T., Nicolaus, M., Rabe, B., and van der Loeff, M.R. (2015). Shallow methylmercury production in the marginal sea ice zone of the central Arctic Ocean. Scientific reports 5, 10318.

Hintelmann, H., Evans, R.D., and Villeneuve, J.Y. (1995). Measurement of mercury methylation in sediments by using enriched stable mercury isotopes combined with methylmercury determination by gas chromatography–inductively coupled plasma mass spectrometry. Journal of Analytical Atomic Spectrometry 10, 619-624.

Hintelmann, H., Keppel‐Jones, K., and Evans, R.D. (2000). Constants of mercury methylation and demethylation rates in sediments and comparison of tracer and ambient mercury availability. Environmental Toxicology and Chemistry 19, 2204-2211.

Hintelmann, H., and Ogrinc, N. (2003). Determination of stable mercury isotopes by ICP/MS and their application in environmental studies, Vol 835 (Washington D.C American Chemical Society).

Horton, T.W., Blum, J.D., Xie, Z., Hren, M., and Chamberlain, C.P. (2009). Stable isotope food‐web analysis and mercury biomagnification in polar bears (Ursus maritimus). Polar Research 28, 443-454.

JENSEN, S., and Jernelöv, A. (1969). Biological methylation of mercury in aquatic organisms. Nature 223, 753-754.

Johnson, K.P., Blum, J.D., Keeler, G.J., and Douglas, T.A. (2008). Investigation of the deposition and emission of mercury in arctic snow during an atmospheric mercury depletion event. Journal of Geophysical Research: Atmospheres 113(D17).

Kerin, E.J., Gilmour, C., Roden, E., Suzuki, M., Coates, J., and Mason, R. (2006). Mercury methylation by dissimilatory iron-reducing bacteria. Applied and Environmental Microbiology 72, 7919-7921.

Koeman, J., Van de Ven, W., De Goeij, J., Tjioe, P., and Van Haaften, J. (1975). Mercury and selenium in marine mammals and birds. Science of the Total Environment 3, 279-287.

Kraepiel, A.M., Keller, K., Chin, H.B., Malcolm, E.G., and Morel, F.M. (2003). Sources and variations of mercury in tuna. Environmental Science & Technology 37, 5551-5558.

Kritee, K., Blum, J.D., Reinfelder, J.R., and Barkay, T. (2013). Microbial stable isotope fractionation of mercury: A synthesis of present understanding and future directions. Chemical Geology 336, 13-25.

Lamborg, C.H., Yiğiterhan, O., Fitzgerald, W.F., Balcom, P.H., Hammerschmidt, C.R., and Murray, J. (2008). Vertical distribution of mercury species at two sites in the Western Black Sea. Marine Chemistry 111, 77-89.

Lee, C.S., and Fisher, N.S. (2017). Bioaccumulation of methylmercury in a marine copepod. Environmental Toxicology and Chemistry 36, 1287-1293.

Lehnherr, I., Louis, V.L.S., Hintelmann, H., and Kirk, J.L. (2011). Methylation of inorganic mercury in polar marine waters. Nature geoscience 4, 298-302.

Leitch, D.R., Carrie, J., Lean, D., Macdonald, R.W., Stern, G.A., and Wang, F. (2007). The delivery of mercury to the Beaufort Sea of the Arctic Ocean by the Mackenzie River. Science of the Total Environment 373, 178-195.

Loseto, L., Stern, G., Deibel, D., Connelly, T., Prokopowicz, A., Lean, D., Fortier, L., and Ferguson, S. (2008). Linking mercury exposure to habitat and feeding behaviour in Beaufort Sea beluga whales. Journal of Marine Systems 74, 1012-1024.

Macdonald, R., and Loseto, L. (2010). Are Arctic Ocean ecosystems exceptionally vulnerable to global emissions of mercury? A call for emphasised research on methylation and the consequences of climate change. Environmental Chemistry 7, 133-138.

Macdonald, R.W., Wang, F., Stern, G., and Outridge, P. (2008). The overlooked role of the ocean in mercury cycling in the Arctic. Marine Pollution Bulletin 56, 1963-1965.

Mason, R., Reinfelder, J., and Morel, F. (1995a). Bioaccumulation of mercury and methylmercury. Water, Air, & Soil Pollution 80, 915-921.

Mason, R., Rolfhus, K., and Fitzgerald, W. (1995b). Methylated and elemental mercury cycling in surface and deep ocean waters of the North Atlantic. In Mercury as a Global Pollutant (Springer), pp. 665-677.

Mason, R., Rolfhus, K.a., and Fitzgerald, W. (1998). Mercury in the north Atlantic. Marine Chemistry 61, 37-53.

Mason, R.P., Choi, A.L., Fitzgerald, W.F., Hammerschmidt, C.R., Lamborg, C.H., Soerensen, A.L., and Sunderland, E.M. (2012). Mercury biogeochemical cycling in the ocean and policy implications. Environmental Research 119, 101-117.

Mason, R.P., and Fitzgerald, W.F. (1993). The distribution and biogeochemical cycling of mercury in the equatorial Pacific Ocean. Deep Sea Research Part I: Oceanographic Research Papers 40, 1897-1924.

Mason, R.P., Reinfelder, J.R., and Morel, F.M. (1996). Uptake, toxicity, and trophic transfer of mercury in a coastal diatom. Environmental Science & Technology 30, 1835-1845.

Mason, R.y., and Fitzgerald, W. (1990). Alkylmercury species in the equatorial Pacific. Nature 347, 457−459.

Monperrus, M., Tessier, E., Amouroux, D., Leynaert, A., Huonnic, P., and Donard, O. (2007). Mercury methylation, demethylation and reduction rates in coastal and marine surface waters of the Mediterranean Sea. Marine Chemistry 107, 49-63.

Munson, K.M., Lamborg, C.H., Swarr, G.J., and Saito, M.A. (2015). Mercury Species Concentrations and Fluxes in the Central Tropical Pacific Ocean. Global Biogeochemical Cycles 29, 656-676.

Obrist, D., Agnan, Y., Jiskra, M., Olson, C.L., Colegrove, D.P., Hueber, J., Moore, C.W., Sonke, J.E., and Helmig, D. (2017). Tundra uptake of atmospheric elemental mercury drives Arctic mercury pollution. Nature 547, 201-204.

Obrist, D., Kirk, J.L., Zhang, L., Sunderland, E.M., Jiskra, M., and Selin, N.E. (2018). A review of global environmental mercury processes in response to human and natural perturbations: Changes of emissions, climate, and land use. Ambio 47, 116-140.

Pacyna, J., and Keeler, G.J. (1995). Sources of mercury in the Arctic. Water, Air, & Soil Pollution 80, 621-632.

Petersen, G., and Munthe, J. (1995). Atmospheric mercury species over central and northern Europe. Model calculations and comparison with observations from the Nordic air and precipitation network for 1987 and 1988. Atmospheric Environment 29, 47-67.

Pomerleau, C., Stern, G.A., Pućko, M., Foster, K.L., Macdonald, R.W., and Fortier, L. (2016). Pan-Arctic concentrations of mercury and stable isotope ratios of carbon (δ 13 C) and nitrogen (δ 15 N) in marine zooplankton. Science of the Total Environment 551, 92-100.

Pućko, M., Burt, A., Walkusz, W., Wang, F., Macdonald, R., Rysgaard, S., Barber, D., Tremblay, J.-É., and Stern, G. (2014). Transformation of mercury at the bottom of the Arctic food web: An overlooked puzzle in the mercury exposure narrative. Environmental Science & Technology 48, 7280-7288.

Reinfelder, J.R., and Fisher, N.S. (1991). The assimilation of elements ingested by marine copepods. Science 251, 794-796.

Riget, F., Muir, D., Kwan, M., Savinova, T., Nyman, M., Woshner, V., and O'Hara, T. (2005). Circumpolar pattern of mercury and cadmium in ringed seals. Science of the Total Environment 351, 312-322.

Routti, H., Letcher, R.J., Born, E.W., Branigan, M., Dietz, R., Evans, T.J., Fisk, A.T., Peacock, E., and Sonne, C. (2011). Spatial and temporal trends of selected trace elements in liver tissue from polar bears (Ursus maritimus) from Alaska, Canada and Greenland. Journal of Environmental Monitoring 13, 2260-2267.

Ruus, A., Øverjordet, I.B., Braaten, H.F.V., Evenset, A., Christensen, G., Heimstad, E.S., Gabrielsen, G.W., and Borgå, K. (2015). Methylmercury biomagnification in an Arctic pelagic food web. Environmental Toxicology and Chemistry 34, 2636-2643.

Schartup, A.T., Qureshi, A., Dassuncao, C., Thackray, C.P., Harding, G., and Sunderland, E.M. (2017). A Model for Methylmercury Uptake and Trophic Transfer by Marine Plankton. Environmental Science & Technology 52, 654–662.

Schroeder, W., Anlauf, K., Barrie, L., Lu, J., Steffen, A., Schneeberger, D., and Berg, T. (1998). Arctic springtime depletion of mercury. Nature 394, 331-332.

Schuster, P.F., Schaefer, K.M., Aiken, G.R., Antweiler, R.C., Dewild, J.F., Gryziec, J.D., Gusmeroli, A., Hugelius, G., Jafarov, E., and Krabbenhoft, D.P. (2018). Permafrost stores a globally significant amount of mercury. Geophysical Research Letters 45, 1463-1471.

Schuster, P.F., Striegl, R.G., Aiken, G.R., Krabbenhoft, D.P., Dewild, J.F., Butler, K., Kamark, B., and Dornblaser, M. (2011). Mercury export from the Yukon River Basin and potential response to a changing climate. Environmental Science & Technology 45, 9262-9267.

Smith, T.G., and Armstrong, F. (1975). Mercury in seals, terrestrial carnivores, and principal food items of the Inuit, from Holman, NWT. Journal of the Fisheries Board of Canada 32, 795-801.

Soerensen, A.L., Jacob, D.J., Schartup, A., Fisher, J.A., Lehnherr, I., St Louis, V.L., Heimbürger, L.E., Sonke, J.E., Krabbenhoft, D.P., and Sunderland, E.M. (2016). A Mass Budget for Mercury and Methylmercury in the Arctic Ocean. Global Biogeochemical Cycles 30, 560-575.

St. Louis, V.L., Derocher, A.E., Stirling, I., Graydon, J.A., Lee, C., Jocksch, E., Richardson, E., Ghorpade, S., Kwan, A.K., and Kirk, J.L. (2011). Differences in mercury bioaccumulation between polar bears (Ursus maritimus) from the Canadian high-and sub-Arctic. Environmental Science & Technology 45, 5922-5928.

Stern, G., and Macdonald, R. (2005). Biogeographic provinces of total and methyl mercury in zooplankton and fish from the Beaufort and Chukchi Seas: results from the SHEBA drift. Environmental Science & Technology 39, 4707-4713.

Sunderland, E.M. (2007). Mercury exposure from domestic and imported estuarine and marine fish in the US seafood market. Environmental Health Perspectives 115, 235-242.

Sunderland, E.M., Krabbenhoft, D.P., Moreau, J.W., Strode, S.A., and Landing, W.M. (2009). Mercury sources, distribution, and bioavailability in the North Pacific Ocean: Insights from data and models. Global Biogeochemical Cycles 23, 1-14.

Tang, K.W., Glud, R.N., Glud, A., Rysgaard, S., and Nielsen, T.G. (2011). Copepod guts as biogeochemical hotspots in the sea: Evidence from microelectrode profiling of Calanus spp. Limnology and Oceanography 56, 666-672.

Ullrich, S.M., Tanton, T.W., and Abdrashitova, S.A. (2001). Mercury in the aquatic environment: a review of factors affecting methylation. Critical Reviews in Environmental Science and Technology 31, 241-293.

Wagemann, R., Innes, S., and Richard, P. (1996). Overview and regional and temporal differences of heavy metals in Arctic whales and ringed seals in the Canadian Arctic. Science of the Total Environment 186, 41-66.

Wang, F., Macdonald, R.W., Armstrong, D.A., and Stern, G.A. (2012). Total and Methylated Mercury in the Beaufort Sea: The Role of Local and Recent Organic Remineralization. Environmental Science & Technology 46, 11821-11828.

Wang, W.-X., and Wong, R.S. (2003). Bioaccumulation kinetics and exposure pathways of inorganic mercury and methylmercury in a marine fish, the sweetlips Plectorhinchus gibbosus. Marine Ecology Progress Series 261, 257-268.

Watras, C.J., and Bloom, N.S. (1992). Mercury and methylmercury, in individual zooplankton: Implications for bioaccumulation. Limnology and Oceanography 37, 1313-1318.

Whalin, L., Kim, E.-H., and Mason, R. (2007). Factors influencing the oxidation, reduction, methylation and demethylation of mercury species in coastal waters. Marine Chemistry 107, 278-294.

Zhang, Y., Jacob, D.J., Dutkiewicz, S., Amos, H.M., Long, M.S., and Sunderland, E.M. (2015). Biogeochemical drivers of the fate of riverine mercury discharged to the global and Arctic oceans. Global Biogeochemical Cycles 29, 854-864.

Chapter 2: Subsurface Seawater Methylmercury Maximum Explains Biotic Mercury Concentrations in the Canadian Arctic

This chapter has been published in:

Scientific Reports, 8(1), 14465. https://doi.org/10.1038/s41598-018-32760-0.

Kang Wang[1], Kathleen M. Munson[1], Alexis Beaupré-Laperrière[2], Alfonso Mucci[2], Robie W. Macdonald[1,3] & Feiyue Wang[1*]

[1]Centre for Earth Observation Science, and Department of Environment and Geography, University of Manitoba, Winnipeg, Manitoba, R3T 2N2, Canada

[2]GEOTOP and Department of Earth and Planetary Sciences, McGill University, Montreal, Quebec, H3A 0E8, Canada

[3]Institute of Ocean Sciences, Department of Fisheries and Oceans, Sidney, British Columbia, V8L 4B2, Canada

Abstract

Mercury (Hg) is a contaminant of major concern in Arctic marine ecosystems. Decades of Hg observations in marine biota from across the Canadian Arctic show generally higher concentrations in the west than in the east. Various hypotheses have attributed this longitudinal biotic Hg gradient to regional differences in atmospheric or terrestrial inputs of inorganic Hg, but it is methylmercury (MeHg) that accumulates and biomagnifies in marine biota. Here, we present high-resolution vertical profiles of total Hg and MeHg in seawater along a transect from the Canada Basin, across the Canadian Arctic Archipelago (CAA) and Baffin Bay, and into the Labrador Sea. Total Hg concentrations are lower in the western Arctic, opposing the biotic Hg distributions. In contrast, MeHg exhibits a distinctive subsurface maximum at shallow depths of 100–300 m, with its peak concentration decreasing eastwards. As this subsurface MeHg maximum lies within the habitat of zooplankton and other lower trophic-level biota, biological uptake of subsurface MeHg and subsequent biomagnification readily explains the biotic Hg concentration gradient. Understanding the risk of MeHg to the Arctic marine ecosystem and Indigenous Peoples will thus require an elucidation of the processes that generate and maintain this subsurface MeHg maximum.

Introduction

Monitoring data collected during the past four decades have shown Hg concentrations in Canadian Arctic marine mammals (e.g., beluga whales, ringed seals, polar bears) to be highly elevated, frequently exceeding toxicity thresholds (AMAP, 2011; Dietz et al., 2013). This has raised major concerns over the health of marine mammals and Indigenous Peoples whose traditional diets include marine mammal tissues. Mercury concentrations in marine biota are generally higher in the Beaufort Sea and western Canadian Arctic Archipelago (CAA) than in the eastern CAA and Baffin Bay (AMAP, 2011; Brown et al., 2018; Dietz et al., 2013). This longitudinal gradient is not limited to apex predators (Brown et al., 2016; Routti et al., 2011), but extends to organisms at lower trophic levels such as zooplankton (e.g., Themisto spp., Calanus spp.) (Pomerleau et al., 2016) (Figure 2-1a). Whereas regional variations in top predator Hg concentrations may be linked to feeding behavior and dietary preference (Brown et al., 2016), observed spatial patterns persist after adjustments are made to account for trophic position (Brown et al., 2018).

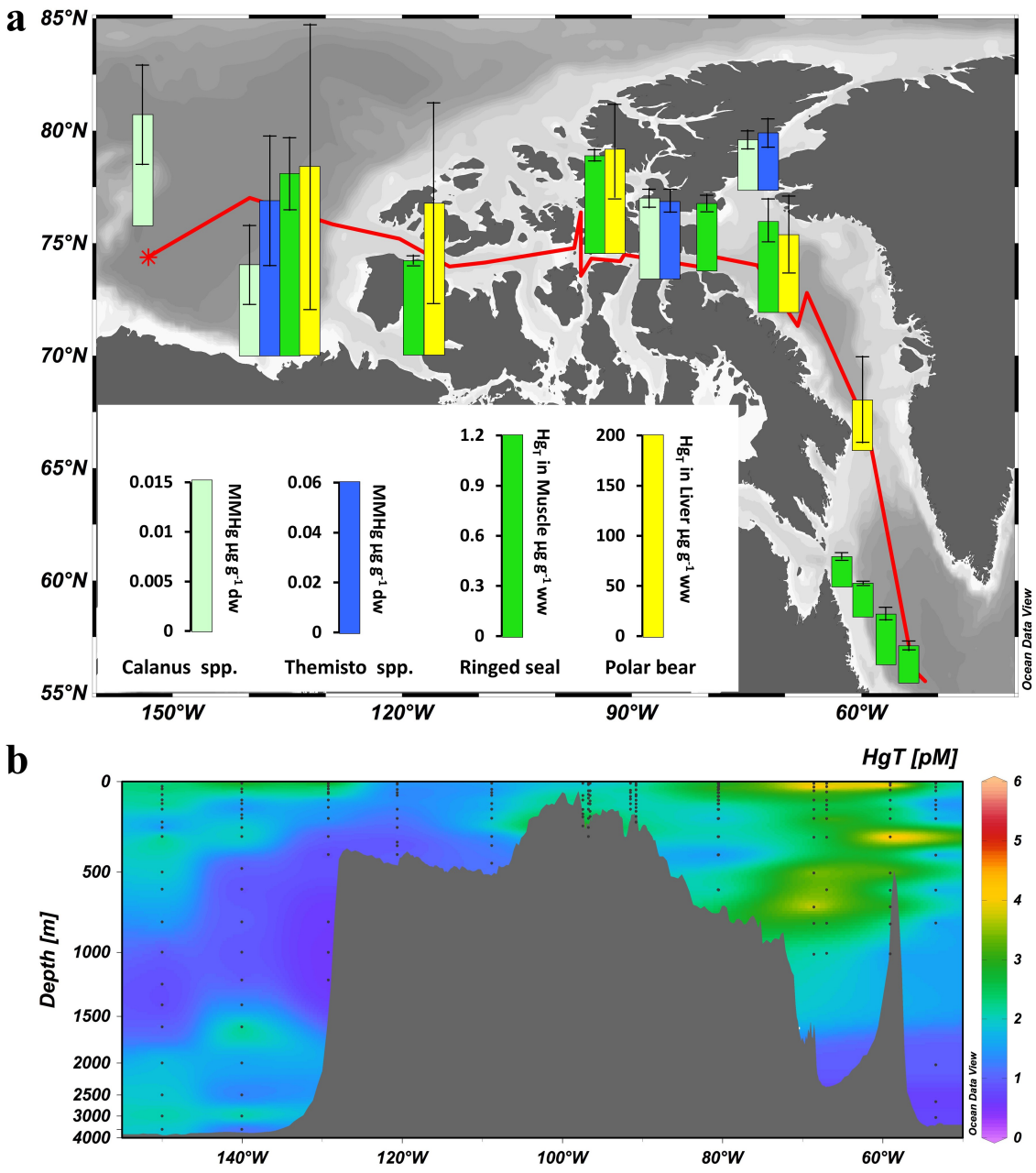

Figure 2-1: Mercury concentrations in the marine food web and seawaters across the Canadian Arctic and Labrador Sea. a, Map showing Hg concentrations in the marine food web, and seawater sampling sites across the Canadian Arctic and Labrador Sea; b, distribution of total Hg (Hg_T); and c, methylmercury (MeHg) in seawater along a longitudinal (west-to-east) section. The bar charts in a show mean concentrations ± one standard deviation of monomethylmercury (MMHg) in *Calanus* spp. and *Themisto* spp. collected from 1998 to 2012 (Pomerleau et al., 2016), Hg_T in muscle of adult ringed seals collected from 2007 and 2011 (Brown et al., 2016, 2018), and Hg_T in liver of polar bears collected from 2005 to 2008 (Brown et al., 2018). The base map with bathymetry was created using Ocean Data View (version 4.0; https://odv.awi.de) (Schlitzer, 2018).

Figure 2-1: Continued

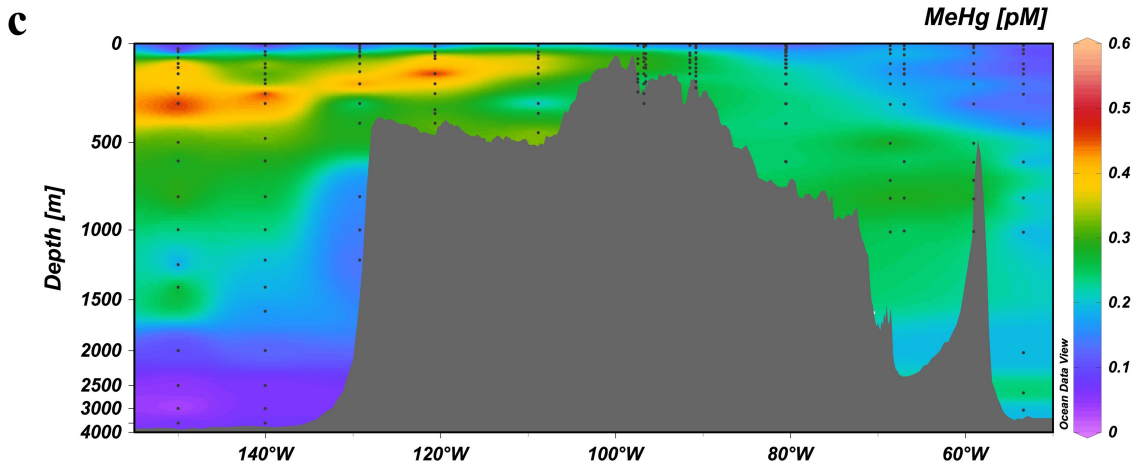

During the 2015 Canadian Arctic GEOTRACES cruises (July 14–September 16, 2015) aboard the Canadian Research Icebreaker CCGS Amundsen, we measured high-resolution vertical profiles of total mercury (Hg_T) (Figure 2-1b) in unfiltered seawater, along a 5200-km transect (150°–53° W) from the Canada Basin in the west, through CAA to Baffin Bay in the east, reaching the Labrador Sea in the North Atlantic Ocean (Figures 2-1a, 2-S1, Table 2-S1). Total Hg concentrations show a distinctive longitudinal gradient along the transect (Figure 2-1b, Table 2-1), with concentrations increasing from the Canada Basin and the western CAA (1.76 ± 1.15 pM) to the eastern CAA and Baffin Bay (2.62 ± 1.97 pM). These results are comparable to the limited Hg_T dataset reported for Canadian Arctic waters (Kirk et al., 2008; Lehnherr et al., 2011; Wang et al., 2012). The lowest concentrations were found in the Labrador Sea (0.65 ± 0.18 pM), slightly higher than those (0.44 ± 0.10 pM, 0.25–0.67 pM) measured in June 2014 in a similar area (Cossa et al., 2017).

Table 2-1: Concentrations of total Hg (Hg_T) and methylmercury (MeHg) in seawater from the Canadian Arctic and Labrador Sea.

Regions	Stations	Depth	Hg_T (pM)	MeHg (pM)
Canada Basin, Beaufort Sea, and Western CAA	CB1–4 CAA6–9	0–500 m	1.90 ± 1.25, 0.73–8.55, n=77	0.30 ± 0.14, 0.02–0.56, n=77
		Full depth	1.76 ± 1.15, 0.55–8.55, n=101	0.27 ± 0.14, 0.02–0.56, n=100
Eastern CAA and Baffin Bay	CAA1–5 BB1–3	0–500 m	2.60 ± 2.06, 0.80–12.35, n=78	0.19 ± 0.08, 0.04–0.44, n=78
		Full depth	2.62 ± 1.97, 0.80–12.35, n=93	0.20 ± 0.09, 0.04–0.44, n=93
Labrador Sea	K1	0–500 m	0.62 ± 0.19, 0.30–0.92, n=9	0.09 ± 0.04, 0.03–0.12, n=9
		Full depth	0.65 ± 0.18, 0.30–0.95, n=14	0.12 ± 0.06, 0.03–0.24, n=15

The low seawater Hg_T concentrations in the Canada Basin, to the west, contrast with expectations based on the hypothesized elevated atmospheric and riverine inputs of Hg into this region. Whereas AMDEs do result in high springtime deposition, the low Canada Basin Hg_T concentrations are consistent with findings that most AMDEs occur in coastal regions and most of the deposited Hg is re-emitted to the atmosphere before snow melts (Johnson et al., 2008), thus limiting its transfer into the ocean. Likewise, Hg transported by rivers, possibly enhanced by tundra uptake, permafrost thawing, or geological enrichment, is likely deposited with sediment in coastal areas (Graydon et al., 2009) or escapes rapidly from the river plume to the atmosphere (Fisher et al., 2012). Furthermore, because MeHg accounts for <1% of the Hg_T in the Mackenzie River water (Graydon et al., 2009; Leitch et al., 2007), and the atmospheric input of Hg is predominantly inorganic (Baya et al., 2015; Johnson et al., 2008; Soerensen et al., 2016), the Hg delivered to Canada Basin waters requires transformation to MeHg, the biomagnifying Hg species, to account for observed higher biotic Hg concentrations. Therefore, elevated input of inorganic Hg in the western relative to the eastern Arctic does not provide, by itself, a plausible mechanism to explain higher biotic Hg

concentrations in the western Canadian Arctic (Figure 2-1b).

Concentrations of MeHg (0.23 ± 0.12 pM, 0.02 to 0.56 pM), measured during the 2015 Canadian Arctic GEOTRACES cruises (Figure 2-1c), are comparable to values reported in previous studies (Kirk et al., 2008; Lehnherr et al., 2011; Wang et al., 2012) and show an overall decoupling from Hg_T distributions in the water column (Figure 2-1c). The improved sampling resolution reveals distinctive vertical and longitudinal variations along the transect. Vertically, MeHg concentrations are lowest at the surface, increase with depth to a subsurface maximum, and subsequently decrease towards the bottom. Longitudinally, the subsurface MeHg peak value is highest (~0.5 pM) in the western part of the section and decreases to ~0.2 pM over the Barrow Strait sill into the eastern CAA, eventually dropping to ~0.1 pM in the Labrador Sea (Figure 2-1c, Table 2-1). The depth of the subsurface MeHg maximum varies from west to east: MeHg peaks at depths of ~300 m at the westernmost station in the Canada Basin and shoals progressively eastward to ~100 m in the western CAA. Farther east, the subsurface MeHg peak remains at ~100 m in the eastern CAA and Baffin Bay, but deepens to ~200 m in the Labrador Sea.

Regional differences in polar bear hair Hg concentrations between the Beaufort Sea and Hudson Bay were tentatively attributed to regional differences in seawater MeHg concentrations that resulted in different degrees of bioaccumulation (St. Louis et al., 2011), but high-resolution (vertical and horizontal) water-column MeHg concentration data were not available at that time to support this hypothesis. The distribution of the subsurface MeHg peak along our transect directly links the spatial distribution of aqueous MeHg concentrations to biotic uptake (Figure 2-1a,c).

Enrichment of MeHg in the subsurface water column (300–1000 m) is a common

feature of many ocean basins (Cossa et al., 2009; Sunderland et al., 2009). A notable difference is that the subsurface MeHg peak occurs at a much shallower depth in the western Canadian Arctic (100–300 m), in agreement with recent reports from the Beaufort Sea (Wang et al., 2012) and the central Arctic Ocean (Heimbürger et al., 2015). This MeHg maximum occurs at shallow depths that are just below the surface productive layer (see Figure 2-S2), which may enhance MeHg availability to organisms at the base of the marine food webs (Heimbürger et al., 2015). Phytoplankton are known to bioconcentrate MeHg from seawater (Mason et al., 1996), and zooplankton bioaccumulate it directly from seawater and by trophic transfer through their diet (Lee & Fisher, 2017; Pućko et al., 2014); as a result, higher phytoplankton and zooplankton MeHg concentrations have been linked to higher seawater MeHg concentrations (Schartup et al., 2017). Among the three most important herbivores in Arctic waters, *Calanus hyperboreus* and *C. finmarchicus* are concentrated in shallow water (<300 m) except during winter, whereas *C. glacialis* spend all life stages in the top 300 m (Darnis & Fortier, 2012; Falk-Petersen et al., 2009). The amphipod consumers of these *Calanus* species, *Themisto* spp., also inhabit shallow waters (Dalpadado et al., 2001), as does Arctic cod (*Boreogadus saida*, <500 m), key species in the Arctic marine food web (Majewski et al., 2016). Given that the MeHg-enriched waters lie within the main habitat of low trophic level marine biota in these waters, spatial variations in MeHg concentrations within the subsurface zone can readily explain the higher biotic Hg concentrations in the western compared to the eastern regions of the section.

Therefore, to understand what controls Arctic biotic Hg distributions and predict future conditions, characterization of atmospheric and terrestrial sources of inorganic Hg

inputs to the Arctic Ocean is not sufficient. Detailed investigations will be required to identify processes controlling the production and loss of MeHg associated with the upper halocline waters of the western Arctic Ocean and how these processes respond to the changing climate. The subsurface seawater MeHg maximum in the oceans is typically attributed to in-situ MeHg production associated with organic matter remineralization (Cossa et al., 2009; Heimbürger et al., 2015; Sunderland et al., 2009; Wang et al., 2012). In the central Arctic Ocean, Heimbürger et al. (2015) suggested that sinking particles are slowed down at the shallow pycnocline where they undergo remineralization and stimulate in-situ MeHg production. It remains unclear what microbial or abiotic processes are responsible for Hg methylation at such shallow depths where dissolved oxygen is well above 75% of the saturation value (Figure 2-S2). Alternatively, the MeHg maximum in the upper halocline in the western Canadian Arctic could be supported by isopycnal transport, along with the metabolite-enriched upper halocline waters, from sediments of the productive Chukchi and Beaufort Shelves (Anderson et al., 2013). Understanding the risk of MeHg to the Arctic marine ecosystem and Indigenous Peoples will thus require an elucidation of the processes that generate and maintain the subsurface seawater MeHg maximum.

Methods

Seawater sampling and analyses were carried out following ultraclean techniques recommended for the GEOTRACES program (Cutter & Bruland, 2012; Lamborg et al., 2012). Seawater was collected onboard the Canadian Research Icebreaker CCGS Amundsen in pre-cleaned, 12-L Teflon-coated Go-Flo bottles mounted on a Trace Metal-

Clean Rosette System. Following rosette retrieval, the Go-Flo bottles were promptly moved to a clean laboratory van where seawater for Hg_T and MeHg analyses was collected into pre-cleaned, 250-mL amber glass bottles (Hammerschmidt et al., 2011). Immediately after collection, the seawater samples were acidified with 0.5% (v:v) ultraclean acid (CMOS grade JT Baker HCl for Hg_T, and trace metal clean grade Fisher Scientific H_2SO_4 for MeHg) and stored at 4 °C until analysis. The acidification breaks down dimethylmercury (DMHg) to monomethylmercury (MMHg) (Black et al., 2009) and, thus, the MeHg reported herein represents the sum of MMHg and DMHg.

Within 48 hr of sampling, Hg_T was analyzed in the Portable In-situ Laboratory for Mercury Speciation (PILMS) onboard the icebreaker (http://www.amundsen.ulaval.ca/capacity/portable-insitu-lab-mercury-speciation.php). The analysis was carried out on a Tekran 2600 Hg analyzer following U.S EPA Method 1631, which involves BrCl oxidation, $SnCl_2$ reduction, gold trap pre-concentration and measurement by cold vapor atomic fluorescence spectrometry (CVAFS). Water samples were analyzed for MeHg at the PILMS or at the Ultra-Clean Trace Elements Laboratory (UCTEL) at the University of Manitoba. Concentrations of MeHg were measured on an automated MeHg analyzer (MERX-M, Brooks Rand) following an adapted ascorbic acid-assisted direct ethylation method (Munson et al., 2014), which involves ethylation, Tenax trap pre-concentration, gas chromatographic separation and CVAFS quantification. The original method (Munson et al., 2014) was modified for use with ~40-mL sample volumes using acetate buffers to adjust pH. Daily calibration curves were prepared by adding standards solutions to filtered seawater to improve recovery from the seawater matrix. The detection limit (DL) was estimated at 0.25 pM and 0.014 pM for Hg_T and

MeHg, respectively, as three times the standard deviation of seven laboratory blank replicates. Whenever seawater was sampled, Milli-Q water was collected in pre-cleaned 250-mL amber glass bottles to serve as field blanks, the concentrations of which were always lower than the DL for both Hg_T and MeHg. Certified reference seawater BCR579 (9.5 ± 2.5 pmol kg^{-1} or 9.7 ± 2.5 pM when corrected for density, Institute for Reference Materials and Measurements, European Commission - Joint Research Centre) was analyzed for Hg_T and the recovery was 93–116%. Since no certified reference seawater is available for MeHg, a 0.01 pmol MMHg spike was used during sample analysis and its recovery was 87–114%.

Seawater fluorescence was measured in real-time with a chlorophyll fluorometer (Seapoint) installed on the rosette. To calibrate the fluorometer output, discrete seawater samples were measured for chlorophyll-α fluorescence concentrations.

Data Availability

The datasets generated during and/or analyzed during the current study are available from the corresponding author on reasonable request.

References

AMAP (2011). AMAP Assessment 2011: Mercury in the Arctic. Arctic Monitoring and Assessment Program: Oslo.

Anderson, L. G., Andersson, P. S., Björk, G., Peter Jones, E., Jutterström, S., & Wåhlström, I. (2013). Source and formation of the upper halocline of the Arctic Ocean. Journal of Geophysical Research: Oceans 118, 410-421.

Baya, P. A., Gosselin, M., Lehnherr, I., St. Louis, V. L., & Hintelmann, H. (2015). Determination of monomethylmercury and dimethylmercury in the Arctic marine boundary layer. Environmental Science & Technology 49, 223-232.

Black, F. J., Conaway, C. H., & Flegal, A. R. (2009). Stability of dimethyl mercury in seawater and its conversion to monomethyl mercury. Environmental Science & Technology 43, 4056-4062.

Brown, T. M., Fisk, A. T., Wang, X., Ferguson, S. H., Young, B. G., Reimer, K. J., & Muir, D. C. (2016). Mercury and cadmium in ringed seals in the Canadian Arctic: Influence of location and diet. Science of the Total Environment 545, 503-511.

Brown, T. M., Macdonald, R. W., Muir, D. C., & Letcher, R. J. (2018). The distribution and trends of persistent organic pollutants and mercury in marine mammals from Canada's Eastern Arctic. Science of the Total Environment 618, 500-517.

Cossa, D., Averty, B., & Pirrone, N. (2009). The origin of methylmercury in open Mediterranean waters. Limnology and Oceanography 54, 837-844.

Cossa, D., Harmelin-Vivien, M., Mellon-Duval, C., Loizeau, V., Averty, B., Crochet, S., Chou, L., Cadiou, J.-F. (2012). Influences of bioavailability, trophic position, and growth on methylmercury in hakes (Merluccius merluccius) from northwestern Mediterranean and northeastern Atlantic. Environmental Science & Technology 46, 4885-4893.

Cossa, D., Heimbürger, L., Sonke, J., Planquette, H., Lherminier, P., García-Ibáñez, M., Pérez, F. F., Sarthou, G. (2018). Sources, cycling and transfer of mercury in the Labrador Sea (Geotraces-Geovide cruise). Marine Chemistry 198, 64-69.

Cutter, G. A., & Bruland, K. W. (2012). Rapid and noncontaminating sampling system for trace elements in global ocean surveys. Limnology and Oceanography: Methods 10, 425-436.

Dalpadado, P., Borkner, N., Bogstad, B., & Mehl, S. (2001). Distribution of Themisto (Amphipoda) spp. in the Barents Sea and predator-prey interactions. ICES Journal of Marine Science 58, 876-895.

Darnis, G., & Fortier, L. (2012). Zooplankton respiration and the export of carbon at depth in the Amundsen Gulf (Arctic Ocean). Journal of Geophysical Research: Oceans 117(C4).

Dietz, R., Sonne, C., Basu, N., Braune, B., O'Hara, T., Letcher, R.J., Scheuhammer, T., Andersen, M., Andreasen, C., and Andriashek, D. (2013). What are the toxicological effects of mercury in Arctic biota? Science of the Total Environment 443, 775-790.

Falk-Petersen, S., Mayzaud, P., Kattner, G., & Sargent, J. R. (2009). Lipids and life strategy of Arctic Calanus. Marine Biology Research 5, 18-39.

Fisher, J. A., Jacob, D. J., Soerensen, A. L., Amos, H. M., Steffen, A., & Sunderland, E. M. (2012). Riverine source of Arctic Ocean mercury inferred from atmospheric observations. Nature Geoscience 5, 499-504.

Graydon, J. A., Emmerton, C. A., Lesack, L. F., & Kelly, E. N. (2009). Mercury in the Mackenzie River delta and estuary: Concentrations and fluxes during open-water conditions. Science of the Total Environment 407, 2980-2988.

Hammerschmidt, C. R., Bowman, K. L., Tabatchnick, M. D., & Lamborg, C. H. (2011). Storage bottle material and cleaning for determination of total mercury in seawater. Limnology and Oceanography: Methods 9, 426-431.

Heimbürger, L.-E., Sonke, J.E., Cossa, D., Point, D., Lagane, C., Laffont, L., Galfond, B.T., Nicolaus, M., Rabe, B., and van der Loeff, M.R. (2015). Shallow methylmercury production in the marginal sea ice zone of the central Arctic Ocean. Scientific Reports 5, 10318.

Johnson, K. P., Blum, J. D., Keeler, G. J., & Douglas, T. A. (2008). Investigation of the deposition and emission of mercury in arctic snow during an atmospheric mercury depletion event. Journal of Geophysical Research: Atmospheres 113(D7).

Kirk, J. L., St. Louis, V. L., Hintelmann, H., Lehnherr, I., Else, B., & Poissant, L. (2008). Methylated mercury species in marine waters of the Canadian high and sub Arctic. Environmental Science & Technology 42, 8367-8373.

Lamborg, C. H., Hammerschmidt, C. R., Gill, G. A., Mason, R. P., & Gichuki, S. (2012). An intercomparison of procedures for the determination of total mercury in seawater and recommendations regarding mercury speciation during GEOTRACES cruises. Limnology and Oceanography: Methods 10, 90-100.

Lee, C. S., & Fisher, N. S. (2017). Bioaccumulation of methylmercury in a marine copepod. Environmental Toxicology and Chemistry 36, 1287-1293.

Lehnherr, I., Louis, V. L. S., Hintelmann, H., & Kirk, J. L. (2011). Methylation of inorganic mercury in polar marine waters. Nature Geoscience 4, 298-302.

Leitch, D. R., Carrie, J., Lean, D., Macdonald, R. W., Stern, G. A., & Wang, F. (2007). The delivery of mercury to the Beaufort Sea of the Arctic Ocean by the Mackenzie River. Science of the Total Environment 373, 178-195.

Majewski, A. R., Walkusz, W., Lynn, B. R., Atchison, S., Eert, J., & Reist, J. D. (2016). Distribution and diet of demersal Arctic Cod, Boreogadus saida, in relation to habitat characteristics in the Canadian Beaufort Sea. Polar Biology 39, 1087-1098.

Mason, R. P., Reinfelder, J. R., & Morel, F. M. (1996). Uptake, toxicity, and trophic transfer of mercury in a coastal diatom. Environmental Science & Technology 30, 1835-1845.

Munson, K. M., Babi, D., & Lamborg, C. H. (2014). Determination of monomethylmercury from seawater with ascorbic acid assisted direct ethylation. Limnology and Oceanography: Methods 12, 1-9.

Obrist, D., Agnan, Y., Jiskra, M., Olson, C.L., Colegrove, D.P., Hueber, J., Moore, C.W., Sonke, J.E., and Helmig, D. (2017). Tundra uptake of atmospheric elemental mercury drives Arctic mercury pollution. Nature 547, 201-204.

Pomerleau, C., Stern, G. A., Pućko, M., Foster, K. L., Macdonald, R. W., & Fortier, L. (2016). Pan-Arctic concentrations of mercury and stable isotope ratios of carbon (δ 13 C) and nitrogen (δ 15 N) in marine zooplankton. Science of the Total Environment 551, 92-100.

Pućko, M., Burt, A., Walkusz, W., Wang, F., Macdonald, R., Rysgaard, S., Barber, D., Tremblay, J.-É., and Stern, G. (2014). Transformation of mercury at the bottom of the Arctic food web: An overlooked puzzle in the mercury exposure narrative. Environmental Science & Technology 48, 7280-7288.

Routti, H., Letcher, R.J., Born, E.W., Branigan, M., Dietz, R., Evans, T.J., Fisk, A.T., Peacock, E., and Sonne, C. (2011). Spatial and temporal trends of selected trace elements in liver tissue from polar bears (Ursus maritimus) from Alaska, Canada and Greenland. Journal of Environmental Monitoring 13, 2260-2267.

Schartup, A. T., Qureshi, A., Dassuncao, C., Thackray, C. P., Harding, G., & Sunderland, E. M. (2017). A Model for Methylmercury Uptake and Trophic Transfer by Marine Plankton. Environmental Science & Technology 52, 654–662.

Schlitzer, R. Ocean Data View. odv.awi.de (2018).

Schroeder, W., Anlauf, K., Barrie, L., Lu, J., Steffen, A., Schneeberger, D., & Berg, T. (1998). Arctic springtime depletion of mercury. Nature 394, 331-332.

Schuster, P.F., Schaefer, K.M., Aiken, G.R., Antweiler, R.C., Dewild, J.F., Gryziec, J.D., Gusmeroli, A., Hugelius, G., Jafarov, E., and Krabbenhoft, D.P. (2018). Permafrost stores a globally significant amount of mercury. Geophysical Research Letters 45, 1463-1471.

Soerensen, A.L., Jacob, D.J., Schartup, A., Fisher, J.A., Lehnherr, I., St Louis, V.L., Heimbürger, L.E., Sonke, J.E., Krabbenhoft, D.P., and Sunderland, E.M. (2016). A Mass Budget for Mercury and Methylmercury in the Arctic Ocean. Global Biogeochemical Cycles 30, 560-575.

St. Louis, V.L., Derocher, A.E., Stirling, I., Graydon, J.A., Lee, C., Jocksch, E., Richardson, E., Ghorpade, S., Kwan, A.K., and Kirk, J.L. (2011). Differences in mercury bioaccumulation between polar bears (Ursus maritimus) from the Canadian high-and sub-Arctic. Environmental Science & Technology 45, 5922-5928.

Sunderland, E. M., Krabbenhoft, D. P., Moreau, J. W., Strode, S. A., & Landing, W. M. (2009). Mercury sources, distribution, and bioavailability in the North Pacific Ocean: Insights from data and models. Global Biogeochemical Cycles 23, 1-14.

Wagemann, R., Innes, S., & Richard, P. (1996). Overview and regional and temporal differences of heavy metals in Arctic whales and ringed seals in the Canadian Arctic. Science of the Total Environment 186, 41-66.

Wang, F., Macdonald, R. W., Armstrong, D. A., & Stern, G. A. (2012). Total and Methylated Mercury in the Beaufort Sea: The Role of Local and Recent Organic Remineralization. Environmental Science & Technology 46, 11821-11828.

Acknowledgements

This work was supported by funding from Natural Science and Engineering Research Council (NSERC) of Canada, ArcticNet, the Canadian Arctic GEOTRACES program, and the Canada Research Chairs Program. We thank W. Xu, A. Elliott, J. Li, M. Colombo, P. Chandan, J. Cullen, Z. Gao, D. Janssen, D. Semienuk, K. Orians, K. Purdon, S. L. Jackson, and R. Fox for rosette sample collection; R. François, J. Cullen, P. Tortell, K. Orians, and K. Brown for organizing the sampling activities; D. Armstrong, M. Soon, and K. Levesque for assistance with logistics; as well as the captains and crew of the Canadian Research Icebreaker CCGS Amundsen. We are grateful to R. Letcher for providing a digital version of polar bear Hg data.

Competing Interests: The authors declare no competing interests.

Publisher's note: Springer Nature remains neutral with regard to jurisdictional claims in published maps and institutional affiliations.

Supplementary Information

Table 2-S1: Detailed information of the stations sampled during the 2015 Canadian Arctic GEOTRACES campaign.

Station	Latitude	Longitude	Water Depth	Sampling Date
K1	56.124°N	53.377°W	3312m	07/14/2015
BB1	66.856°N	59.058°W	1040m	08/03/2015
BB2	72.753°N	67.001°W	2371m	08/09/2015
BB3	71.409°N	68.598°W	1272m	08/06/2015
CAA1	74.521°N	80.611°W	636m	08/10/2015
CAA2	74.321°N	80.499°W	702m	08/10/2015
CAA3	73.984°N	80.465°W	690m	08/11/2015
CAA4	74.123°N	91.521°W	193m	08/14/2015
CAA5	74.533°N	90.802°W	259m	08/13/2015
CAA6	74.761°N	97.433°W	260m	08/15/2015
CAA7	73.666°N	96.552°W	219m	08/15/2015
CAA8	74.139°N	108.837°W	563m	09/23/2015
CAA9	76.331°N	96.754°W	336m	09/26/2015
CB1	75.118°N	120.628°W	466m	09/07/2015
CB2	75.799°N	129.247°W	1365m	09/08/2015
CB3	76.990°N	140.036°W	3731m	09/12/2015
CB4	74.999°N	149.987°W	3830m	09/16/2015

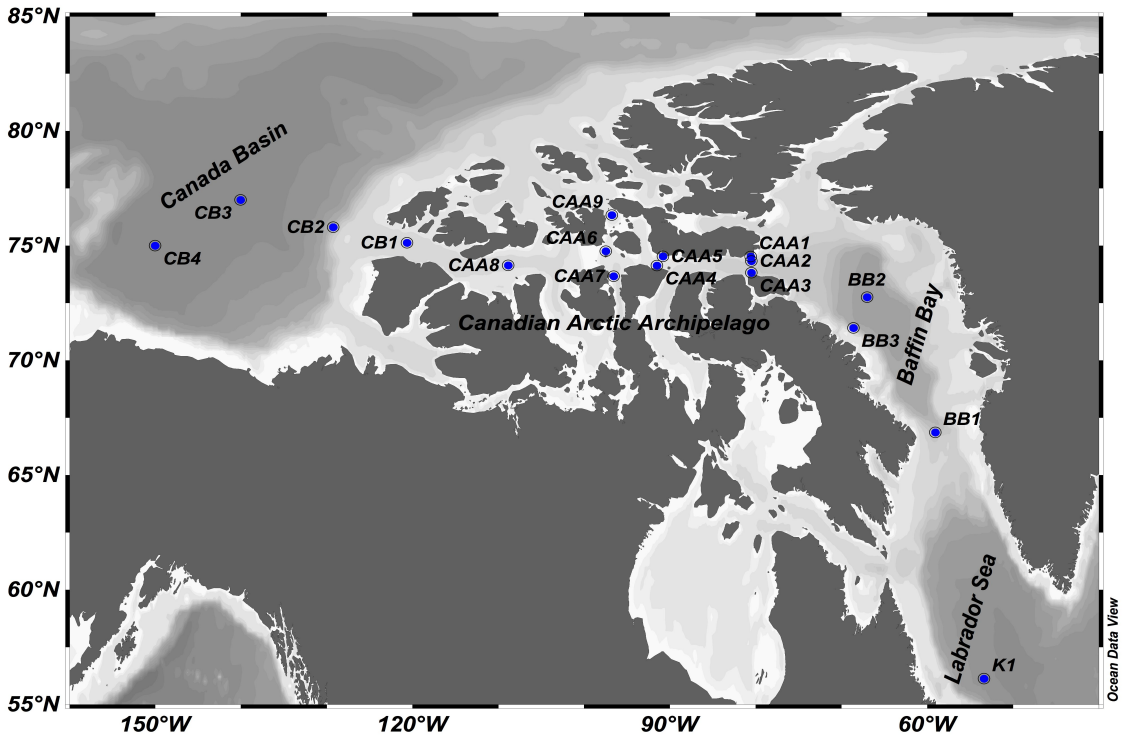

Figure 2-S1: Location map of sampling stations during 2015 Canadian Arctic GEOTRACES Cruises.

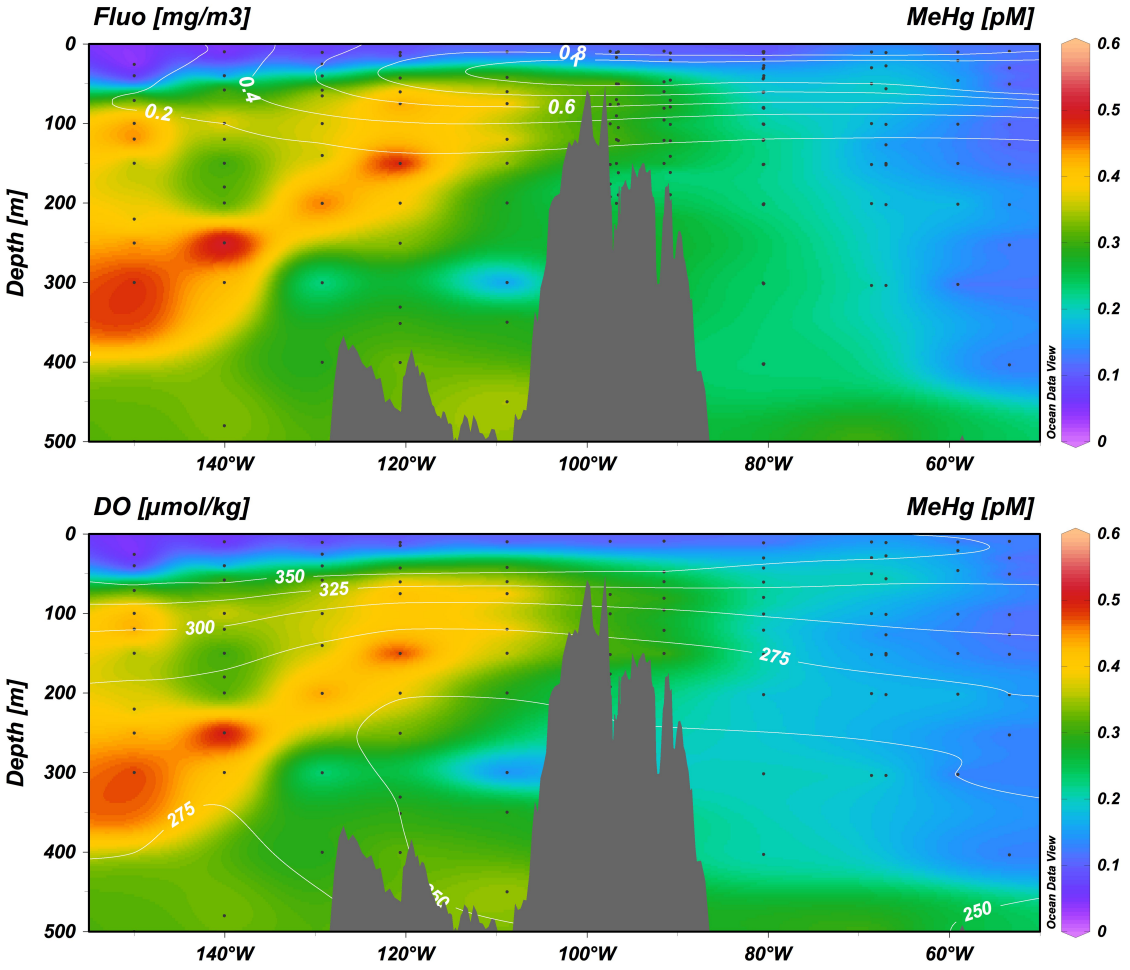

Figure 2-S2: Distributions of methylmercury (MeHg, color coded) overlaid with the contours of the chlorophyll-α fluorescence (Fluo, top) and dissolved oxygen (DO, bottom) in the upper 500 m seawater across the Canadian Arctic and Labrador Sea.

Chapter 3: Determining Seawater Mercury Methylation and Demethylation Rates by the Seawater Incubation Approach: A Critique

Abstract

The discovery of a subsurface methylmercury (MeHg) maximum in the Arctic and in global oceans highlights the importance of understanding the production and loss of MeHg in seawater. However, the rates of in-situ mercury (Hg) methylation and demethylation in seawater are poorly known. Two different approaches have been used: the earlier one was based on the spatial distribution of MeHg and other Hg species in seawater, whereas recent studies favored seawater incubation studies with the addition of isotope enriched Hg species. The reaction rates determined by these approaches differ by several orders of magnitude. When determining Hg methylation and demethylation rates in Arctic seawater using the seawater incubation approach, we observed major issues, including unexplainable methylation and demethylation at time zero and poor data fitting. A critical analysis of previous incubation studies showed similar deficiencies, especially when the Hg was added at low concentrations to resemble ambient seawater conditions. This raises questions concerning the validity of the Hg methylation and demethylation rates determined by the seawater incubation approach, and calls for the development of alternative methods in determining these important rate constants in seawater.

3.1 Introduction

Humans are exposed to mercury (Hg) mainly through consumption of marine products, where Hg is primarily in the form of monomethylmercury (MMHg) (Mason et al., 2012; Sunderland, 2007). Marine animals accumulate MMHg from their prey, and ultimately from seawater (Schartup et al., 2017). In the world ocean, maximum concentrations of methylated Hg (MeHg, sum of MMHg and dimethylmercury (DMHg)) are typically found in subsurface waters and within the net organic matter (OM) remineralization zone (Cossa et al., 2009; Cossa et al., 2011; Mason and Fitzgerald, 1990; Sunderland et al., 2009). In the Arctic, subsurface MeHg enrichment has been found to occur at much shallower depths, just below the productive surface waters (Heimbürger et al., 2015; Wang et al., 2012; Wang et al., 2018). This provides an efficient pathway for MeHg bioaccumulation (Heimbürger et al., 2015), and explains the spatial trend of biotic Hg in the Arctic (Wang et al., 2018). However, the processes responsible for the subsurface MeHg enrichment remain poorly known. Most studies attribute it to in-situ methylation of inorganic Hg(II) in the water column, and the methylation process appears to be associated with OM remineralization (Cossa et al., 2009; Cossa et al., 2011; Mason and Fitzgerald, 1990; Heimbürger et al., 2015; Sunderland et al., 2009; Wang et al., 2012). Another process determining MeHg concentrations is demethylation, which can occur microbially, photolytically, or via other abiotic processes (DiMento and Mason, 2017; Monperrus et al., 2007; Munson et al., 2018). Understanding Hg methylation and demethylation has important implications in predicting the seawater MeHg distribution in future conditions and better assessing the risks of MeHg exposure to the marine ecosystem. However, our knowledge on both processes is insufficient and limited. In

particular, the reaction rates estimated vary widely and the reaction mechanisms remain poorly known.

Two approaches have been used to estimate the rates of Hg methylation and demethylation in seawater. Based on the distributions of Hg species in the North Atlantic Ocean and Equatorial Pacific Ocean, earlier studies estimated that the production and loss rates were 5×10^{-5} d^{-1} and 2×10^{-4} d^{-1} for DMHg, and 2×10^{-4} d^{-1} and $(0.5–5.0) \times 10^{-3}$ d^{-1} for MMHg, respectively (Mason et al., 1995; Mason and Fitzgerald, 1993). However, methylation and demethylation are not the only processes responsible for the rates of change, and MMHg concentration is by other processes such as particle scavenging. The second approach involves incubation of seawater with additions of Hg species typically labeled with stable isotopes (Lehnherr et al., 2011; Mason and Sullivan, 1999; Monperrus et al., 2007; Munson, 2014; Munson et al., 2018; Whalin et al., 2007). The methylation rates (k_m, <0.0002 to 0.13 d^{-1}) and demethylation rates (k_d, 0.01 to 1.64 d^{-1}) determined from these incubation studies are up to four orders of magnitude higher than those from the first approach. Several studies have observed problems that were difficult to explain when using the seawater incubation approach to determine Hg methylation and demethylation rates. For instance, methylation and demethylation were observed immediately after the Hg addition (Lehnherr et al., 2011; Munson, 2014; Munson et al., 2018), and the transformations were found in time zero (t_0) samples preserved with acid even prior to the Hg addition (Munson, 2014). The initial methylation and demethylation are unexpected, and can lead to inaccuracies in the rate estimation. Furthermore, in incubation studies methylation and demethylation are typically estimated based on a first-order kinetics, even though the data may not follow a first-order kinetics (Munson, 2014;

Munson et al., 2018; Whalin et al., 2007).

Seawater incubation studies were also used to investigate mechanisms of methylation and demethylation. Earlier incubation studies assume methylation is due to microbial activities (Lehnherr et al., 2011; Monperrus et al., 2007), whereas recent studies suggest that abiotic methylation might play an important role (Munson, 2014; Munson et al., 2018). For demethylation in the euphotic zone, most studies agree that the process is driven by photolysis with some contributions from microbial decomposition (DiMento and Mason, 2017; Lehnherr et al., 2011; Monperrus et al., 2007; Whalin et al., 2007). For demethylation in the aphotic zone, both microbial (Lehnherr et al., 2011; Monperrus et al., 2007; Whalin et al., 2007) and abiotic (Munson, 2014; Munson et al., 2018) demethylation processes have been implied. In either case, the roles of biotic and abiotic mechanisms in methylation and demethylation have not been assessed systematically, as these studies employed unfiltered (Lehnherr et al., 2011; Mason and Sullivan, 1999) or filtered (Monperrus et al., 2007; Munson, 2014; Munson et al., 2018) seawater in which biological activities could not be ruled out.

In the present study, seawater incubation studies were conducted in marine waters collected from different stations across the Canadian Arctic. Modifications were made with the aim to study both the methylation and demethylation mechanisms and to determine their reaction rates. The modifications included measurements at t_0 to examine the initial methylation and demethylation, high temporal resolution measurements to test whether the reactions follow first-order kinetics, and use of sterilized seawater as a control to differentiate biotic and abiotic processes. Results from our incubation studies were compared to literature studies to test the validity of the seawater incubation

approach in determining the methylation and demethylation rates.

3.2 Material and Methods

3.2.1 Study Sites and Sampling

As part of the ArcticNet/Canadian Arctic GEOTRACES cruises, we carried out seawater incubation experiments with Hg isotope additions onboard the Canadian research icebreaker CCGS *Amundsen* in August and September 2015 (Figure 3-1). Seawater for incubations was collected from three stations in the Canadian Arctic: station BB2 in Baffin Bay (depth: 2369 m) and station CB4 in the Canada Basin (depth: 3578 m) represent open ocean conditions, and station CAA5 in the Canadian Arctic Archipelago (depth: 254 m) represents shallow, coastal conditions. In these regions, at least three water masses can be distinguished: the Polar Mixed Layer at the surface (<50 m), the Pacific Halocline Water at intermediate depths (~50–200 m), and the Atlantic Water at deeper depths (>200 m) (Mclaughlin et al., 2004).

Seawater was collected from Teflon coated Go-Flo bottles (12 L) mounted on a trace metal clean rosette system aboard the icebreaker. Dissolved oxygen (DO) was measured in-situ with an oxygen probe attached to the rosette system, and calibrated against Winkler titrations at more than two discrete data points per cast (Table 3-1). Immediately after the rosette was recovered from seawater, the Go-Flo bottles were moved to a clean laboratory van, where seawater from different depths was decanted to pre-cleaned glass carboys (2.5 L), which were rinsed three times with the water to be sampled. To prevent potential cross-contamination, the clean-hands-dirty-hands protocol was followed during the sampling process (Fitzgerald, 1999). At all three stations,

incubation seawater was collected at a depth of 150 m, where MeHg typically peaks in the Arctic (Heimbürger et al., 2015; Wang et al., 2012; Wang et al., 2018). At CB4, seawater for incubations was also collected at the subsurface chlorophyll maximum (SCM) depth (70 m) where there is abundant biological activity, and at the 500 m depth to represent the intermediate water.

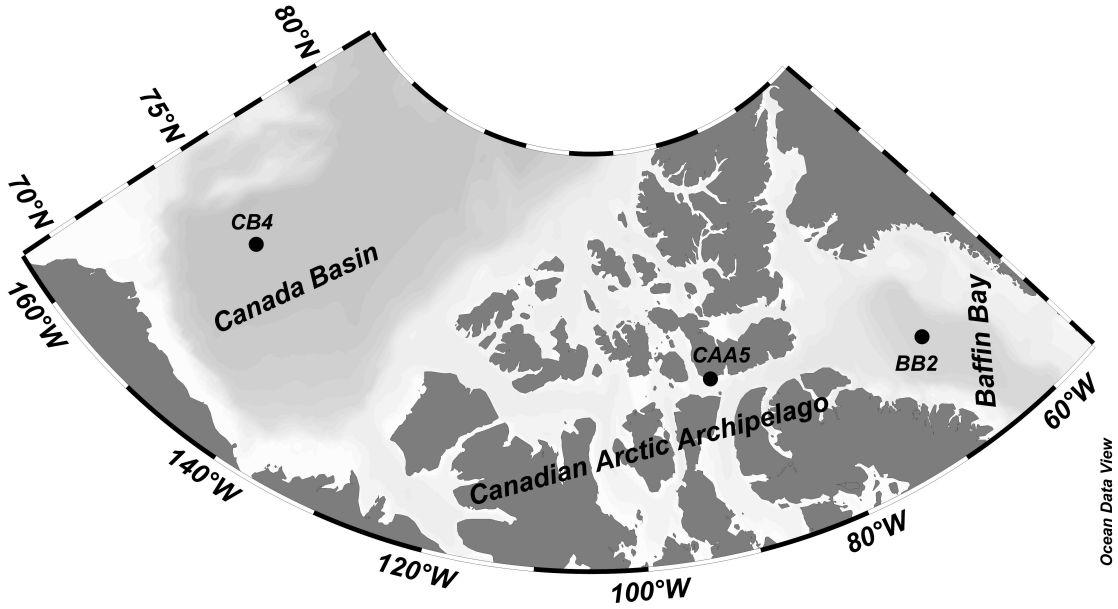

Figure 3-1: Location map of stations where seawater was collected for for incubation experiments.

Table 3-1: Concentrations of ambient seawater Hg species and details of sampling stations in the Canadian Arctic.

Station	Latitude	Longitude	Date	Depth (m)	DO (µmol/Kg)	MeHg (ng/L)	Inorganic Hg(II) (ng/L)
BB2	72.752°N	66.994°W	08/09/2015	150	312	0.03	0.46
CAA5	74.533°N	90.802°W	08/13/2015	150	267	0.03	0.31
CB4	74.999°N	149.987°W	09/15/2015	70	356	0.09	0.35
				150	286	0.12	0.24
				500	279	0.06	0.30

3.2.2 Incubation Experiments

The stock solutions of isotopically labeled inorganic $^{202}Hg(II)$ and $MM^{198}Hg$ were prepared separately. For inorganic $^{202}Hg(II)$, the stock solution ($^{202}Hg(NO_3)_2$, 100 mg/L) was prepared by dissolving 10 mg of elemental ^{202}Hg (Trace Sciences International Corp., ^{202}Hg composes >98% of all the Hg) in 5 mL of concentrated HNO_3 (trace metal clean grade, Sigma-Aldrich), which was then diluted with 95 ml Milli-Q water (Element Grade, Millipore) in a pre-cleaned 125 ml Teflon bottle. C. Lamborg provided the $MM^{198}Hg$ stock solution, which was prepared by methylating $Hg^{198}O$ (Oak Ridge National Laboratory, ^{198}Hg >93%) with methylcobalamin following the procedure described in Hintelmann and Ogrinc (2003). The stock solutions of both inorganic $^{202}Hg(II)$ and $MM^{198}Hg$ were double bagged and refrigerated (4 ºC) during storage and shipment to the icebreaker.

Prior to the incubation experiments, the seawater went through various treatments of filtration and/or sterilization (Figure 3-2) at the Portable *In-situ* Laboratory for Mercury Speciation onboard the icebreaker. Larger particles were removed by filtering the seawater through a 0.2 μm GH Polypro filter (Pall Laboratory, 47mm). Sterilization was done by heating the seawater to 121−127 ºC for 35 min in a sterilizer (All American Electric Sterilizer, 25X), to eliminate living organisms. Sterilization treatment was not applied to marine waters collected at the CB4 station.

To start incubation, seawater after various treatments was transferred into pre-cleaned amber, borosilicate glass bottles (250 mL). Inorganic $^{202}Hg(II)$ and $MM^{198}Hg$ were then added into the bottles to reach target concentrations of 2.5 ng/L and 0.5 ng/L, respectively. Immediately after the additions of isotopically enriched Hg species, the

incubation bottles were refrigerated at 4 ºC to mimic the dark cold conditions of the Arctic seawater (Lehnherr et al., 2011). Incubations were terminated with 0.5% (v/v) H_2SO_4 (trace metal clean grade, Fisher Scientific) at the time points of 0.5, 4, 12, 24 and 36 h (Figure 3-2). True t_0 samples were collected in the CB4 experiments, by terminating the incubations prior to the isotopic Hg addition (Figure 3-2). Most of the incubations were performed in triplicate. The samples were transported to the Ultra-Clean Trace Elements Laboratory (UCTEL) at the University of Manitoba for analysis.

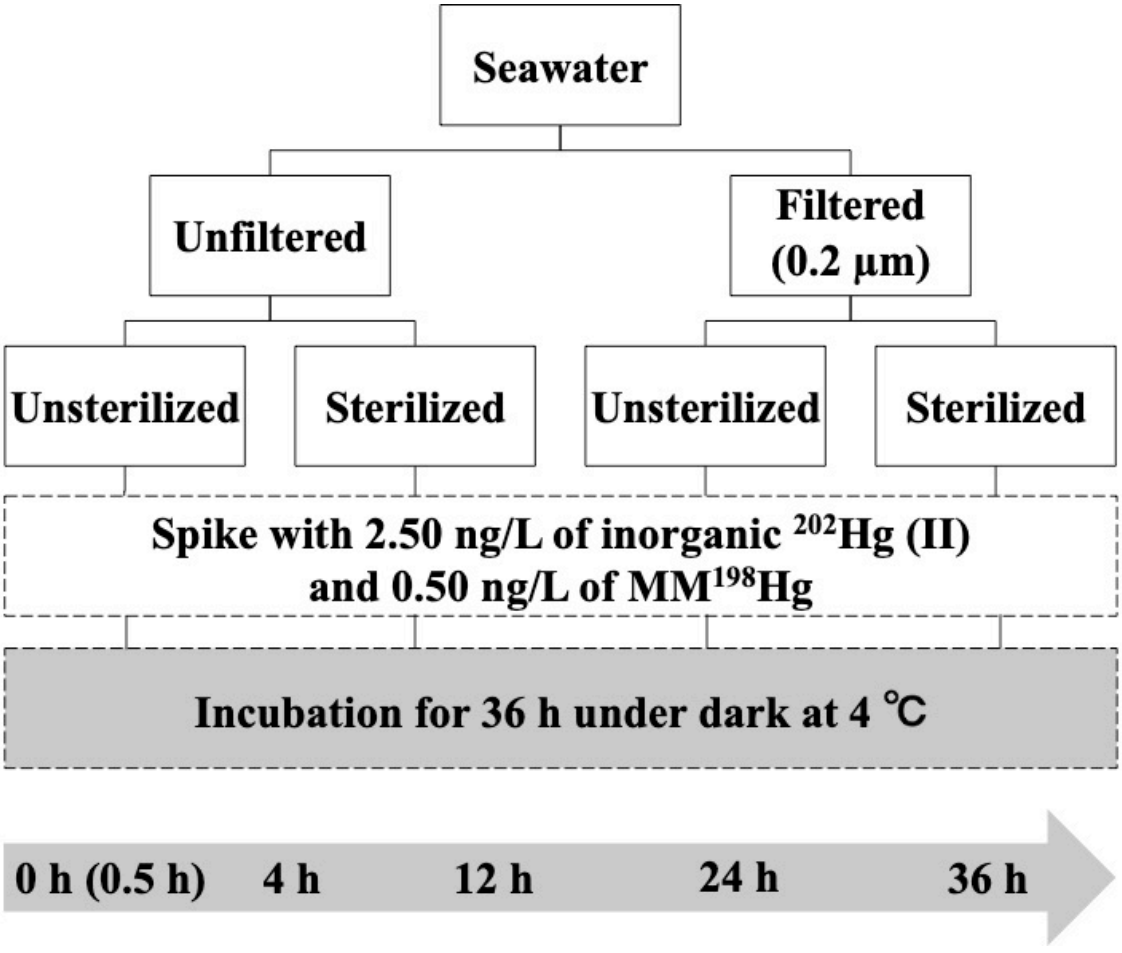

Figure 3-2: Flow chart of the procedures for seawater incubation experiments.

3.2.3 Analysis of Mercury Species Isotopes

For both inorganic Hg(II) and MMHg, the concentrations and isotopic abundances were measured at UCTEL. The analysis of inorganic Hg(II) and MMHg concentrations followed an adapted ascorbic acid-assisted direct ethylation method (Munson et al., 2014), which involves ethylation with $NaB(Et)_4$, Tenax trap pre-concentration, gas chromatographic separation, pyrolysis, and quantification of Hg species by cold-vapour atomic fluorescence spectroscopy (CVAFS) on an automated methylmercury analyzer (MERX-M, Brooks Rand) (U.S.EPA 1630). The Hg(0) exhausted from the MERX-M was introduced via a polyethylene line to an inductively-coupled plasma mass spectrometer (ICP-MS; PerkinElmer Elan DRC II) for the determination of Hg species-specific isotope abundance.

Typical calibration curves for the determination of inorganic Hg(II) and MMHg concentrations by CVAFS are shown in Figure 3-S1. Figure 3-S2 shows an example chromatogram of Hg isotopes by CVAFS-ICP-MS, with typical calibration curves for isotopic measurements of inorganic Hg(II) and MMHg given in Figure 3-S3. The isotopic abundances of the Hg species were quantified by integrating the relative counts of different isotopes peaks using MATLAB scripts. In this study, only three out of the seven Hg isotopes (202, 200, and 198) were quantified for further calculations.

3.2.4 Calculation for Mercury Methylation and Demethylation

The measured Hg isotopes were from three different sources: Hg in the ambient seawater and the two isotopically enriched Hg species added to incubation bottles. For example, the measured $MM^{202}Hg$ in a seawater sample at an incubation time t was

contributed from the ambient seawater $MM^{202}Hg$, the minor fraction of $MM^{202}Hg$ in the isotopically enriched $MM^{198}Hg$, and the $MM^{202}Hg$ methylated from the added inorganic $^{202}Hg(II)$. While IUPAC values were used as the isotopic ratios for ambient seawater Hg species, the isotopic ratios for the added Hg species were from direct measurements instead of values certified by manufacturers (Trace Sciences International Corp., and Oak Ridge National Laboratory) to prevent potential changes of isotope ratios during stock solution preparation (see Appendix for details). With a matrix inverse approach (Hintelmann and Evans, 1997; Hintelmann and Ogrinc, 2003), we calculated the contributions of different sources in the measured isotopes abundance of inorganic Hg(II) and MMHg (see Appendix for details). During the calculation, ^{200}Hg, ^{202}Hg and ^{198}Hg were used as tracer isotopes for ambient seawater Hg, added inorganic $^{202}Hg(II)$ and $MM^{198}Hg$, respectively.

With the Hg species converted from added Hg species known, potential Hg methylation and demethylation in incubations can thus be quantified. The methylation percentages during incubations were calculated by dividing the formed MMHg by the methylation substrate (detailed calculations are shown in Appendix). Here the Hg methylation substrate used was the sum of the added inorganic Hg(II) and produced MMHg, which were measured directly for different time points. In previous studies, the Hg methylation substrate used was inorganic Hg(II), which was quantified either by assuming the added inorganic Hg(II) remains constant (Monperrus et al., 2007), or estimating the available inorganic Hg(II) based on an exponential decrease observed in separate incubations (Lehnherr et al., 2011). The demethylation percentages in our incubations were estimated by quantifying the ratio of inorganic $^{198}Hg(II)$ to the added

$MM^{198}Hg$ (see Appendix for detailed calculation). The calculation was similar to that of Monperrus et al. (2007), which quantified the ratios of formed inorganic $^{201}Hg(II)$ to added $MM^{201}Hg$. In our study, the remaining $MM^{198}Hg$ and resulting $^{198}Hg(II)$ were summed to represent the added $MM^{198}Hg$ available for demethylation. Because the transformation rate of MMHg to Hg(0) is three orders of magnitude lower than that of MMHg to inorganic Hg(II) (Lehnherr et al., 2011), Hg(0) was not included as methylation substrate in our calculation. As DMHg quickly decomposes to MMHg in acidic conditions (Black et al., 2009), the MMHg measured in this study was the sum of MMHg and DMHg. Therefore, the potential Hg methylation here represents the overall conversion of inorganic Hg(II) to MeHg, whereas the potential demethylation represents the transformation of MMHg to inorganic Hg(II). In our incubations, neither methylation nor demethylation rates were quantified, because the time series data cannot be fit to first-order reaction curve.

3.2.5 Data Quality Assurance and Quality Control

When analyzing ambient seawater Hg species concentrations, the detection limit (DL) and lower limit of quantification (LLOQ) were calculated as three and ten times the standard deviation of seven laboratory blanks, respectively (Table 3-2). For isotope abundance analysis of Hg species, DL and LLOQ were calculated with the same method (Table 3-2). When collecting incubation samples, Milli-Q water was sampled into pre-cleaned 250-mL glass bottles to serve as field blanks. For both Hg species, the concentrations and isotope abundances in field blanks were lower than DL and LLOQ.

Table 3-2: Detection limit and lower limit of quantification of Hg isotopes in monomethylmercury (MMHg) and inorganic Hg(II).

		Detection limit		Lower Limit of quantification	
		MMHg	Inorganic Hg(II)	MMHg	Inorganic Hg(II)
Hg concentration		0.003 ng/L	0.05 ng/L	0.009 ng/L	0.17 ng/L
Hg isotopes	^{198}Hg	0.08 pg	0.29 pg	0.28 pg	0.97 pg
	^{200}Hg	0.18 pg	0.68 pg	0.60 pg	2.27 pg
	^{202}Hg	0.24 pg	0.88 pg	0.80 pg	2.93 pg

3.3 Results

3.3.1 Methylation

Our attempt to determine Hg methylation in Arctic seawater was not successful due to measurement uncertainties at the very low concentrations of MM^{202}Hg methylated from the added inorganic ^{202}Hg(II) in incubation experiments. The MM^{202}Hg concentrations in many incubated seawater samples were lower than the DL or LLOQ, and no samples had a MM^{202}Hg concentration higher than two times of LLOQ. At these low concentrations, the analytical uncertainties are large enough to result in negative values of methylated MM^{202}Hg concentrations and methylation percentages. The unrealistic negative values suggest that Hg methylation either did not occur or occurred at extremely slow rates. In the Canadian Arctic Archipelago, an earlier incubation study estimated a seawater Hg methylation rate of 0.0068 ± 0.0039 d^{-1} (0.0006−0.013 d^{-1}) (Lehnherr et al., 2011), which is at the lower end of k_m values reported from incubation studies with seawater from other oceans, such as the Mediterranean Sea (<0.0002−0.063 d^{-1}) (Monperrus et al., 2007), the Sargasso Sea (0.002−0.052 d^{-1}) (Munson, 2014), and the Central Tropical Pacific Ocean (0.002−0.042 d^{-1}) (Munson et al., 2018). In the Atlantic coastal region, no measureable seawater Hg methylation was observed in the incubations

(Whalin et al., 2007), probably also due to the higher DL and LLOQ and slow methylation rates (<0.086 d^{-1}).

3.3.2 Demethylation

In contrast to methylation, the inorganic ^{198}Hg produced from demethylation of $MM^{198}Hg$ in the incubation experiments was always above the LLOQ (ranging from 2.6 to 36.3 times LLOQ), confirming that demethylation of the added $MM^{198}Hg$ occurred in all the incubation experiments with seawater from all stations and depths and under all treatments (Figures 3-3 and 3-4). However, the demethylation from our incubation studies did not follow first-order kinetics (Figures 3-3 and 3-4), making it impossible to estimate a first-order demethylation rate constant. Instead, the demethylation in this study is reported as a demethylation percentage. As shown in Figures 3-3 and 3-4, the demethylation percentages are high (39.6 ± 15.2%, 10.5−80.0%) throughout the incubations.

In previous incubations, aquatic particles were reported to enhance MeHg demethylation, in either biotic or abiotic mechanisms (Monperrus et al., 2007; Munson, 2014; Munson et al., 2018). In our incubations with unsterilized seawater at all three stations, demethylation percentages do not show significant differences (t test, $p > 0.05$) in filtered and unfiltered waters (Figure 3-3, 3-4). In incubations with sterilized waters, however, the demethylation percentages are different in filtered and unfiltered waters. In the CAA5 incubations, the demethylation percentages are significantly higher (t test, $p < 0.0001$) in unfiltered seawater (55.9 ± 0.8%, 54.7−56.6%) than in filtered seawater (36.2 ± 5.5%, 28.3−41.5%), suggesting that particles may have enhanced demethylation. In the

BB2 incubations, however, demethylation percentages are significantly lower (t test, $p < 0.0001$) in unfiltered waters (39.0 ± 3.9%, 33.6−42.6%) than in filtered waters (56.3 ± 2.3%, 53.6−59.3%), suggesting an inhibitory effect by particles. The differences in demethylation percentages were observed in the initial stages, and maintained throughout the whole incubation period. Our results thus suggest that the presence of particles only affects abiotic demethylation of MMHg, although the process by which the particles affect demethylation remains unknown.

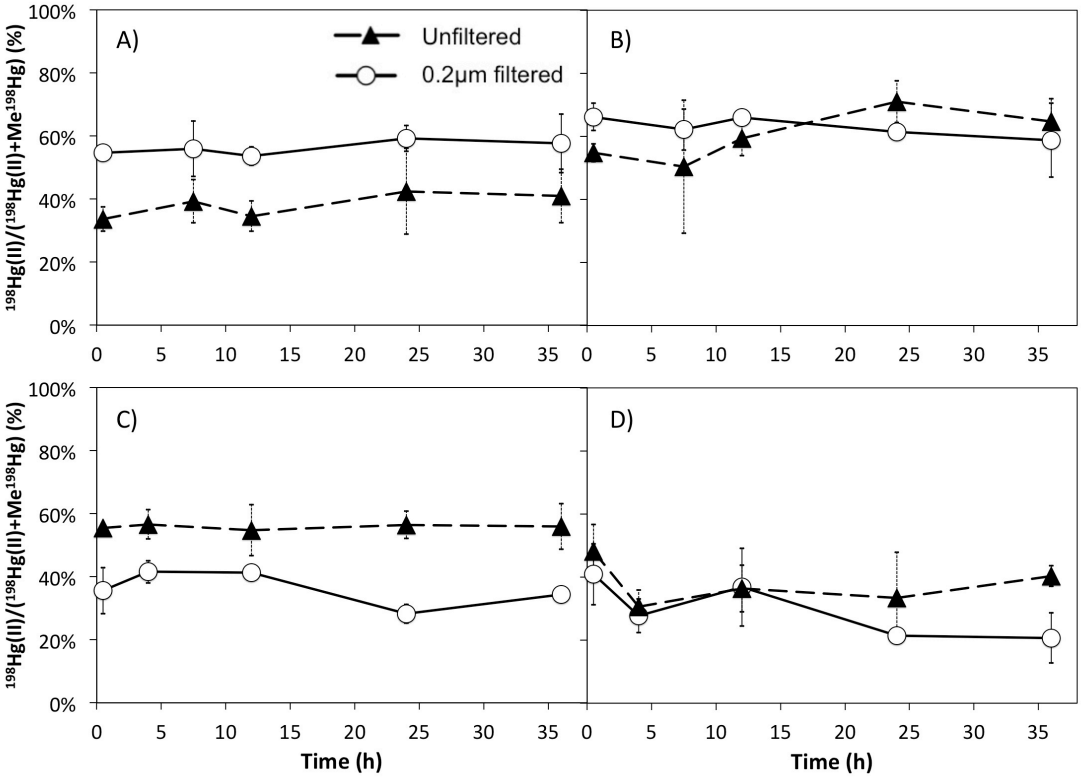

Figure 3-3: Demethylation of monomethylmercury (MMHg) in A) sterilized and B) unsterilized seawater from BB2 in Baffin Bay, as well as C) sterilized and D) unsterilized seawater from CAA5 in the Canadian Arctic Archipelago.

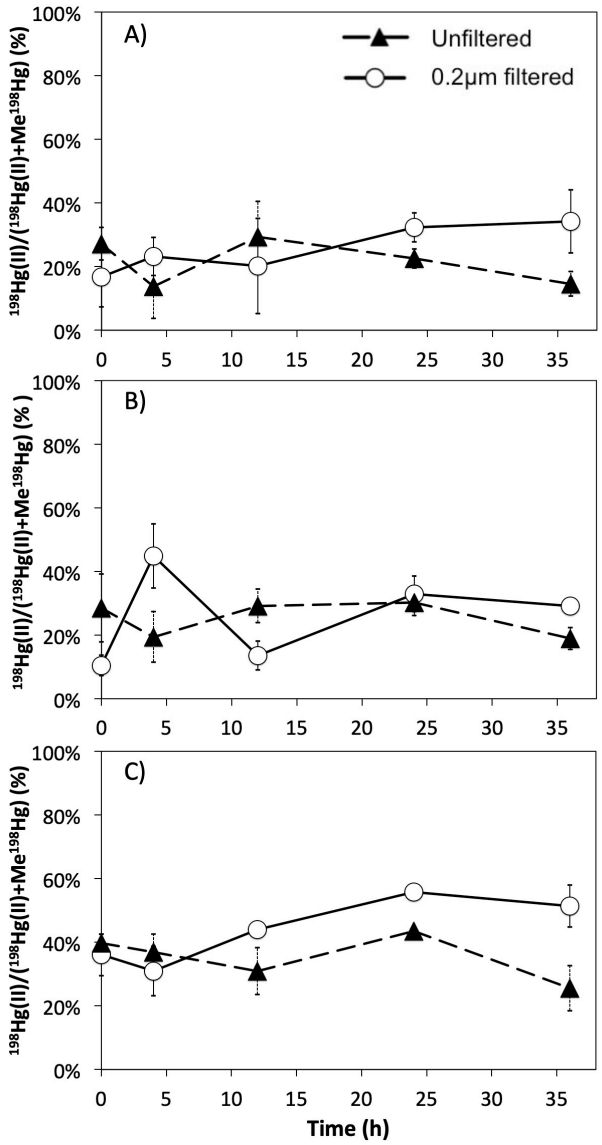

Figure 3-4: Demethylation of monomethylmercury (MMHg) in seawater from CB4 in Canada Basin at depth of A) 70 m (subsurface chlorophyll maximum), B) 150 m and C) 500 m.

3.4 Discussion

While we were not able to determine k_m and k_d from our incubation studies, k_m and k_d values were reported from several incubation studies in the literature (Table 3-3). However, a careful examination of these studies reveals some major deficiencies with the seawater incubation approach, including 1) unrealistically high concentrations of

inorganic Hg(II) added in the incubation study; 2) unexplainable Hg methylation and demethylation in the initial stage of incubation; and 3) unexplainable methylation and demethylation kinetics.

3.4.1 Unrealistically High Concentrations of Added Inorganic Mercury

The only other incubation study on k_m in Arctic seawater was conducted by Lehnherr et al. (2011). In their study, inorganic Hg(II) was added to seawater from the Canadian Arctic Archipelago to a target concentration of 76 ng/L, which was over two orders of magnitudes higher than that in the ambient Arctic seawater (0.21−0.56 ng/L). With the large amount inorganic Hg added, Lehnherr et al. (2011) was able to determine the amount of MMHg produced and thus k_m, but the extent to which this can be applied to the ambient Arctic seawater remains unknown.

Table 3-3: Detailed information of incubation studies that determined mercury methylation and demethylation in seawater.

Region	Month & year	Inorganic Hg(II) added (ng/L)	MMHg added (ng/L)	Time points (h)	Initial demethylation %	Does methylation follow first-order kinetics?	Does demethylation follow first-order kinetics?	References
The Canadian Arctic Archipelago	Sep−Oct 2007	76	0.05	~0.5, 12, 24	Not given	Yes[a]	Yes[a]	Lehnherr et al., 2011
The Central Tropical Pacific Ocean 0°, 8°N, 17°N	Oct 2011	0.35	0.11	0.5−2, 24	56−99%	N/A	N/A	Munson et al., 2018
The Central Tropical Pacific Ocean 12°S	Oct 2011	0.35	0.11	0.5−2, 3, 6, 12, 24, 36	56−99%	No	Yes, partially[b]	Munson et al., 2018
The Sargasso Sea	Apr 2012	0.44	0.14	≤2, 24	67−75%	N/A	N/A	Munson, 2014
The Sargasso Sea	Oct 2012	1.40	0.27	0, 0.5, 2, 4, 8, 12, 24	97−99%	No	Yes, partially[c]	Munson, 2014
The Mediterranean Sea	May & Jul 2005	1.0	0.1	24	Not measured	N/A	N/A	Monpperrus et al., 2007
The Atlantic Coastal Regions	May 2003 to Jul 2004	Not given	Not given	Not given	Not given	Not measurable	Yes, mixed[d]	Whalin et al., 2007
The Canada Arctic	Aug & Sep 2015	2.5	0.5	0 (0.5), 4, 12, 24, 36	10.5−66.1%	Not measurable	No	This study

[a] The methylation and demethylation time-series data only had two to three time points.

[b] Two out of four sets of demethylation time-series data were fit to first-order reaction curve, based on four or five of the six time points available.

[c] Two out of four sets of demethylation time-series data were fit to first-order reaction curve, based on three of the seven time points available.

[d] Three out of five sets of demethylation time-series data from dark incubations were fit to first-order reaction curve, but two of them only had three time points.

3.4.2 Unexplainable Initial Methylation and Demethylation

Several incubation studies observed rapid initial methylation immediately following the addition of inorganic (II) (Lehnherr et al., 2011; Munson et al., 2014, 2018; Monpperrus et al., 2007) (Table 3-3). To better examine the timeframe of this initial methylation, in the Sargasso Sea experiments (Munson, 2014), the incubations were stopped with the addition of H_2SO_4 before the inorganic $^{202}Hg(II)$ addition to collect true time zero (t_0) samples. Methylation was observed even in these t_0 samples, and the Hg methylation at t_0 accounted for a substantial fraction (up to 61%) of the total methylation after 24 h (Munson, 2014). In a separate incubation study with seawater from the Sargasso Sea, the methylation at t_0 was not measured; however, the Hg methylation within the first 2 h was sufficient to account for the total methylation over the 24-h incubations (Munson, 2014).

Lehnherr et al. (2011) attributed the initial methylation to abiotic mechanisms (Eckley and Hintelmann, 2005) such as methylation of inorganic Hg(II) by dead bacterial cells (Ramamoorthy et al., 1982). The rapid Hg methylation can also be explained by microbial mechanisms. In incubations with cultured sulfate- and iron-reducing bacteria, MMHg production was observed ~10 min after the inorganic Hg(II) addition (Schaefer et al., 2011). Another incubation with sulfate reducing bacteria demonstrated Hg methylation ~1 min after the addition of inorganic Hg(II) (Graham et al., 2012). However, none of these biotic and abiotic methylation mechanisms can explain the observed Hg methylation at t_0. Therefore, the methylation rates reported by previous studies are largely from the unexplainable t_0 Hg methylation, and cannot be used to reflect Hg methylation after time zero.

Similarly, initial demethylation was also observed in incubations in our current and previous studies (Tables 3-3 and 3-4). In our incubations, the initial demethylation percentages (39.1 ± 15.2%, 10.5−66.1%) were high enough to account for the total demethylation percentages observed over the 36-h incubations (39.1 ± 15.8%, 14.6−64.7%) (Table 3-4). In the BB2 and CAA5 incubations, the samples for initial demethylation were collected at 0.5 h after $MM^{198}Hg$ addition; in the CB4 incubations, the marine waters were acidified prior to addition of $MM^{198}Hg$, to collect the samples at true t_0. Once again, even at true t_0, considerable demethylation occurred (26.5 ± 10.2%). The significantly higher (t test, $p < 0.01$) demethylation percentages at time 0.5 h (48.5 ± 10.9%) than those at t_0 (26.5 ± 10.2%) were more likely due to the differences between incubated waters rather than continual demethylation after t_0, as suggested by the significantly higher (t test, $p < 0.05$) demethylation percentages after initial stages of the BB2 and CAA5 incubations (46.7 ± 13.8%) than those of the CB4 incubations (30.3 ± 8.9%). In previous studies, high initial demethylation percentages were also observed at both t_0 and shortly after the MMHg addition (Table 3-3). While the demethylation observed shortly after MMHg addition can possibly be attributed to biotic or abiotic degradation, the demethylation at t_0 was unexpected and could not be explained by known demethylation mechanisms. After the initial stage, the demethylation percentages stayed at similar levels over time (Figures 3-3 and 3-4). Therefore, the reaction rates must be low for the continual demethylation after the initial stage. The initial demethylation in previous incubations (Munson 2014; Munson et al., 2018) suggests that their demethylation rates have overestimated the reaction rates of continual demethylation.

Table 3-4: Demethylation percentages in marine waters from different stations across the Canadian Arctic.

Station	Depth	Filtration	Sterilization	Initial Demethylation %	Total Demethylation % at the End	% of Initial Demethylation in Total Demethylation
BB2	150 m	Unfiltered	Unsterilized	54.7	64.7	84.5
			Sterilized	33.6	41.0	91.0
		0.2 μm filtered	Unsterilized	66.1	58.7	112.6
			Sterilized	55.7	57.7	96.5
CAA5	150 m	Unfiltered	Unsterilized	48.1	40.3	119.4
			Sterilized	55.5	55.9	99.3
		0.2 μm filtered	Unsterilized	40.9	20.7	197.6
			Sterilized	33.6	34.4	97.7
CB4	70 m (SCM)	Unfiltered	Unsterilized	27.2*	14.6	186.3
		0.2 μm filtered	Unsterilized	16.7*	34.2	48.8
	150 m	Unfiltered	Unsterilized	28.6*	18.9	151.3
		0.2 μm filtered	Unsterilized	10.5*	29.2	36.0
	500 m	Unfiltered	Unsterilized	39.7*	25.5	155.7
		0.2 μm filtered	Unsterilized	36.0*	51.4	70.0

* Values at t_0 were taken as the initial methylation percentages, instead of values at 0.5 h as other incubations.

3.4.3 Unexplainable Methylation and Demethylation Kinetics

In all the incubation studies, k_m and k_d were estimated on the assumption that Hg methylation and demethylation in seawater follow a first-order kinetics. For the k_m calculation, Lehnherr et al. (2011) fit the methylation fraction time-series data to first-order reaction curves, and all other studies (Monperrus et al., 2007; Munson, 2014; Munson et al., 2018) estimated k_m with a linear regression model, and divided the ending Hg methylation ratios by incubation time (Table 3-3). For the k_d calculation, some studies (Lehnherr et al., 2011; Munson, 2014; Munson et al., 2018; Whalin et al., 2007) estimated it as the slope of the linear best fit line of ln (MMHg) over time, and others (Monperrus et al., 2007; Munson et al., 2018) used a linear regression model and divided ending demethylation ratios by incubation time (Table 3-3). All these calculations would only be valid if the time series data follow a first-order reaction curve. The considerable methylation and demethylation at or immediately after t_0 as discussed above suggests that this assumption is unlikely to hold.

With only one or two time points (beginning and end of incubations) in some incubation studies (Monperrus et al., 2007; Munson, 2014; Munson et al., 2018), it remains untested whether the time series data throughout the incubation period can fit to first-order reaction curve, especially given the considerable methylation and demethylation at or immediately after t_0. Samples were collected at higher temporal resolution in the incubations with seawater from the Atlantic coastal regions (Whalin et al., 2007), the Sargasso Sea (October 2012) (Munson, 2014) and the South Pacific Ocean station (12°S) (Munson et al., 2018). Except for the demethylation time series data in a few incubations (Munson, 2014; Munson et al., 2018; Whalin et al., 2007), the time series

data in most incubations could not fit to a first-order reaction curve. In our experiments, samples were collected at high temporal resolution, but none of the time series data followed a first-reaction curve (Figures 3-3 and 3-4).

Results from the few studies that managed to fit data in determining k_m (Lehnherr et al., 2011) and k_d (Lehnherr et al., 2011; Munson et al., 2014; Munson et al., 2018; Whalin et al., 2007) are also problematic. The Canadian Arctic Archipelago incubations (Lehnherr et al., 2011) only had two to three time points available for curve fitting, thus with poor temporal resolution. When calculating k_m, the inorganic Hg(II) substrate at different time points was estimated by an exponentially decreasing curve from separate incubations (Lehnherr et al., 2011). However, no information was provided as to whether the waters used were from the same stations and depths as the incubations for methylation and demethylation. In the studies with higher temporal resolution (Munson, 2014; Munson et al., 2018; Whalin et al., 2007), the attempts to fit demethylation data failed for many incubations, and most of the successful fittings were based on a few arbitrarily selected data points instead of using the data points from the entire incubation period (Table 3-3). Given the difficulties encountered by incubation studies in fitting data to first-order reaction curve, we conclude that the methylation and demethylation rates reported from incubations studies does not properly reflect the Hg methylation and demethylation in seawater.

3.5 Conclusion

Our incubation studies with Canadian Arctic seawater failed to determine Hg methylation rate in marine waters, suggesting either methylation did not occur or the rate

was too slow to be detected at the low levels of inorganic ^{202}Hg(II) added in the incubation. High demethylation percentages were observed in our experiments. Our results also show that aquatic particles may play a more complicated role in demethylation, and the role was limited to the abiotic mechanism and during the initial stage of demethylation.

A critical review of the existing incubation studies with Hg isotope additions shows that this approach has major problems when used for rate determination of Hg methylation and demethylation in seawater. One major problem is the observed methylation and demethylation at time zero, which cannot be explained by the known mechanisms. The other problem is the unexplainable reaction kinetics. As methylation and demethylation are assumed to be first-order reactions, the calculation of k_m and k_d relies on fitting the time series data to a first-order reaction curve. However, the existing incubations were either with time series data at low temporal resolutions, or the time series data did not fit to a first-order reaction curve. Given these problems, caution is advised when using the k_m and k_d values reported from incubation studies. Novel and more reliable approaches are required to determine these important reaction rates in seawater.

References

Black, F.J., Conaway, C.H., and Flegal, A.R. (2009). Stability of dimethyl mercury in seawater and its conversion to monomethyl mercury. Environmental Science & Technology 43, 4056-4062.

Cossa, D., Averty, B., and Pirrone, N. (2009). The origin of methylmercury in open Mediterranean waters. Limnology and Oceanography 54, 837-844.

Cossa, D., Heimbürger, L.-E., Lannuzel, D., Rintoul, S.R., Butler, E.C., Bowie, A.R., Averty, B., Watson, R.J., and Remenyi, T. (2011). Mercury in the Southern Ocean. Geochimica et Cosmochimica Acta 75, 4037-4052.

DiMento, B.P., and Mason, R.P. (2017). Factors controlling the photochemical degradation of methylmercury in coastal and oceanic waters. Marine Chemistry 196, 116-125.

Eckley, C.S., and Hintelmann, H. (2006). Determination of mercury methylation potentials in the water column of lakes across Canada. Science of the Total Environment 368, 111-125.

U.S. Environment Protection Agency (2001). Method 1630. Methyl Mercury in Water by Distillation, Aqueous Ethylation, Purge and Trap, and Cold Vapor Atomic Fluorescence Spectrometry, US EPA, Washington, D.C.

Fitzgerald, W.F. (1999). Clean hands, dirty hands: Clair Patterson and the aquatic biogeochemistry of mercury. Clean Hands: Clair Patterson's Crusade Against Environmental Lead Contamination, 119-137.

Graham, A. M., Bullock, A. L., Maizel, A. C., Elias, D. A., & Gilmour, C. C. (2012). Detailed assessment of the kinetics of Hg-cell association, Hg methylation, and methylmercury degradation in several Desulfovibrio species. Applied and Environmental Microbiology 78, 7337-7346.

Heimbürger, L.-E., Sonke, J.E., Cossa, D., Point, D., Lagane, C., Laffont, L., Galfond, B.T., Nicolaus, M., Rabe, B., and van der Loeff, M.R. (2015). Shallow methylmercury production in the marginal sea ice zone of the central Arctic Ocean. Scientific Reports 5, 10318.

Hintelmann, H., and Evans, R. (1997). Application of stable isotopes in environmental tracer studies–Measurement of monomethylmercury (CH_3Hg^+) by isotope dilution ICP-MS and detection of species transformation. Fresenius' Journal of Analytical Chemistry 358, 378-385.

Hintelmann, H., and Ogrinc, N. (2003). Determination of stable mercury isotopes by ICP/MS and their application in environmental studies, American Chemical Society Synposium Series 835, 321-338.

Lehnherr, I., Louis, V.L.S., Hintelmann, H., and Kirk, J.L. (2011). Methylation of inorganic mercury in polar marine waters. Nature Geoscience 4, 298-302.

Mason, R., Rolfhus, K., and Fitzgerald, W. (1995). Methylated and elemental mercury cycling in surface and deep ocean waters of the North Atlantic. Water, Air, and Soil Pollution 80, 665-677.

Mason, R.a., and Sullivan, K. (1999). The distribution and speciation of mercury in the South and equatorial Atlantic. Deep Sea Research Part II: Topical Studies in Oceanography 46, 937-956.

Mason, R.P., Choi, A.L., Fitzgerald, W.F., Hammerschmidt, C.R., Lamborg, C.H., Soerensen, A.L., and Sunderland, E.M. (2012). Mercury biogeochemical cycling in the ocean and policy implications. Environmental Research 119, 101-117.

Mason, R.P., and Fitzgerald, W.F. (1993). The distribution and biogeochemical cycling of mercury in the equatorial Pacific Ocean. Deep Sea Research Part I: Oceanographic Research Papers 40, 1897-1924.

Mason, R.y., and Fitzgerald, W. (1990). Alkylmercury species in the equatorial Pacific. Nature 347, 457−459.

Mclaughlin, F., Carmack, E., Ingram, R., Williams, W., and Michel, C. (2006). Oceanography of the Northwest Passage. In: Robinson, A.R., Brink, K. (Eds.), The Sea, vol. 14, Chapter 31. Harvard University Press, Cambridge.

Monperrus, M., Tessier, E., Amouroux, D., Leynaert, A., Huonnic, P., and Donard, O. (2007). Mercury methylation, demethylation and reduction rates in coastal and marine surface waters of the Mediterranean Sea. Marine Chemistry 107, 49-63.

Munson, K.M. (2014). Transformations of mercury in the marine water column. Phd Thesis. Massachusetts Institute of Technology and Woods Hole Oceanographic Institution, Cambridge.

Munson, K.M., Babi, D., and Lamborg, C.H. (2014). Determination of monomethylmercury from seawater with ascorbic acid-assisted direct ethylation. Limnology and Oceanography: Methods 12, 1-9.

Munson, K. M., Lamborg, C. H., Boiteau, R. M., and Saito, M. A. (2018) Dynamic mercury methylation and demethylation in oligotrophic marine water. Biogeosciences 15, 6451-6460.

Munson, K.M., Lamborg, C.H., Swarr, G.J., and Saito, M.A. (2015). Mercury Species Concentrations and Fluxes in the Central Tropical Pacific Ocean. Global Biogeochemical Cycles 29, 656-676.

Ramamoorthy, S., Cheng, T., and Kushner, D. (1982). Effect of microbial life stages on the fate of methylmercury in natural waters. Bulletin of Environmental Contamination and Toxicology 29, 167-173.

Schaefer, J.K., Rocks, S.S., Zheng, W., Liang, L., Gu, B., and Morel, F.M. (2011). Active transport, substrate specificity, and methylation of Hg (II) in anaerobic bacteria. Proceedings of the National Academy of Sciences 108, 8714-8719.

Sunderland, E.M. (2007). Mercury exposure from domestic and imported estuarine and marine fish in the US seafood market. Environmental Health Perspectives 115, 235-242.

Sunderland, E.M., Krabbenhoft, D.P., Moreau, J.W., Strode, S.A., and Landing, W.M. (2009). Mercury sources, distribution, and bioavailability in the North Pacific Ocean: Insights from data and models. Global Biogeochemical Cycles 23, 1-14.

Wang, F., Macdonald, R.W., Armstrong, D.A., and Stern, G.A. (2012). Total and Methylated Mercury in the Beaufort Sea: The Role of Local and Recent Organic Remineralization. Environmental Science & Technology 46, 11821-11828.

Wang, K., Munson, K.M., Beaupré-Laperrière, A., Mucci, A., Macdonald, R.M., Wang, F. (2018). Subsurface seawater methylmercury maximum explains biotic mercury concentrations in the Canadian Arctic. Scientific Reports, 8(1), 14465. https://doi.org/10.1038/s41598-018-32760-0.

Whalin, L., Kim, E.-H., and Mason, R. (2007). Factors influencing the oxidation, reduction, methylation and demethylation of mercury species in coastal waters. Marine Chemistry 107, 278-294.

Supplementary Information

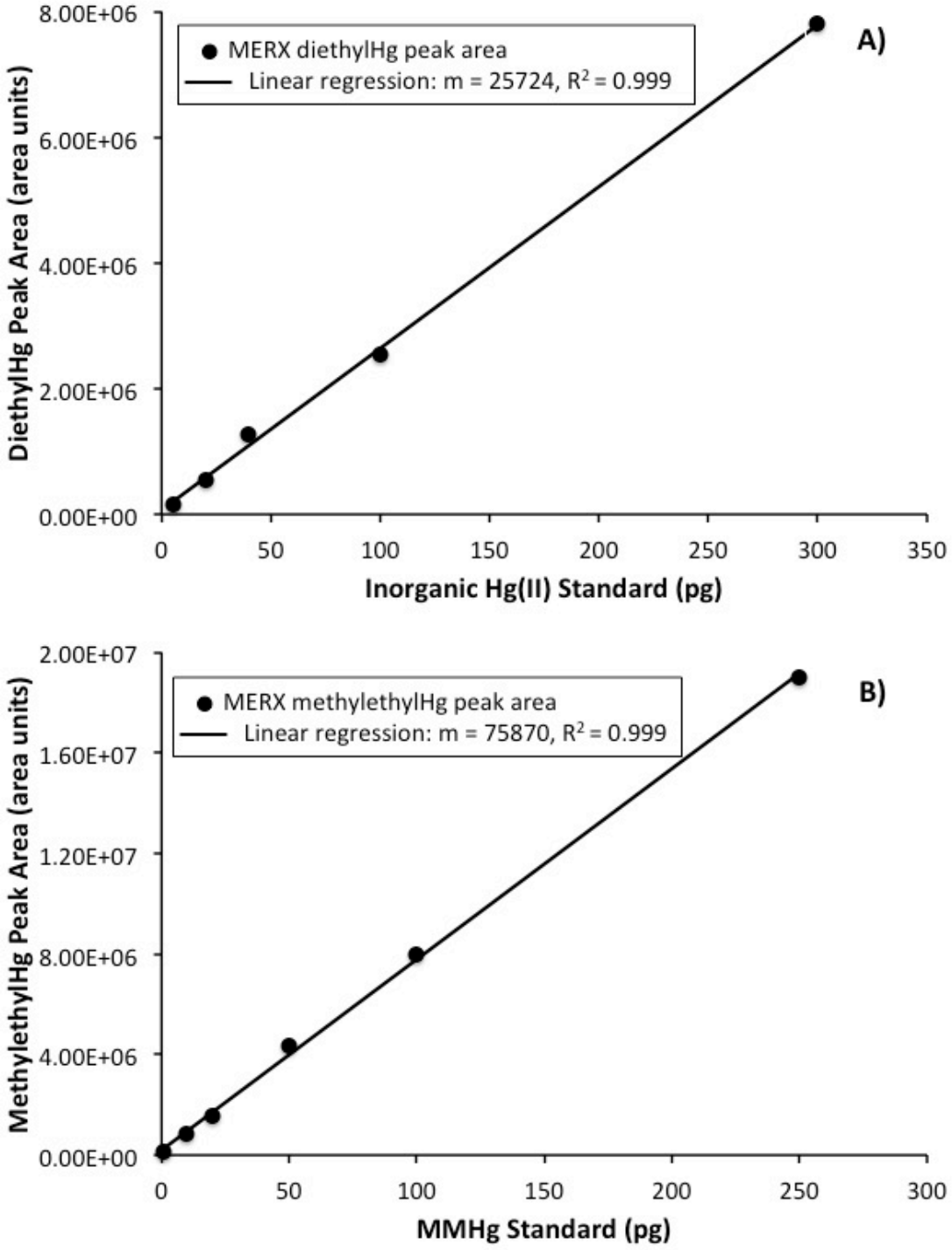

Figure 3-S1: Typical calibration curves for the determination of A) inorganic Hg(II) and B) monomethylmercury (MMHg) in MERX-M.

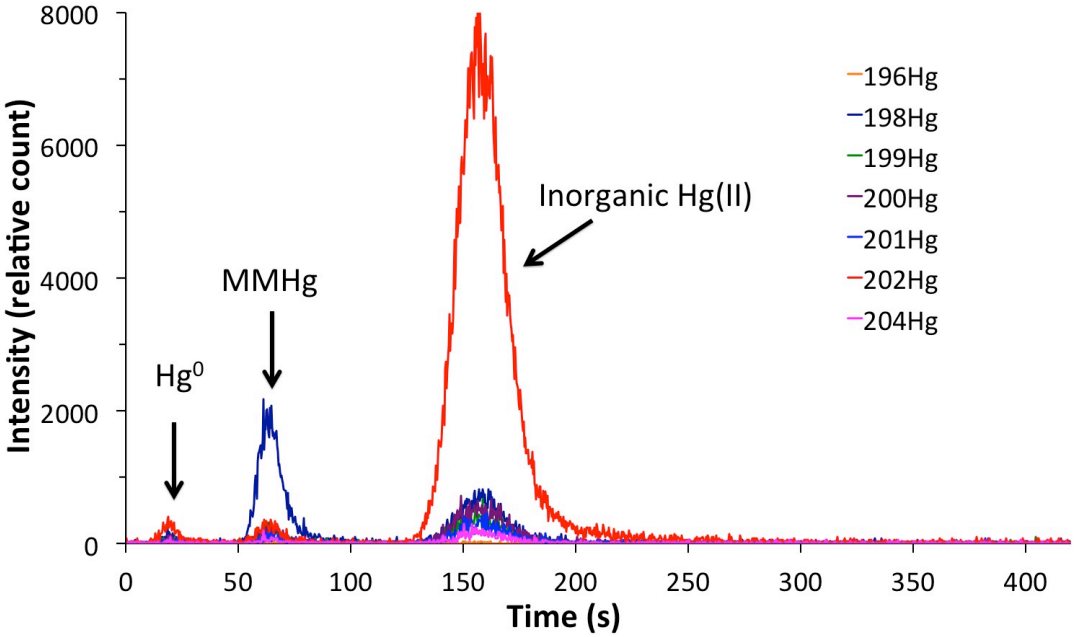

Figure 3-S2: Example chromatogram for Hg isotopic determination by ICP-MS.

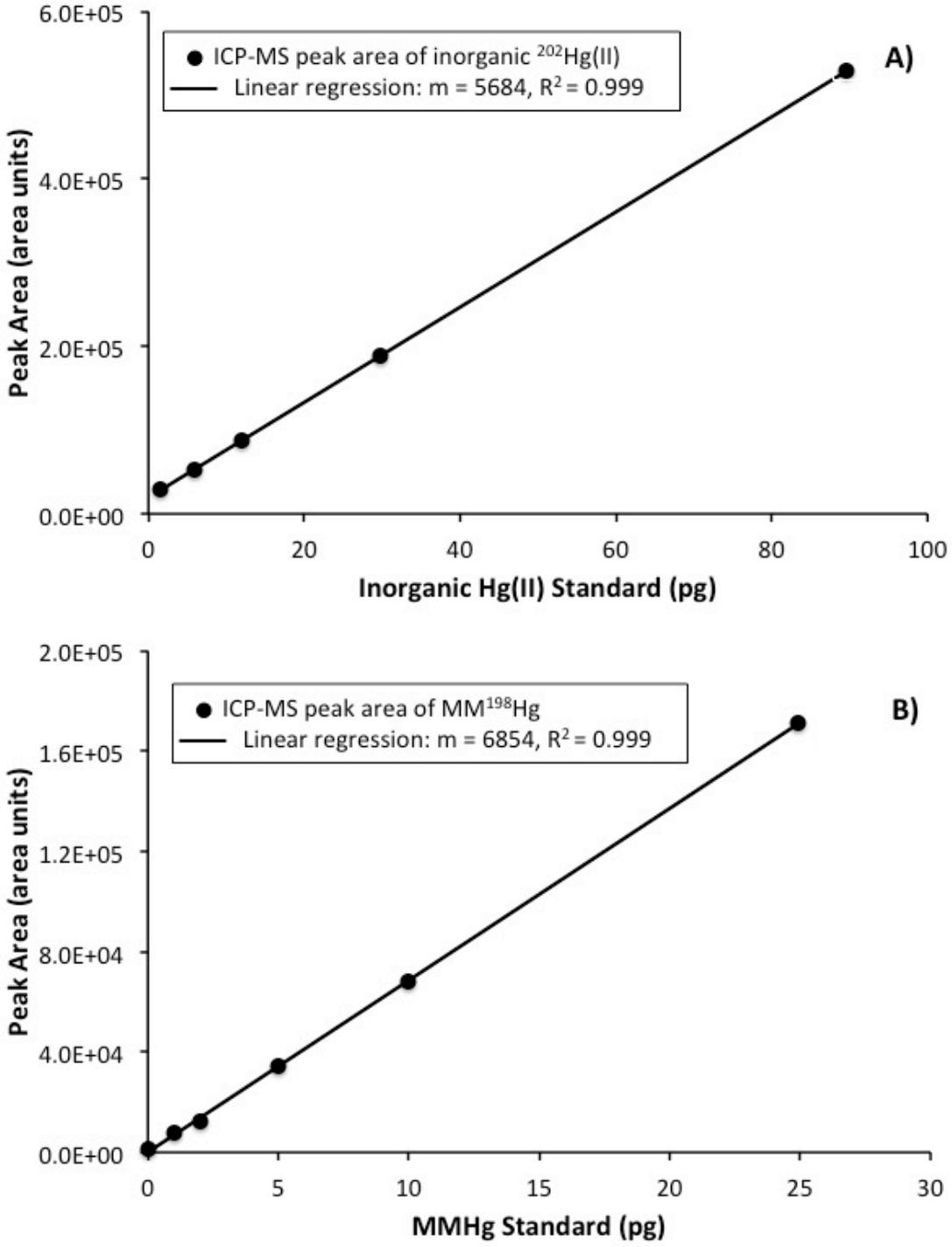

Figure 3-S3: Typical calibration curves for the determination of Hg isotopes in A) inorganic Hg(II) (^{202}Hg), and B) MMHg (^{198}Hg) by ICP-MS.

Chapter 4: Sources of Methylmercury in the Canadian Arctic Seawater: In-situ Production vs. Long-range Advection

Abstract

A subsurface enrichment of methylmercury (MeHg), a neurotoxin, has been observed at shallow depths in several regions of the Arctic Ocean, but its source remains unknown. Here, we discuss the source of seawater MeHg in the Canadian Arctic by linking the MeHg distributions with ancillary data. The subsurface enrichment of MeHg and its significant correlations with nutrients and apparent oxygen utilization appear to indicate that the MeHg in seawater is produced in-situ in the water column and in association with organic matter remineralization. However, the remineralization signatures in the Canadian Arctic are primarily transported from Chukchi Sea, instead of produced in-situ. Water mass analysis shows that the shallow enrichment of MeHg generally follows the distribution of Upper Halocline Water (UHW). Concentrations of MeHg exhibit significant correlation with N*, and the MeHg-to-N* slope decreases progressively from west to east. As the negative N* values originate from denitrification in the Chukchi Sea sediment, the accompanying MeHg also likely originates from there and migrates within UHW to the Canadian Arctic. In contrast to the quasi-conservative N*, MeHg would be progressively lost through demethylation as UHW moves eastwards, resulting in the decreasing MeHg-to-N* slope. The long-distance transport implies that the half-life of MeHg in Arctic seawater below the euphotic zone must be much longer than previously reported.

4.1 Introduction

Mercury (Hg) elicits major concerns in the Arctic for its health implications to Indigenous Peoples and wildlife (AMAP, 2011, 2018). The top predators are primarily exposed to Hg in the form of monomethylmercury (MMHg), which biomagnifies in the food web. Because the ocean is the principal source of Hg in the apex predators, it is of great importance to understand the Hg speciation and distribution in Arctic seawater. However, measurements of seawater Hg species are scarce in the Arctic, due to analytical and logistical constraints.

High-resolution vertical profiles of Hg species have been measured in the Beaufort Sea (Wang et al., 2012a) and central Arctic Ocean (Heimbürger et al., 2015). Both studies have found a subsurface peak of methylated Hg (MeHg, sum of MMHg and dimethylmercury (DMHg)) at shallow depths, just below the productive surface layer. The MeHg enrichments in bioactive shallow waters can enhance its biological uptake at the base of marine food webs, and eventually lead to elevated biotic Hg levels in the Arctic (Heimbürger et al., 2015; Wang et al., 2018). This has been shown to readily explain why biotic Hg levels are higher in the western Canadian Arctic than in the east (Wang et al., 2018). Despite the importance of seawater MeHg, its sources are still being debated (Mason et al., 2012). Globally, atmospheric deposition and riverine transport are considered minor sources for oceanic MeHg (Mason et al., 2012). Although these two sources are modeled to play more important roles in the Arctic Ocean than in other oceans, neither are considered major sources of seawater MeHg (Soerensen et al., 2016).

The commonly held view is that seawater MeHg is primarily produced by in-situ Hg methylation in the water column (Lehnherr 2014; Mason et al., 2012). With the recent

development of reliable methods to measure Hg species in seawater, it has become evident that MeHg is ubiquitously enriched in oxyclines of the world's oceans (Bowman et al., 2015, 2016; Bratkič et al., 2016; Cossa et al., 2009, 2011; Gionfriddo et al., 2016; Hammerschmidt and Bowman, 2012; Heimbürger et al., 2010, 2015; Mason and Fitzgerald, 1990; Mason et al., 2015; Sunderland et al., 2009; Wang et al., 2012a). As MeHg concentrations often show significant correlations with nutrients and apparent oxygen utilization (AOU), this subsurface enrichment is generally attributed to enhanced MeHg production by bacteria within the organic matter (OM) remineralization zone (Cossa et al., 2009; Heimbürger et al., 2010; Sunderland et al., 2009). However, what methylates inorganic Hg to MeHg in the subsurface water remains unknown. So far, the known gene cluster responsible for Hg methylation, *hgcA-hgcB*, has been found only in anaerobic microorganisms (e.g., sulfate- or iron-reducers) (Parks et al., 2013; Podar et al., 2015). The dissolved oxygen (DO) concentrations in the MeHg enriched subsurface waters in most of the studied oceans (Bowman et al., 2015; Cossa et al., 2011; Heimbürger et al., 2015; Wang et al., 2012a), except the Black Sea (Lamborg et al., 2008), were high enough that the *hgcA-hgcB* possessing anaerobes are unlikely to thrive and methylate inorganic Hg. Recently, *hgcA-hgcB*-like genes were found in aerophilic bacterium *Nitrospina* (Gionfriddo et al., 2016), but it remains unknown whether they are capable of methylating Hg.

Alternatively, subsurface seawater MeHg could originate from Hg methylation in marine sediments. Mercury methylation in deep ocean sediments is less studied and not considered an important source of MeHg in open oceans (Mason et al., 2012), as indicated by the low MeHg concentrations in bottom waters (Cossa et al., 2009;

Heimbürger et al., 2015; Munson et al., 2015). However, Hg methylation is known to occur in estuarine, coastal and shelf sediments where microbial organisms possessing *hgcA-hgcB* thrive (Hammerschmidt et al., 2004; Hammerschmidt and Fitzgerald, 2006; Hollweg et al., 2009, 2010). While the isopycnal advection of MeHg from shelf sediments may support the subsurface enrichment in open oceans, its relative contribution is largely controlled by the loss rate of marine MeHg. On the basis of fast demethylation rates calculated from incubation studies (Lehnherr et al., 2011; Monperrus et al., 2007), the MeHg produced in shelf regions was deemed not able to advect over long distances to account for the subsurface enrichment in open oceans (Wang et al., 2012a). However, these demethylation rates are much higher than those estimated from spatial distribution of Hg species (Mason et al., 1995; Mason and Fitzgerald, 1993); as pointed in Chapter 3, major uncertainties exist in the incubation studies for the rate determination. If the demethylation rates from incubation studies do underestimate the lifetime of MeHg in seawater, the long-range transport of MeHg of the shelf sediment origin could serve as the source for the subsurface MeHg enrichment in the Arctic Ocean.

As part of the 2015 Canadian Arctic GEOTRACES cruises, we measured total Hg (Hg_T) and MeHg in high-resolution vertical profiles at 16 stations in the Canadian Arctic. Other oceanographic variables (e.g., temperature, salinity, nutrients) were also monitored during the cruises, which traversed ~ 3600 km from Baffin Bay in the east, through the Canadian Arctic Archipelago (CAA), and into the Canada Basin in the west (Figure 4-1). Based on the relationships between Hg distribution and ancillary data, here we discuss the potential source(s) of seawater MeHg in the Canadian Arctic.

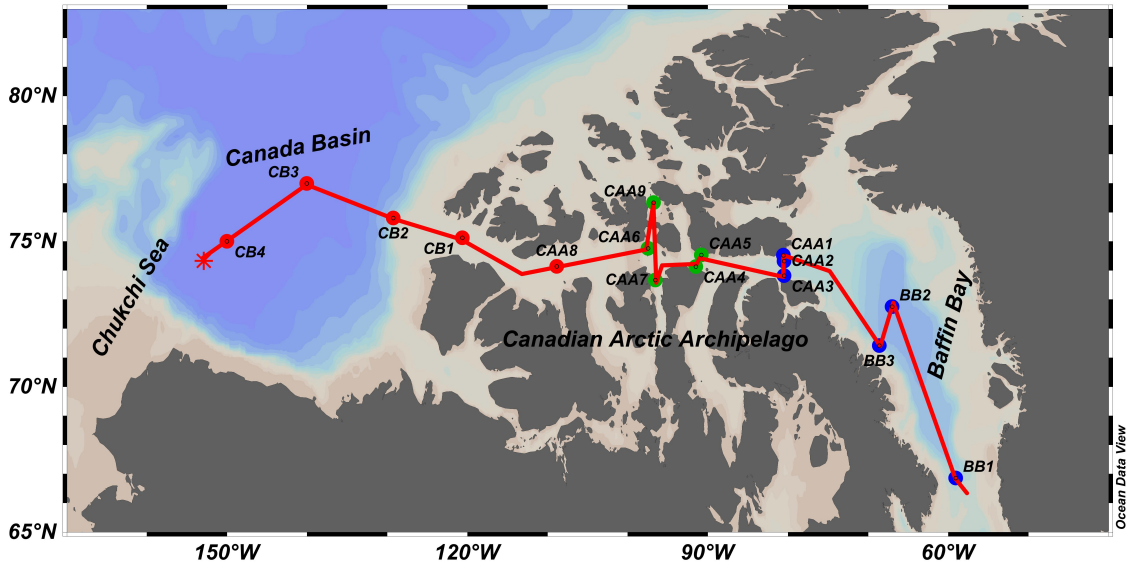

Figure 4-1: A map showing the cruise track and sampling stations across the Canadian Arctic. The stations are colored coded in red, green and blue for the western, central, and eastern Canadian Arctic, respectively.

4.2 Materials and Methods

4.2.1 Regional Water Mass Analysis

The water masses in our study area were analyzed by collaborators A. Beaupré-Laperrière and A. Mucci of McGill University with an optimum multiparameter (OMP) algorithm. The OMP analysis (Karstensen, 2006) is a weighted, linear least squares, mass balance algorithm developed from the earlier work of Mackas et al. (1987) and Tomczak and Large (1989). This algorithm has been extensively used to determine water mass distributions in many areas of the world's oceans, including the Canadian (Macdonald et al., 1989; Lansard et al., 2012) and Alaskan (Alkire and Trefry, 2006) Beaufort Sea. Briefly, the method finds the best fitting fraction (x) of (n + 1) source water types that contribute to the observed values of the n selected tracers in a parcel of water via solution of an over-determined system of linear equations that minimizes the residual error. In this study, we used salinity, total alkalinity (TA), and $\delta^{18}O$ of seawater as conservative tracers

as well as potential temperature, DO and the dissolved inorganic carbon (DIC) concentrations as non-conservative tracers, to constrain the water mass analysis. Non-conservative tracers should be applied with caution in OMP, because of biological activity (respiration and photosynthesis) and exchange of heat and gases with the atmosphere.

We defined the most representative properties for each source water type that are appropriate for our water mass analysis in the study region (Table 4-S1). The analysis was divided in two areas, the first extending from the Canada Basin and the Beaufort Sea to western Barrow Strait, and the second from eastern Barrow Strait through Lancaster Sound, into Baffin Bay. The two areas are separated by a 125-m sill in Barrow Strait, which effectively restricts the east-west circulation of water masses to shallower depths (Bidleman et al., 2007). Thus, we used distinct definitions for Atlantic-origin water having entered the CAA through the Canada Basin (N-ATW) and Baffin Bay (S-ATW). Whereas in some studies (Shadwick et al., 2011) surface waters of the CAA are considered a combination of Meteoric Water (MW; here assumed to be equivalent in properties to Mackenzie River water), Sea-Ice Melt (SIM) and Upper Halocline Water (UHW), we included the Polar Mixed Layer (PML) water in our analysis, as defined by Lansard et al. (2012). This results in UHW fractions that reflect the contribution of water that retains the distinctive characteristics it acquired in the Pacific Ocean, having not resided in the Canada Basin long enough to undergo transformation and/or dilution. Baffin Bay Arctic Water (BBAW) represents the combined (indistinguishable using the available data) inputs of Arctic water entering Baffin Bay through Nares Strait, eastern Davis Strait and Lancaster Sound, including the remnants of UHW.

4.2.2 Sample Collection and Analysis

Collection and analysis of seawater samples for Hg_T and MeHg were carried out following ultraclean techniques recommended for the GEOTRACES program (Hammerschmidt et al., 2012; Lamborg et al., 2012). The detailed procedures were described in Chapter 2 of this study. In addition to Hg species, we also collected ancillary data, including the parameters used in the OMP analysis. Salinity, temperature, density and fluorescence of the seawater were measured with a CTD (Seabird SBE-911plus) and a Seapoint fluorometer, respectively. Dissolved oxygen was measured in real-time by an oxygen probe (SBE-43), which was calibrated against discrete seawater samples analyzed by Winkler titration (Grasshoff et al., 2009). The concentrations of soluble reactive phosphorus (SRP), nitrate and silicate were measured aboard on the samples collected from the Go-Flo bottles, as detailed in an earlier study (Tremblay et al., 2008). The samples for TA, DIC and $\delta^{18}O$ were collected and analyzed with the technique described elsewhere (Lansard et al., 2012).

4.3 Results

Using the OMP analysis, we quantified the water masses fractions in the study area (Figure 4-S1). The water mass and circulation regimes are different in the west and east of the shallow sill in Barrow Strait. The water masses from the surface to bottom are PML, UHW, N-ATW and CBDW in the west, and PML, UHW, S-ATW and BBDW in the east. Note that in Baffin Bay, UHW is replaced by BBAW, which is a combination of UHW and the Arctic waters entering this region from different routes. Both MW and SIM comprise a substantial fraction in the surface water, especially at the westernmost station.

In the east, the fractions of UHW and BBAW are larger in the surface water and comparable to that of PML. One outstanding feature of the Canadian Arctic hydrology is that the water masses in the upper layer shoal when flowing from the Canada Basin towards the CAA: the core UHW depth rises from ~250 m at the westernmost station to ~100 m in central CAA; through the same path, the bottom depth of PML shoals from ~180 m to <100 m.

As detailed in Chapter 2, Hg_T concentration averages 2.17 ± 1.65 pM (0.55– 12.35 pM) in our study area, and increases from the Canada Basin and western CAA to the eastern CAA and Baffin Bay (Figure 4-2a). The results are consistent with the limited datasets measured in the Canadian Arctic (Kirk et al., 2008; Lehnherr et al., 2011; Wang et al., 2012a). In the Canada Basin and Baffin Bay, the Hg_T displays a transient-type distribution, with elevated concentrations in the surface and deep waters, and lower concentrations at mid-depths. In the CAA, the Hg_T concentrations stay constant with depth at most stations.

The MeHg concentration averages 0.23 ± 0.12 pM (0.02–0.56 pM) (Figure 4-2b), and its ratio to Hg_T has an average value of 0.16 ± 0.12 (0.01–0.52). In contrast to the spatial distribution of Hg_T, MeHg concentrations are significantly higher (t test, $p < 0.0001$) in the Canada Basin and western CAA (0.27 ± 0.14 pM, 0.02–0.56 pM) than in the eastern CAA and Baffin Bay (0.20 ± 0.09 pM, 0.04–0.44 pM) (Table 2-1 in Chapter 2 of this study), agreeing with previous measurements (Kirk et al., 2008; Lehnherr et al., 2011; Wang et al., 2012a). With improved sampling resolution, our MeHg measurements reveal distinctive vertical and longitudinal variations in the Canadian Arctic, as detailed in Chapter 2. Consistent with the profiles in the central Arctic Ocean (Heimbürger et al.,

2015), the MeHg concentrations are elevated in ATW across the Canadian Arctic. In Baffin Bay, the MeHg concentrations in S-ATW are even higher than those of the subsurface peaks (Figure 4-2b).

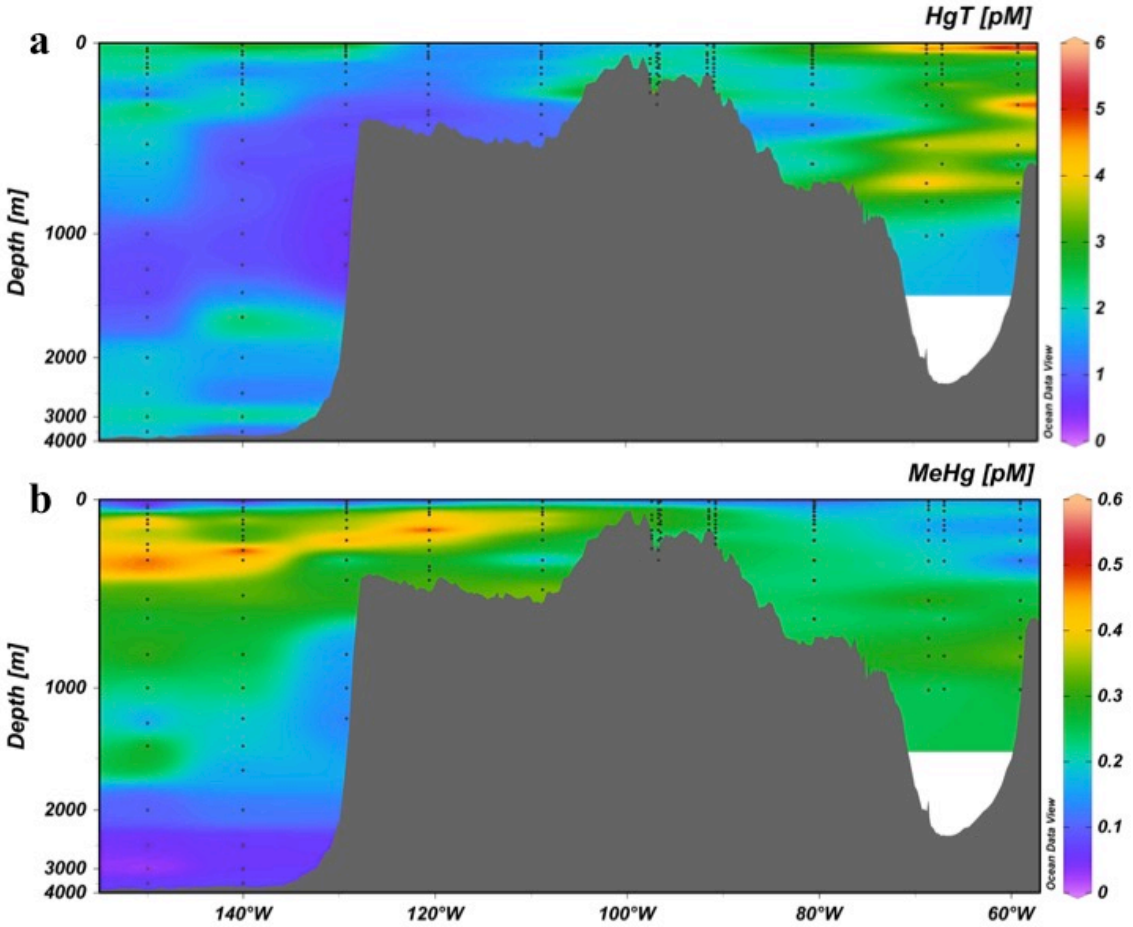

Figure 4-2: Distribution of total Hg (Hg_T, a) and methylmercury (MeHg, b) in seawater along the longitudinal (west-to-east) section in the Canadian Arctic.

4.4 Discussion

4.4.1 Distribution of Hg_T in the Canadian Arctic

In the Canada Basin and Baffin Bay, Hg_T is enhanced in the surface water. This is consistent with the Hg_T profiles observed in other oceans, where surface enrichment is generally attributed to atmospheric deposition (Fitzgerald et al., 2007; Mason et al., 2012). In the Beaufort Sea (Wang et al., 2012a) and central Arctic Ocean (Heimbürger et

al., 2015), however, the high concentrations of Hg_T in surface waters are also supported by Hg inputs of river runoff and sea-ice melt. In river water and sea-ice melt water, the Hg_T concentrations are usually much higher than in seawater. According to previous measurements, the water Hg_T concentrations were 33.5 ± 0.7 pM at the Mackenzie River mouth (Wang et al., 2012a). In the Beaufort Sea and McClure Strait, the Hg_T concentrations in the samples of first-year ice and multi-year ice were with a range of 2.5–20 pM and 0.65–60.8 pM, respectively (Beattie, et al., 2014; Chaulk et al., 2011). In this study, the MW and SIM comprise up to 10% and 20% in surface waters, respectively (Fig S1a, b). Therefore, Hg inputs by the MW and SIM must be important sources of the surface Hg_T enhancement, as concluded in previous studies (Heimbürber et al., 2015; Wang et al., 2012a).

In Baffin Bay surface waters, the Hg_T enhancement is more prominent than in the Canada Basin (Figure 4-2a), whereas the MW and SIM proportions are smaller (Figure 4-S1a, b). Therefore, the surface Hg_T enrichment in this area cannot be fully explained by Hg from the two fresh water masses. While direct measurements of atmospheric Hg deposition are scarce in the Arctic and limited to coastal regions (AMAP, 2011), atmospheric concentrations of gaseous elemental Hg (GEM) in the marine boundary layer were monitored onboard the icebreakers along the cruise tracks in the Canadian Arctic from 2008 to 2015 (Munson et al., manuscript in preparation). The results show that the atmospheric GEM concentrations are higher in Baffin Bay than in the Canada Basin. This spatial distribution pattern suggests an enhanced atmospheric Hg deposition in Baffin Bay, which explains the more prominent Hg_T surface enrichment in this region. Meanwhile, Hg input by melt water of glaciers from surrounding islands (e.g.,

Greenland) is another potential source of the surface Hg_T enrichment in Baffin Bay.

The Hg_T profiles in the Canada Basin match well with those observed in the Beaufort Sea and central Arctic Ocean (Heimbürger et al., 2015; Wang et al., 2012a). The increasing concentrations in bottom waters were not observed in the Beaufort Sea, because the stations sampled are not deep enough (<1000 m) (Wang et al., 2012a). The decreasing Hg_T concentrations below surface waters are likely the results of particle scavenging. In bottom waters, the elevated concentrations could be due to Hg release from OM remineralization (Bowman et al., 2015; Munson et al., 2015) and/or Hg diffusion from sediment sources (Heimbürger et al., 2015). In Baffin Bay, the vertical distribution below the surface layer can also be explained by particle scavenging and OM remineralization; Hg transport with seawater circulation may also have played a role. In the east of Greenland, the Hg_T profiles have concentrations and patterns similar to those in Baffin Bay (Mason et al., 1998). As S-ATW and part of BBAW flow into Baffin Bay through the regions east of Greenland, the Hg present in this area can be transported with the water masses and result in similar Hg_T distribution patterns in Baffin Bay. In the CAA, the constant concentrations with depth can be attributed to the enhanced scavenging process by the abundant inputs of terrestrial particulate matter in this region.

4.4.2 Source of MeHg in the Canadian Arctic: In-situ Production vs. Long-range Advection

In our measurements, the surface depletion of MeHg (Figure 4-2b) likely results from photodemethylation (Wang et al., 2012a) and evasion to the atmosphere (Baya et al., 2015). As all stations experienced at least 11.5 h of sunlight and lacked sea ice cover

during the sampling dates, the loss of MeHg by both mechanisms was well facilitated. In the Canadian Arctic, MeHg concentrations have significant relationships with nutrients ($r^2 = 0.42$, $p < 0.0001$ for SRP; $r^2 = 0.20$, $p < 0.0001$ for nitrate, and $r^2 = 0.30$, $p < 0.0001$ for silicate) and AOU ($r^2 = 0.15$, $p < 0.0001$) (Table 4-1). In the upper layer (where $f_{PML}+f_{UHW} > 0.5$), the relationships between MeHg and remineralization proxies are even stronger, with r^2 at 0.62 and 0.21 for the MeHg–SRP and MeHg–AOU correlations (for both, $p < 0.0001$), respectively (Table 4-1). The subsurface enrichment of MeHg and its significant correlations with remineralization proxies are also observed in other oceans, where they are used to support the association between seawater Hg methylation and OM remineralization (Cossa et al., 2009, 2011; Sunderland et al., 2009). In some regions, although the MeHg concentrations show significant correlations with AOU or nutrients, the percentage of MeHg in Hg_T does not significantly increase with these proxies (Canário et al., 2016; Munson et al., 2015). The methylation in these regions is thus considered more of a steady state process than one promoted by OM remineralization. In this study, the proportion of MeHg in Hg_T has significant relationships with AOU ($r^2 = 0.11$, $p < 0.0001$) and SRP ($r^2 = 0.40$, $p < 0.0001$) (Table 4-1), confirming the stimulation of OM remineralization on Hg methylation. Whereas the distribution of MeHg in the upper water column matches well with that of remineralization proxies, such matches break down in deep waters and especially in CBDW (Figure 4-S2). While SRP and AOU remain high, concentrations of MeHg decrease steadily with depth. In the Mediterranean Sea (Cossa et al., 2009) and North Pacific Ocean (Sunderland et al., 2009), the deficient MeHg concentrations comparing to remineralization proxies were also observed in deep waters. Both studies attributed the deficient MeHg to its demethylation as seawater ages.

Here, the decreasing MeHg concentrations may also results from its demethylation with time, as suggested by the long residence time (up to 300 years) of CBDW (Tanhua et al., 2009).

Table 4-1: Relationship between MeHg (pM) and apparent oxygen utilization (AOU, µmol/L) and nutrients (soluble reactive phosphorus (SRP), nitrate, silicate; µmol/L), and between fraction of MeHg in total Hg (Hg_T) and AOU and SRP in the Canadian Arctic.

Relationships	Full depth	Upper layer ($f_{PML}+f_{UHW} > 0.5$)
MeHg – AOU	MeHg = 0.00100 AOU + 0.169 *(n = 193, r^2 = 0.15, p < 0.0001)*	MeHg = 0.00130 AOU + 0.166 *(n = 115, r^2 = 0.21, p < 0.0001)*
MeHg – SRP	MeHg = 0.256 SRP – 0.0311 *(n = 190, r^2 = 0.42, p < 0.0001)*	MeHg = 0.279 SRP – 0.0645 *(n = 110, r^2 = 0.62, p < 0.0001)*
MeHg – nitrate	MeHg = 0.0105 nitrate + 0.125 *(n = 181, r^2 = 0.20, p < 0.0001)*	MeHg = 0.0171 nitrate + 0.0942 *(n = 109, r^2 = 0.41, p < 0.0001)*
MeHg – silicate	MeHg = 0.00749 silicate + 0.122 *(n = 188, r^2 = 0.30, p < 0.0001)*	MeHg = 0.0101 silicate + 0.0866 *(n = 112, r^2 = 0.49, p < 0.0001)*
MeHg:Hg_T – AOU	MeHg:Hg_T = 0.000691 AOU + 0.113 *(n = 192, r^2 = 0.07, p < 0.0001)*	MeHg:Hg_T = 0.000859 AOU + 0.101 *(n = 114, r^2 = 0.11, p < 0.0001)*
MeHg:Hg_T – SRP	MeHg:Hg_T = 0.170 SRP - 0.0197 *(n = 189, r^2 = 0.20, p < 0.0001)*	MeHg:Hg_T = 0.207 SRP - 0.0733 *(n = 110, r^2 = 0.40, p < 0.0001)*

In previous studies, the regression coefficient of MeHg concentrations (pmol/L) versus AOU extent (µmol/L) has been used to represent the seawater methylation capacity (Cossa et al., 2009; Heimbürger et al., 2010; Munson et al., 2015). In the upper layer of the Canadian Arctic, the Hg methylation capacity falls in the ranges measured in the world's oceans. The regression coefficient (0.00130, Table 4-1) is comparable to that measured by Wang et al. (2012a) in the Beaufort Sea (0.0011), higher than that in the Central Tropical Pacific Ocean (0.0004) (Munson et al., 2015), but lower than those in the Southern Ocean (0.0031) (Cossa et al., 2011), the Mediterranean Sea (~0.0040) (Cossa et al., 2009; Heimbürger et al., 2010), and the North Pacific Ocean (~0.0040) (Sunderland et al., 2009). For regression calculated for each individual station, 12 of the

16 relationships between MeHg and AOU have $p < 0.10$ (four relationships have $p < 0.05$), and their regression coefficients vary from 0.0009 to 0.0037 (Table 4-S2). In the Canadian Arctic, the regression coefficients generally exhibit a decreasing trend from west to east, mirroring the spatial trend of MeHg concentrations. In the Central Tropical Pacific Ocean, the low methylation capacity of intermediate waters was attributed to limitations by Hg_T substrate or associated compounds or requirements by microbial methylation activity (Munson et al., 2015). As the Hg_T concentrations have an opposite spatial trend, the lower methylation capacity might reflect the limitations of methylation activities by some compounds or conditions in the eastern regions.

In contrast to other oceans, the high nutrients and low DO in subsurface waters in the Canada Basin are predominantly advective features (Wheeler et al., 1997). Therefore, the accompanying MeHg enrichment may, likewise, derive from advection (Figure 4-S3). The prominent nutrient maximum (~120–200 m; salinity 33.1) in the Canada Basin is produced by regeneration under the "green belts" of Chukchi Sea where OM remineralization occurs extensively in bottom water and sediments (Anderson et al., 2013; Jones and Anderson, 1986). The products of regeneration are subsequently transported into the Arctic Ocean interior along with dense winter water (Macdonald et al., 1989; Wheeler et al., 1997). Although few studies have examined Hg methylation on the Chukchi Shelf sediments, other anaerobic processes such as denitrification are known to occur extensively (Chang and Devol, 2009; McTigue et al., 2016). Below, we provide an alternative explanation that the subsurface MeHg peak observed in the Canadian Arctic is primarily an advective feature; that is, much of the MeHg is originally produced in the Chukchi Shelf, presumably via anaerobic Hg methylators in the sediment, and

transported to the Canadian Arctic via the UHW which also forms in Chukchi Sea (Jones and Anderson, 1986).

As shown in Figure 4-S3a, the distribution pattern of MeHg closely tracks the core of UHW in the western Canadian Arctic, with the peak depths of both MeHg and f_{UHW} shoaling as the water moves eastward to the CAA. In the eastern Canadian Arctic, UHW is mixed with water from Nares Strait and Davis Strait and forms BBAW, thus does not carry elevated MeHg concentrations.

That the Chukchi Shelf is the origin of the MeHg peak is further supported by the relationship between MeHg and a quasi-conservative tracer, N*:

$$N^* = [NO_3^-] - 16\,[SRP] + 2.9\ (\mu mol/L)$$

N* provides a measurement of denitrification and N_2 fixation (Gruber and Sarmiento, 1997). As shown in Figure 4-S3b, the distribution pattern of MeHg follows the general pattern of N* throughout the Canadian Arctic. This relationship becomes much more evident when MeHg concentrations are plotted against N* values in the upper layer of the Canadian Arctic (Figure 4-3b).

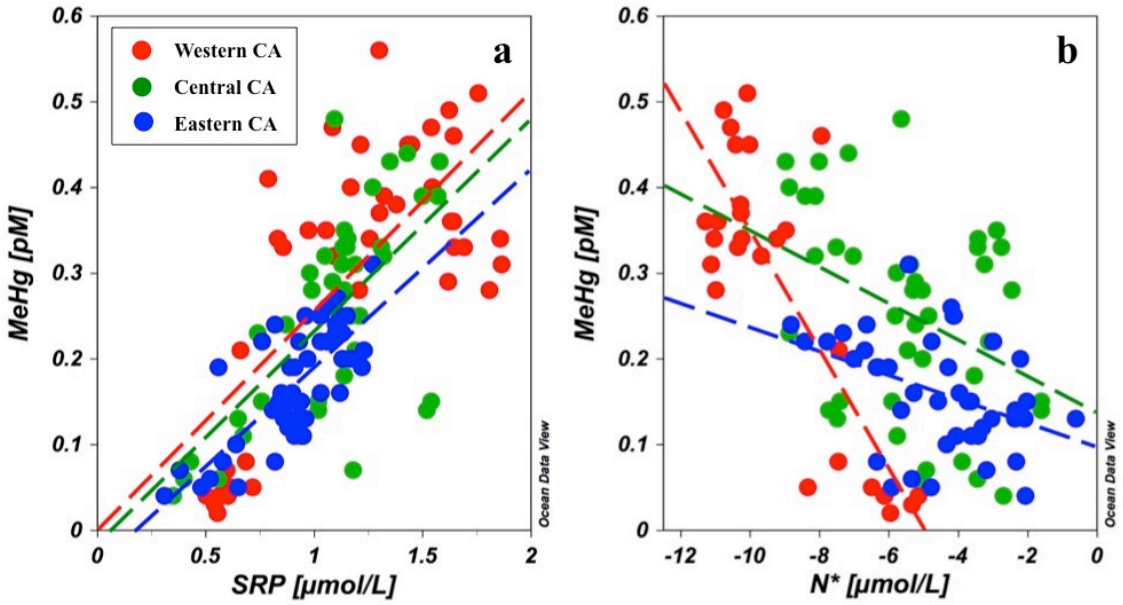

Figure 4-3: Relationship between methylmercury (MeHg) and soluble reactive phosphorus (SRP, a) or N* (b) in the upper layer of the water column (fPML+fUHW > 0.5) in the western (red), central (green) and eastern (blue) Canadian Arctic (see Figure 4-1 for the station locations).

Not only is there a significant negative relationship between the two parameters throughout the Canadian Arctic, the slope of the MeHg vs. N* relationship also decreases considerably and progressively from the western Canadian Arctic (slope = –0.069 pmol/µmol) to the central (slope = –0.021 pmol/µmol) and eastern Canadian Arctic (slope = –0.014 pmol/µmol) (Figure 4-3b, Table 4-2). As the negative N* values in the Canadian Arctic originate from denitrification in the Chukchi Sea sediment (Chang and Devol, 2009; McTigue et al., 2016), the accompanying MeHg also likely originates from the Chukchi Shelf sediments (Figure 4-3b). In contrast to N*, which is quasi-conservative (Gruber and Sarmiento, 1997), MeHg would be progressively lost as the UHW advects from the Chukchi Sea eastwards and through the CAA, as suggested by the decreasing slope between MeHg and N* (Figure 4-3b). A similar correlation is also seen between MeHg and SRP (Figure 4-3a, Table 4-2), although the eastward change in slope is not

significant since SRP is not conservative and can be taken up by primary production in the euphotic zone.

Table 4-2: Relationship between seawater methylated mercury (MeHg, pM) and soluble reactive phosphorus (SRP, µmol/L) or N* (µmol/L) in the upper layer of the Canadian Arctic.

Region	n	MeHg – SRP	MeHg – N*
Western Canadian Arctic (Stations in red circles)	27	MeHg = 0.285 SRP – 0.0639 *(r^2 = 0.69, $p < 0.0001$)*	MeHg = –0.0689 N* – 0.342 *(r^2 = 0.69, $p < 0.0001$)*
Central Canadian Arctic (Stations in green circles)	41	MeHg = 0.248 SRP – 0.0148 *(r^2 = 0.42, $p < 0.0001$)*	MeHg = –0.0210 N* + 0.140 *(r^2 = 0.14, $p = 0.015$)*
Eastern Canadian Arctic (Stations in blue circles)	42	MeHg = 0.222 SRP + 0.0353 *(r^2 = 0.55, $p < 0.0001$)*	MeHg = –0.0139 N* + 0.0970 *(r^2 = 0.16, $p = 0.008$)*
Throughout Canadian Arctic	110	MeHg = 0.279 SRP – 0.0645 *(r^2 = 0.62, $p < 0.0001$)*	MeHg = –0.0659 N* – 0.0264 *(r^2 = 0.31, $p < 0.0001$)*

MeHg is particle reactive and can be transported with particles along isopycnals. Jackson et al. (2010) observed that suspended particulate matter and particulate organic carbon concentrations are higher in UHW than in waters above and below it in the Canada Basin. The accumulation and remineralization of these particles at the lower boundary of UHW (i.e., pycnocline separating UHW from N-ATW), rather than its core would explain why peak MeHg concentrations are found slightly deeper than the UHW core (Figure 4-S3a) as well as the AOU and nutrient maxima (Figure 4-S3c, d). A similar "mismatch" between the depths of the MeHg and AOU peaks has been observed in the Atlantic Ocean, and was also attributed to the particle reactivity of MeHg (Mason and Sulivan, 1999). Microbial demethylation of MeHg could also occur in oxygenated waters (Lehnherr et al., 2011; Monperrus et al., 2007), and may have contributed to some of the low MeHg values in UHW (Figure 4-S3a). These processes are summarized in Figure 4-4.

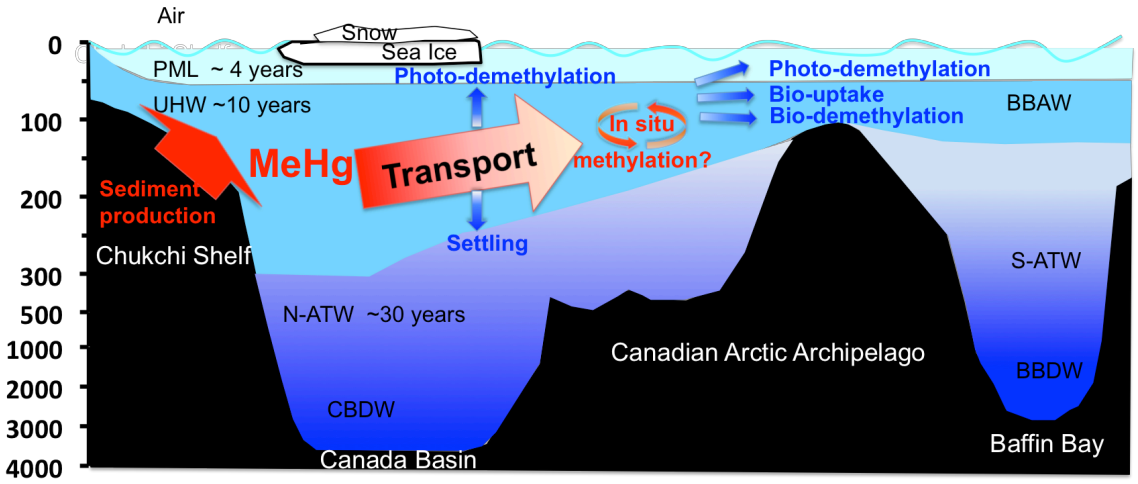

Figure 4-4: A schematic representation of the major processes governing the formation and transport of methylmercury (MeHg) in the Canadian Arctic.

In addition to the main peak near the UHW bottom, there appears to be a second, less pronounced MeHg enrichment at an even shallower depth (~150 m in the Canada Basin shoaling up to ~75 m in the CAA). Although less frequently observed, a near-surface MeHg peak at the depth of the subsurface chlorophyll maximum (SCM) has been reported at a few locations in the North (Bowman et al., 2015) and South Atlantic (Pongratz and Heumann, 1999) as well as in the Mediterranean Sea (Heimbürger et al., 2010). This peak has been attributed to MeHg production by enhanced surface water remineralization of the authocthonous OM. In the western Canadian Arctic, however, this near-surface MeHg enrichment does not correlate to the chlorophyll a concentrations, which were, based on fluorescence measurements, at extremely low levels (Figure 4-S3e). Therefore, our data do not support the hypothesis of in-situ production as an important source of the near-surface MeHg peak. Instead, it appears to be part of the subsurface peak associated with the advection of MeHg and loss by photolytic and microbial demethylation, bio-uptake and particle settling.

In contrast to the fast photolytic demethylation in the euphotic zone (Monperrus et al., 2007), microbial or chemical loss of MeHg in the deeper, aphotic zone must be slow enough to allow its transportation from its source region in the Chukchi Shelf to the Canadian Arctic (Figure 4-4). As the distance between the Chukchi Shelf and the stations in the western Canadian Arctic is >1000 km and the mean annual current velocity in the top 300 m is ~4 cm s^{-1} (Wang et al., 2012b), our data would imply a first-order MeHg loss rate in the order of 10^{-4} d^{-1}, which is in good agreement with the loss rates of MMHg (~10^{-4} d^{-1}) and DMHg (2×10^{-4} d^{-1}) derived from modeling their distributions in the deep Pacific (Mason and Fitzgerald, 1993) and Atlantic (Mason et al., 1995) waters. In contrast, the loss rate is two-to-three orders of magnitude lower than the non-photolytic demethylation rates of MMHg recently estimated based on dark incubations of seawater from the surface and oxycline of the CAA (0.36 d^{-1}) (Lehnherr et al., 2011), the surface coastal Atlantic (<0.09–0.43 d^{-1}) (Whalin et al., 2007) and the surface Mediterranean Sea (<0.015–0.109 d^{-1}) (Monperrus et al., 2007). In these incubation experiments, the loss rate was measured on isotopically labeled MMHg added to the seawater. The compatibility of our results with those of Mason and Fitzgerald (1993) and Mason et al. (1995) implies that incubation studies may have considerably overestimated the loss rate of MMHg, as the ambient seawater MMHg is likely bound to ligands and particles and thus more stable than the freshly added MMHg. Problems with using the seawater incubation approach to determine MeHg demethylation rate are further detailed in Chapter 3.

4.5 Conclusion

In this study, we discussed the Hg_T and MeHg distribution in the Canadian Arctic seawater. Concentrations of Hg_T are higher in the eastern CAA and Baffin Bay than in the western CAA and Canada Basin. The surface enrichment of Hg_T in the Canada Basin and Baffin Bay can be attributed to riverine input, sea-ice melt and atmospheric deposition.

In the Canadian Arctic, MeHg peaks in subsurface waters and significantly correlates with AOU and nutrients, appearing to indicate a major source of in-situ production associated with OM remineralization. However, further analysis with water mass and N* reveals that this MeHg is more likely originated from anaerobic Chukchi Shelf sediments and advected within UHW to the Canadian Arctic. The long-distance transport and long lifetime of MeHg in Arctic seawater imply that production hotspots like the Chukchi Shelf can have widespread consequences for Hg exposure in the Arctic Ocean food webs.

References

Alkire, M.B., and Trefry, J.H. (2006). Transport of spring floodwater from rivers under ice to the Alaskan Beaufort Sea. Journal of Geophysical Research: Oceans 111(C12).

AMAP (2011). AMAP Assessment 2011: Mercury in the Arctic. Arctic Monitoring and Assessment Program: Oslo.

AMAP (2018). AMAP Assessment 2018: Biological effects of contaminants on Arctic wildlife and fish. Mercury in the Arctic. Arctic Monitoring and Assessment Program: Tromsø.

Anderson, L.G., Andersson, P.S., Björk, G., Peter Jones, E., Jutterström, S., and Wåhlström, I. (2013). Source and formation of the upper halocline of the Arctic Ocean. Journal of Geophysical Research: Oceans 118, 410-421.

Avramescu, M.-L., Yumvihoze, E., Hintelmann, H., Ridal, J., Fortin, D., and Lean, D.R. (2011). Biogeochemical factors influencing net mercury methylation in contaminated freshwater sediments from the St. Lawrence River in Cornwall, Ontario, Canada. Science of the Total Environment 409, 968-978.

Baya, P.A., Gosselin, M., Lehnherr, I., St. Louis, V.L., and Hintelmann, H. (2015). Determination of monomethylmercury and dimethylmercury in the Arctic marine boundary layer. Environmental Science & Technology 49, 223-232.

Beattie, S., Armstrong, D., Chaulk, A., Comte, J., Gosselin, M., and Wang, F. (2014). Total and Methylated Mercury in Arctic Multiyear Sea Ice. Environmental Science & Technology 48, 5575-5582.

Benoit, J., Gilmour, C.C., Heyes, A., Mason, R., and Miller, C. (2003). Geochemical and biological controls over methylmercury production and degradation in aquatic ecosystems. In Biogeochemistry of Environmentally Important Trace Elements (American Chemical Society), pp. 262-279.

Bidleman, T., Kylin, H., Jantunen, L., Helm, P., and Macdonald, R. (2007). Hexachlorocyclohexanes in the Canadian Archipelago. 1. Spatial Distribution and Pathways of α-, β-, and γ-HCHs in Surface Water. Environmental Science & Technology 41, 2688-2695.

Bowman, K.L., Hammerschmidt, C.R., Lamborg, C.H., and Swarr, G. (2015). Mercury in the north Atlantic ocean: The US GEOTRACES zonal and meridional sections. Deep Sea Research Part II: Topical Studies in Oceanography 116, 251-261.

Bowman, K.L., Hammerschmidt, C.R., Lamborg, C.H., Swarr, G.J., and Agather, A.M. (2016). Distribution of mercury species across a zonal section of the eastern tropical South Pacific Ocean (US GEOTRACES GP16). Marine Chemistry 186, 156-166.

Bratkič, A., Vahčič, M., Kotnik, J., Obu Vazner, K., Begu, E., Woodward, E.M.S., and Horvat, M. (2016). Mercury presence and speciation in the South Atlantic Ocean along the 40° S transect. Global Biogeochemical Cycles 30, 105-119.

Canário, J., Santos-Echeandia, J., Padeiro, A., Amaro, E., Strass, V., Klaas, C., Hoppema, M., Ossebaar, S., Koch, B.P., and Laglera, L.M. (2017). Mercury and methylmercury in the Atlantic sector of the Southern Ocean. Deep Sea Research Part II: Topical Studies in Oceanography 138, 52-62.

Chang, B.X., and Devol, A.H. (2009). Seasonal and spatial patterns of sedimentary denitrification rates in the Chukchi Sea. Deep Sea Research Part II: Topical Studies in Oceanography 56, 1339-1350.

Chaulk, A., Stern, G.A., Armstrong, D., Barber, D.G., and Wang, F. (2011). Mercury Distribution and Transport Across the Ocean− Sea-Ice− Atmosphere Interface in the Arctic Ocean. Environmental Science & Technology 45, 1866-1872.

Compeau, G., and Bartha, R. (1985). Sulfate-reducing bacteria: principal methylators of mercury in anoxic estuarine sediment. Applied and Environmental Microbiology 50, 498-502.

Cossa, D., Averty, B., and Pirrone, N. (2009). The origin of methylmercury in open Mediterranean waters. Limnology and Oceanography 54, 837-844.

Cossa, D., Heimbürger, L.-E., Lannuzel, D., Rintoul, S.R., Butler, E.C., Bowie, A.R., Averty, B., Watson, R.J., and Remenyi, T. (2011). Mercury in the Southern Ocean. Geochimica et Cosmochimica Acta 75, 4037-4052.

Fitzgerald, W.F., Lamborg, C.H., and Hammerschmidt, C.R. (2007). Marine biogeochemical cycling of mercury. Chemical Reviews 107, 641-662.

Gilmour, C.C., Henry, E.A., and Mitchell, R. (1992). Sulfate stimulation of mercury methylation in freshwater sediments. Environmental Science & Technology 26, 2281-2287.

Gionfriddo, C.M., Tate, M.T., Wick, R.R., Schultz, M.B., Zemla, A., Thelen, M.P., Schofield, R., Krabbenhoft, D.P., Holt, K.E., and Moreau, J.W. (2016). Microbial mercury methylation in Antarctic sea ice. Nature microbiology 1, 16127.

Grasshoff, K., Kremling, K., and Ehrhardt, M. (2009). Methods of seawater analysis (John Wiley & Sons).

Gruber, N., and Sarmiento, J.L. (1997). Global patterns of marine nitrogen fixation and denitrification. Global Biogeochemical Cycles 11, 235-266.

Hammerschmidt, C.R., Bowman, K.L., Tabatchnick, M.D., and Lamborg, C.H. (2011). Storage bottle material and cleaning for determination of total mercury in seawater. Limnol Oceanogr Methods 9, 426-431.

Hammerschmidt, C.R., and Fitzgerald, W.F. (2004). Geochemical controls on the production and distribution of methylmercury in near-shore marine sediments. Environmental Science & Technology 38, 1487-1495.

Hammerschmidt, C.R., and Fitzgerald, W.F. (2006). Methylmercury cycling in sediments on the continental shelf of southern New England. Geochimica et Cosmochimica Acta 70, 918-930.

Hammerschmidt, C.R., Fitzgerald, W.F., Lamborg, C.H., Balcom, P.H., and Visscher, P.T. (2004). Biogeochemistry of methylmercury in sediments of Long Island Sound. Marine Chemistry 90, 31-52.

Heimbürger, L.-E., Cossa, D., Marty, J.-C., Migon, C., Averty, B., Dufour, A., and Ras, J. (2010). Methyl mercury distributions in relation to the presence of nano-and picophytoplankton in an oceanic water column (Ligurian Sea, North-western Mediterranean). Geochimica et Cosmochimica Acta 74, 5549-5559.

Heimbürger, L.-E., Sonke, J.E., Cossa, D., Point, D., Lagane, C., Laffont, L., Galfond, B.T., Nicolaus, M., Rabe, B., and van der Loeff, M.R. (2015). Shallow methylmercury production in the marginal sea ice zone of the central Arctic Ocean. Scientific Reports 5, 10318.

Hollweg, T., Gilmour, C., and Mason, R. (2009). Methylmercury production in sediments of Chesapeake Bay and the mid-Atlantic continental margin. Marine Chemistry 114, 86-101.

Hollweg, T., Gilmour, C., and Mason, R. (2010). Mercury and methylmercury cycling in sediments of the mid-Atlantic continental shelf and slope. Limnology and Oceanography 55, 2703-2722.

Jackson, J., Allen, S., Carmack, E., and McLaughlin, F. (2010). Suspended particles in the Canada Basin from optical and bottle data, 2003-2008. Ocean Science 6, 799.

Jones, E., and Anderson, L. (1986). On the origin of the chemical properties of the Arctic Ocean halocline. Journal of Geophysical Research: Oceans 91, 10759-10767.

Karstensen, J. (2006). OMP (Optimum Multiparameter) Analysis-User Group (Lamont-Doherty Earth Obs. Palisades, NY).

Kirk, J.L., St. Louis, V.L., Hintelmann, H., Lehnherr, I., Else, B., and Poissant, L. (2008). Methylated mercury species in marine waters of the Canadian high and sub Arctic. Environmental Science & Technology 42, 8367-8373.

Kraepiel, A.M., Keller, K., Chin, H.B., Malcolm, E.G., and Morel, F.M. (2003). Sources and variations of mercury in tuna. Environmental Science & Technology 37, 5551-5558.

Lamborg, C.H., Hammerschmidt, C.R., Gill, G.A., Mason, R.P., and Gichuki, S. (2012). An intercomparison of procedures for the determination of total mercury in seawater and

recommendations regarding mercury speciation during GEOTRACES cruises. Limnology and Oceanography: Methods 10, 90-100.

Lamborg, C.H., Yiğiterhan, O., Fitzgerald, W.F., Balcom, P.H., Hammerschmidt, C.R., and Murray, J. (2008). Vertical distribution of mercury species at two sites in the Western Black Sea. Marine Chemistry 111, 77-89.

Lansard, B., Mucci, A., Miller, L.A., Macdonald, R.W., and Gratton, Y. (2012). Seasonal variability of water mass distribution in the southeastern Beaufort Sea determined by total alkalinity and δ18O. Journal of Geophysical Research: Oceans 117(C3).

Lehnherr, I. (2014). Methylmercury biogeochemistry: a review with special reference to Arctic aquatic ecosystems. Environmental Reviews 22, 229-243.

Lehnherr, I., Louis, V.L.S., Hintelmann, H., and Kirk, J.L. (2011). Methylation of inorganic mercury in polar marine waters. Nature Geoscience 4, 298-302.

Macdonald, R., Carmack, E., McLaughlin, F., Iseki, K., Macdonald, D., and O'Brien, M. (1989). Composition and modification of water masses in the Mackenzie Shelf Estuary. Journal of Geophysical Research: Oceans 94, 18057-18070.

Mackas, D.L., Denman, K.L., and Bennett, A.F. (1987). Least squares multiple tracer analysis of water mass composition. Journal of Geophysical Research: Oceans 92, 2907-2918.

Mason, R., Rolfhus, K., and Fitzgerald, W. (1995). Methylated and elemental mercury cycling in surface and deep ocean waters of the North Atlantic. In Mercury as a Global Pollutant (Springer), pp. 665-677.

Mason, R., Rolfhus, K.a., and Fitzgerald, W. (1998). Mercury in the north Atlantic. Marine Chemistry 61, 37-53.

Mason, R.a., and Sullivan, K. (1999). The distribution and speciation of mercury in the South and equatorial Atlantic. Deep Sea Research Part II: Topical Studies in Oceanography 46, 937-956.

Mason, R.P., Choi, A.L., Fitzgerald, W.F., Hammerschmidt, C.R., Lamborg, C.H., Soerensen, A.L., and Sunderland, E.M. (2012). Mercury biogeochemical cycling in the ocean and policy implications. Environmental Research 119, 101-117.

Mason, R.P., and Fitzgerald, W.F. (1993). The distribution and biogeochemical cycling of mercury in the equatorial Pacific Ocean. Deep Sea Research Part I: Oceanographic Research Papers 40, 1897-1924.

Mason, R.y., and Fitzgerald, W. (1990). Alkylmercury species in the equatorial Pacific. Nature 347, 457−459.

McTigue, N., Gardner, W., Dunton, K., and Hardison, A. (2016). Biotic and abiotic controls on co-occurring nitrogen cycling processes in shallow Arctic shelf sediments. Nature Communications 7, 13145.

Miller, L.A., Papakyriakou, T.N., Collins, R.E., Deming, J.W., Ehn, J.K., Macdonald, R.W., Mucci, A., Owens, O., Raudsepp, M., and Sutherland, N. (2011). Carbon dynamics in sea ice: A winter flux time series. Journal of Geophysical Research: Oceans 116(C2).

Monperrus, M., Tessier, E., Amouroux, D., Leynaert, A., Huonnic, P., and Donard, O. (2007). Mercury methylation, demethylation and reduction rates in coastal and marine surface waters of the Mediterranean Sea. Marine Chemistry 107, 49-63.

Munson, K.M., Lamborg, C.H., Swarr, G.J., and Saito, M.A. (2015). Mercury Species Concentrations and Fluxes in the Central Tropical Pacific Ocean. Global Biogeochemical Cycles 29, 656-676.

Parks, J.M., Johs, A., Podar, M., Bridou, R., Hurt, R.A., Smith, S.D., Tomanicek, S.J., Qian, Y., Brown, S.D., and Brandt, C.C. (2013). The genetic basis for bacterial mercury methylation. Science 339, 1332-1335.

Podar, M., Gilmour, C.C., Brandt, C.C., Soren, A., Brown, S.D., Crable, B.R., Palumbo, A.V., Somenahally, A.C., and Elias, D.A. (2015). Global prevalence and distribution of genes and microorganisms involved in mercury methylation. Science Advances 1, e1500675.

Pongratz, R., and Heumann, K.G. (1999). Production of methylated mercury, lead, and cadmium by marine bacteria as a significant natural source for atmospheric heavy metals in polar regions. Chemosphere 39, 89-102.

Rysgaard, S., Glud, R.N., Sejr, M., Bendtsen, J., and Christensen, P. (2007). Inorganic carbon transport during sea ice growth and decay: A carbon pump in polar seas. Journal of Geophysical Research: Oceans 112(C3).

Shadwick, E., Thomas, H., Chierici, M., Else, B., Fransson, A., Michel, C., Miller, L., Mucci, A., Niemi, A., and Papakyriakou, T. (2011). Seasonal variability of the inorganic carbon system in the Amundsen Gulf region of the southeastern Beaufort Sea. Limnology and Oceanography 56, 303-322.

Soerensen, A.L., Jacob, D.J., Schartup, A., Fisher, J.A., Lehnherr, I., St Louis, V.L., Heimbürger, L.E., Sonke, J.E., Krabbenhoft, D.P., and Sunderland, E.M. (2016). A Mass Budget for Mercury and Methylmercury in the Arctic Ocean. Global Biogeochemical Cycles 30, 560-575.

Sunderland, E.M., Krabbenhoft, D.P., Moreau, J.W., Strode, S.A., and Landing, W.M. (2009). Mercury sources, distribution, and bioavailability in the North Pacific Ocean: Insights from data and models. Global Biogeochemical Cycles 23, 1-14.

Tanhua, T., Jones, E.P., Jeansson, E., Jutterström, S., Smethie, W.M., Wallace, D.W., and Anderson, L.G. (2009). Ventilation of the Arctic Ocean: Mean ages and inventories of anthropogenic CO2 and CFC-11. Journal of Geophysical Research: Oceans 114(C1).

Tomczak, M., and Large, D.G. (1989). Optimum multiparameter analysis of mixing in the thermocline of the eastern Indian Ocean. Journal of Geophysical Research: Oceans 94, 16141-16149.

Tremblay, J.É., Simpson, K., Martin, J., Miller, L., Gratton, Y., Barber, D., and Price, N.M. (2008). Vertical stability and the annual dynamics of nutrients and chlorophyll fluorescence in the coastal, southeast Beaufort Sea. Journal of Geophysical Research: Oceans 113(C7).

Wang, F., Macdonald, R.W., Armstrong, D.A., and Stern, G.A. (2012a). Total and Methylated Mercury in the Beaufort Sea: The Role of Local and Recent Organic Remineralization. Environmental Science & Technology 46, 11821-11828.

Wang, Q., Myers, P.G., Hu, X., and Bush, A.B. (2012b). Flow constraints on pathways through the Canadian Arctic Archipelago. Atmosphere-Ocean 50, 373-385.

Wang, K., Munson, K.M., Beaupré-Laperrière, A., Mucci, A., Macdonald, R.M., Wang, F. (2018). Subsurface seawater methylmercury maximum explains biotic mercury concentrations in the Canadian Arctic. Scientific Reports, 8(1), 14465. https://doi.org/10.1038/s41598-018-32760-0.

Whalin, L., Kim, E.-H., and Mason, R. (2007). Factors influencing the oxidation, reduction, methylation and demethylation of mercury species in coastal waters. Marine Chemistry 107, 278-294.

Wheeler, P., Watkins, J., and Hansing, R. (1997). Nutrients, organic carbon and organic nitrogen in the upper water column of the Arctic Ocean: implications for the sources of dissolved organic carbon. Deep Sea Research Part II: Topical Studies in Oceanography 44, 1571-1592.

Yamamoto-Kawai, M., McLaughlin, F., Carmack, E., Nishino, S., Shimada, K., and Kurita, N. (2009). Surface freshening of the Canada Basin, 2003–2007: River runoff versus sea ice meltwater. Journal of Geophysical Research: Oceans 114(C1).

Supplementary Information

Table 4-S1: Definitions of source-water masses with multi-parameters.

Source-water masses	Salinity	$\delta^{18}O$ (‰)	TA (µmol/kg)	DIC (µmol/kg)	Pot.Temp. (°C)	DO (µmol/kg)
MW[a] Meteoric Water (Mackenzie River)	0	-19.94 ± 1.27	1714 ± 200	1700 ± 60	0 to +20	330
SIM Sea-ice melt	5.0 ± 0.5[b,c]	-2.00 ± 0.50[d]	415 ± 35[b,c]	330 ± 30[b,c]	0 ± 0.2	380
PML[e] Polar Mixed Layer	31.8 ± 0.1	-2.2 ± 0.2	2256 ± 12	2162 ± 14	-1.65 ± 0.05	331
UHW Upper Halocline (Pacific) Water	33.15 ± 0.10	-1.40 ± 0.01	2291 ± 15	2245 ± 20	-1.48 ± 0.02	263
N-ATW Northern (Arctic) Atlantic Water	34.83 ± 0.01	+0.20	2307 ± 20	2166 ± 18	0.70 ± 0.05	253
CBDW Canada Basin Deep Water	34.90 ± 0.01	+0.27 ± 0.01	2309 ± 12	2160 ± 10	-0.50	291
BBAW Baffin Bay Arctic Water	33.52 ± 0.02	-1.25 ± 0.05	2249 ± 2	2149 ± 2	-1.50	319
S-ATW Southern (Labrador Sea) Atlantic Water	34.47 ± 0.03	-0.14	2274 ± 6	2153 ± 4	3.24	280
BBDW Baffin Bay Deep Water	34.49	-0.45 ± 0.01	2296 ± 4	2265 ± 7	-0.25 ± 0.05	136

± values represent ranges derived from the use of two or more observations for a single source-water definition, rather than uncertainties.

a: Arctic Great Rivers Observatory Project; 2009-2012.

b: Rysgaard et al. (2007).

c: Miller et al. (2011).

d: Yamamoto-Kawai et al. (2009).

e: Lansard et al. (2012).

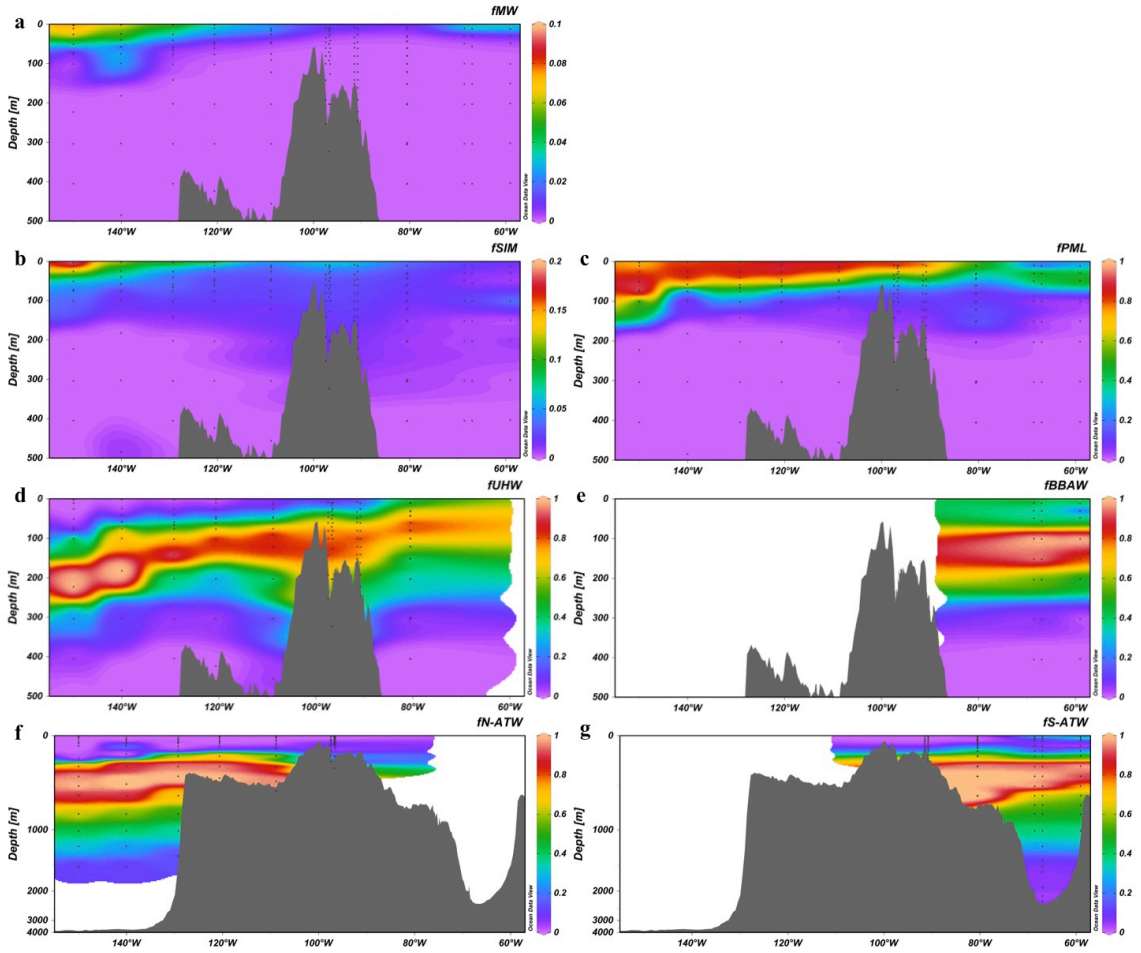

Figure 4-S1: Source-water mass fractions in the seawater along the longitudinal (west-to-east) section in the Canadian Arctic: a) MW, Meteoric Water; b) SIM, Sea-Ice Melt; c) PML, Polar Mixed Layer; d) UHW, Upper Halocline Water; e) BBAW, Baffin Bay Arctic Water; f) N-ATW, North-flowing Atlantic Water; g) S-ATW, South Atlantic Water. The water masses of CBDW and BBDW are located in the bottom of the Canada Basin and Baffin Bay, respectively.

Table 4-S2: Equation parameters of the methylated mercury (MeHg, pM) versus apparent oxygen utilization (AOU, µmol/L) relationship at each individual station in the upper layer of the Canadian Arctic.

Station	Regression coefficient	Origin	r^2	p	N
BB1	0.0006	0.1191	0.14	>0.10	5
BB2	-0.0010	0.2100	0.41	<0.05	9
BB3	0.0009	0.1585	0.45	<0.10	6
CAA1	0.0013	0.0958	0.47	<0.10	6
CAA2	0.0010	0.0885	0.44	<0.10	7
CAA3	0.0015	0.1206	0.60	<0.10	9
CAA4	0.0017	0.2218	0.64	<0.05	7
CAA5	0.0012	0.0865	0.33	<0.10	9
CAA6	0.0014	0.1420	0.58	<0.05	7
CAA7	0.0010	0.2069	0.17	>0.10	7
CAA8	0.0025	0.2622	0.64	<0.10	5
CAA9	0.0014	0.2219	0.27	<0.10	10
CB1	0.0036	0.2264	0.68	<0.05	5
CB2	0.0023	0.1778	0.41	<0.10	7
CB3	0.0014	0.1934	0.16	>0.10	9
CB4	0.0030	0.1431	0.46	<0.05	7

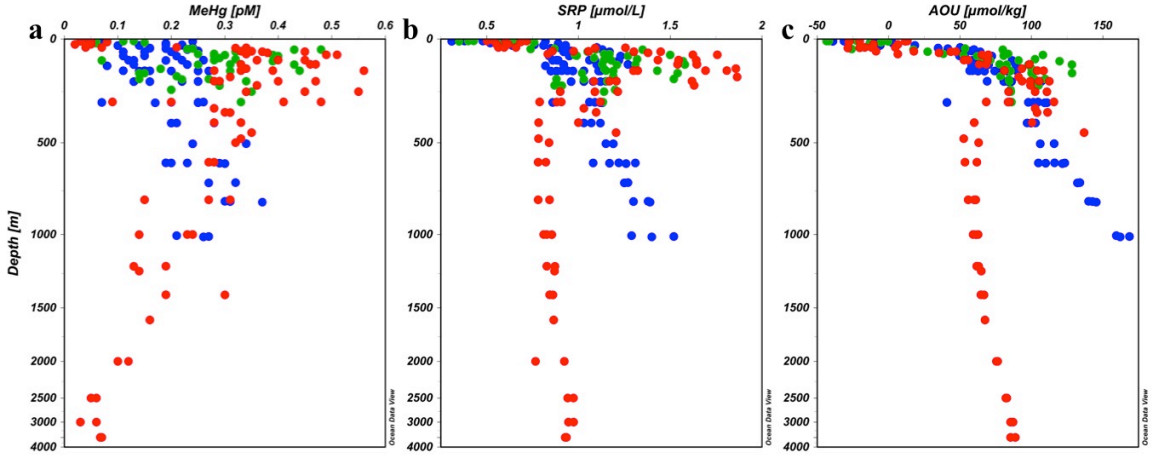

Figure 4-S2: Vertical profiles of methylmercury (MeHg, a), soluble reactive phosphorus (SRP, b) and apparent oxygen utilization (AOU, c).

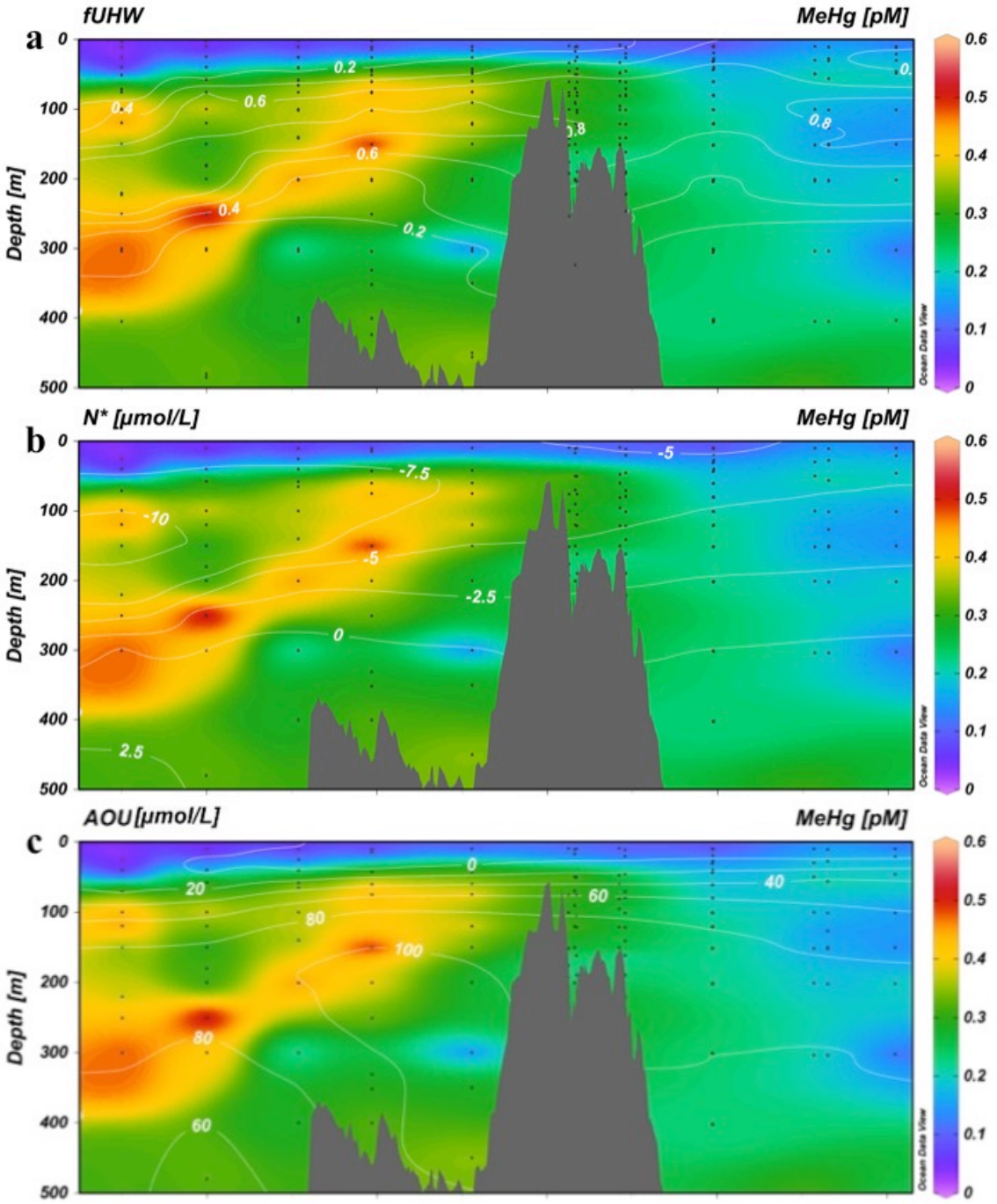

Figure 4-S3: The distributions of methylmercury (MeHg, color coded) overlaid with the contours of the fraction of the upper halocline water (f_{UHW}, a) and the concentration of N* (b), apparent oxygen utilization (AOU, c), SRP (d), and fluorescence (e) in the upper 500 m of the Canadian Arctic.

Figure 4-S3: Continued

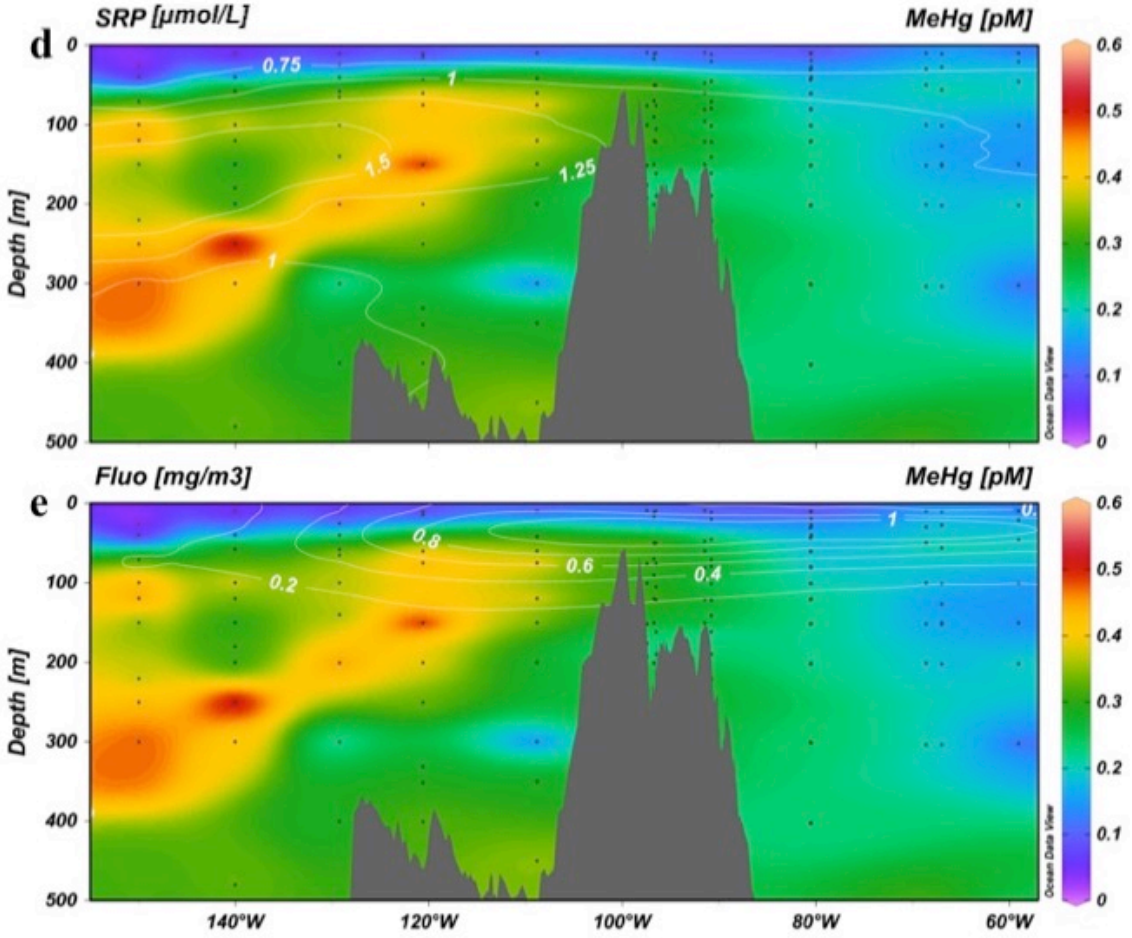

Chapter 5: Bioaccumulation Pathways of Monomethylmercury in an Arctic Marine Copepod

Abstract

Monomethylmercury (MMHg) is a contaminant of major concern in the Arctic marine ecosystem, due to its biomagnification and potential toxicity in marine mammals and Indigenous Peoples. Extensive efforts have been undertaken in the past decades to understand mercury (Hg) and MMHg concentrations in higher trophic-level animals; however, much less is known about Hg dynamics at the base of Arctic marine food web. Based on a series of incubation experiments with the addition of isotopically enriched inorganic Hg(II), here we report MMHg bioaccumulation in *Calanus hyperboreus*, a key herbivorous copepod that serves as a major energy source to higher trophic level organisms in the Arctic marine food web. Our results show that the copepod preferentially bioaccumulated MMHg over inorganic Hg, and that the MMHg uptake was primarily via trophic transfer with a minor contribution from seawater bioconcentration. Mercury methylation ratios determined from incubation experiments do not support the hypothesis of Hg methylation enhancement in the copepod guts or fecal pellets, suggesting these microenvironments are unlikely hotspots for Hg methylation. Our results also suggest an inhibitory effect of marine algae on Hg methylation in seawater, which may contribute to the low concentrations of methylated Hg at the depth of the subsurface chlorophyll a maximum in the world's oceans.

5.1 Introduction

Monomethylmercury (MMHg) is a neurotoxin and its elevated concentrations in Arctic marine mammals elicit major concerns over the health of these animals (AMAP, 2011; AMAP, 2018). In the Arctic, the methylated mercury (MeHg, sum of MMHg and dimethylmercury (DMHg)) peaks in subsurface seawater (Heimbürger et al., 2015; Wang et al., 2012; Wang et al., 2018), which readily explains the longitudinal gradients of biotic mercury (Hg) levels in the Canadian Arctic (Wang et al., 2018). Through the process of bioaccumulation, MMHg concentrations can increase over 10^6 times from seawater (often <0.1 ng/L) to top predators such as ringed seals (*Phoca hispida*), beluga whales (*Delphinapterus leucas*) and polar bears (*Ursus maritimus*), where they frequently exceed toxicity thresholds (AMAP, 2011, 2018). As Indigenous Peoples rely on marine mammal tissues as their traditional diets, the high Hg concentrations in these animals also raise concerns over human health (AMAP, 2009, 2011).

Most of the literature studies on biotic Hg in the Arctic have focused on top predators (AMAP, 2011, 2018). However, the most critical step in Hg bioaccumulation and biomagnification occurs at lower trophic levels such as phytoplankton and zooplankton (Foster et al., 2012; Lee and Fisher, 2017; Pućko et al., 2014; Schartup et al., 2017). In marine ecosystems, the bioaccumulation factor (BAF) of MMHg, calculated as the ratio of the MMHg concentration in biota (typically in wet weight) to that in water, can reach 10^5 L/kg for phytoplankton, and further increase 2–10 times per increasing trophic level (Hammerschmidt et al., 2013). Zooplankton also plays an important role in the bioaccumulation process, as it builds up MMHg from seawater and phytoplankton, and facilitates its transfer to marine animals at higher trophic level (Lee and Fisher, 2017;

Schartup et al., 2017). Despite their importance, few studies have examined bioconcentration and biomagnification of MMHg at the base of marine food web (Schartup et al., 2017), especially in the Arctic (Foster et al., 2012; Pućko et al., 2014).

In the Arctic marine ecosystem, *Calanus hyperboreus* is a key zooplankton species because of its abundance and large size (Hirche, 1997). This species and other *Calanus* species constitute most of the overall zooplankton biomass, reserve large amounts of lipids (Darnis and Fortier, 2012), and serve as major energy sources to higher trophic level organisms (Hop and Gjøsæter, 2013). Of particular interest is a recent revelation that *C. hyperboreus* may play a key role in Hg transformation (Pućko et al., 2014). While the total Hg (Hg_T) concentration in *C. hyperboreus* was similar to its prey of pelagic particulate organic matter (POM), this species shifted the Hg speciation from being primarily inorganic Hg in the pelagic POM (>99.5%) and ambient seawater (>90%) to MMHg (>50%) in its tissues. As dietary uptake only supplied ~30% of the MMHg in *C. hyperboreus*, Pućko et al. (2014) speculated that the rest of MMHg in the copepod must be either from bioconcentration from the ambient seawater, or produced by the copepod, presumably in its guts where anaerobic environment is known to develop (Tang et al., 2011). The latter, if true, would provide a new mechanism for in-situ MeHg production in the seawater column. The anoxic conditions can also form inside the fresh fecal pellets of zooplankton (Alldredge and Cohen, 1987), and favors the anaerobic Hg methylation. However, there has been no experimental study on whether Hg methylation occurs in the zooplankton guts or fecal pellets.

In this study, we performed a series of incubation experiments with the addition of isotopic enriched inorganic Hg(II) to study Hg bioaccumulation in *C. hyperboreus* and

estimate the relative contributions from different pathways, including seawater bioconcentration, trophic transfer, and the potential Hg methylation in guts. In addition to the MMHg production in copepod guts, we also examined the potential enhancement of Hg methylation in fecal pellets.

5.2 Material and Methods

5.2.1 Study Sites and Sampling

In collaboration with P. Stief and R. Glud of the Southern Denmark University, the incubation experiments were carried out in May 2014 at the Arctic Station (69°15′N, 53°31′W), a field station affiliated with the University of Copenhagen, in Disko Bay, Southwest Greenland (Figure 5-1). Seawater and copepods were freshly collected onboard *R/V Porsild* at a 320-m deep station (69°13′N, 53°23′W), which is located in Davis Strait approximately 2 km off the coast. There are three water masses at the sampling site: the Polar Mixed Layer at the surface (<50 m), the Pacific Water (50–200 m) flowing in through the Lancaster Sound and Nares Strait, and the Atlantic Water (from 200 m to the bottom) flowing in with the Western Greenland Currents (Tang et al., 2004).

Seawater was collected at the depth of 150 m where MeHg typically peaks (Wang et al., 2018) by using 30-L Niskin bottles installed on a frame with a Seabird CTD. Copepods were collected by vertical hauls from the top 200 m depths, using a WP-3 net (200 μm mesh size) with a large non-filtering cod-end. Immediately after collection, the copepods were transferred to a thermo box with seawater at the in-situ temperature under dark conditions. Immediately after collection, stage V copepodites, adult males and

females of *C. hyperboreus* were selected by prosome length (Scott et al., 2000), and starved for 24 h prior to the incubation experiments.

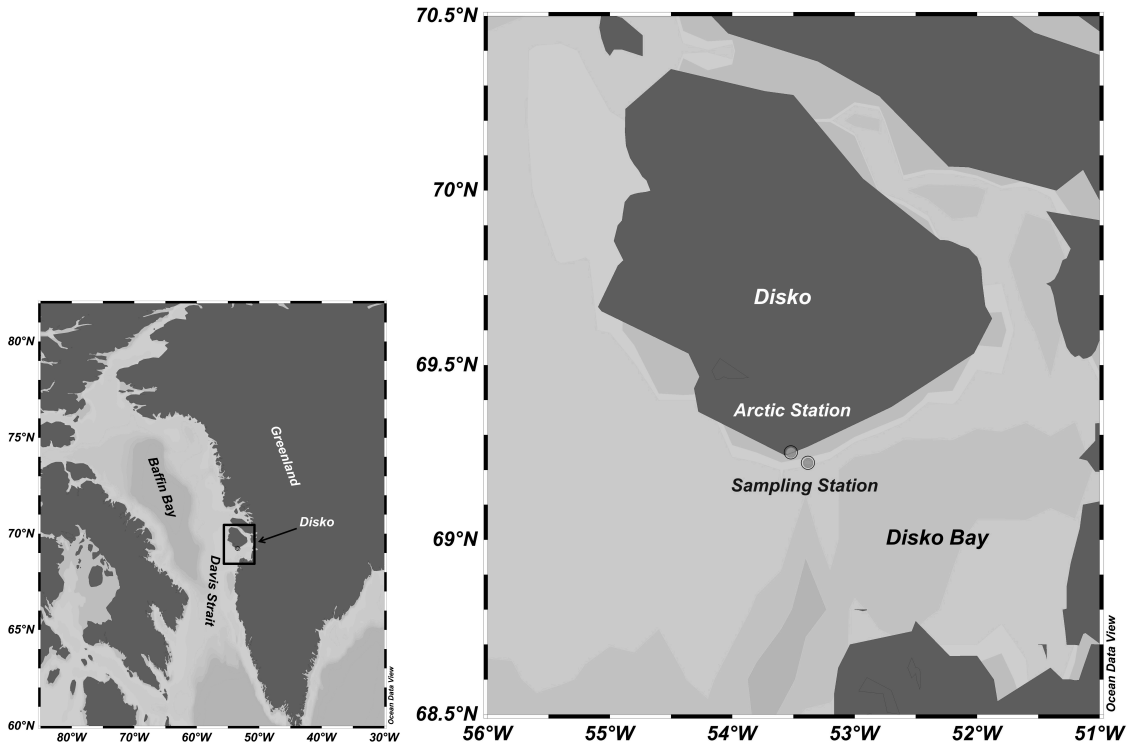

Figure 5-1: The map of the Disko Bay, Greenland, showing the sampling station and the Arctic Station where incubation experiments were performed.

5.2.2 Incubation Experiments

The incubation experiments were performed in four groups (Figure 5-2). The incubation seawater had a dissolved oxygen (DO) concentration of over 80% air saturation, similar to that in seawater at 150 m in the Arctic. The cryptophyte *Rhodomonas salina* fed to the copepods was from filtered seawater cultures in exponential growth phase (Nørregaard et al., 2014). Group 1–3 incubations were performed in duplicates, and Group 4 incubations were performed in triplicates.

Incubation Group 1 without algae and copepods served as a control study. Groups 2 with algae only and 3 with starving copepods only aimed to measure bioconcentration

of Hg species from seawater to algae and copepod, respectively. Group 4 with both algae and copepods aimed to study copepod uptake of Hg species from seawater bioconcentration, trophic transfer, as well as the potential for Hg methylation in the anoxic guts. In addition to the potential gut methylation, Group 4 also aimed to test the potential Hg methylation in fecal pellets of *C. hyperboreus*. As the copepods were not fed in Group 3, the gut DO would not be fully depleted in the starving individuals (Tang et al., 2011) and fecal pellets would not be produced. Therefore, anaerobic Hg methylation would not occur in guts of copepods of Group 3 incubations.

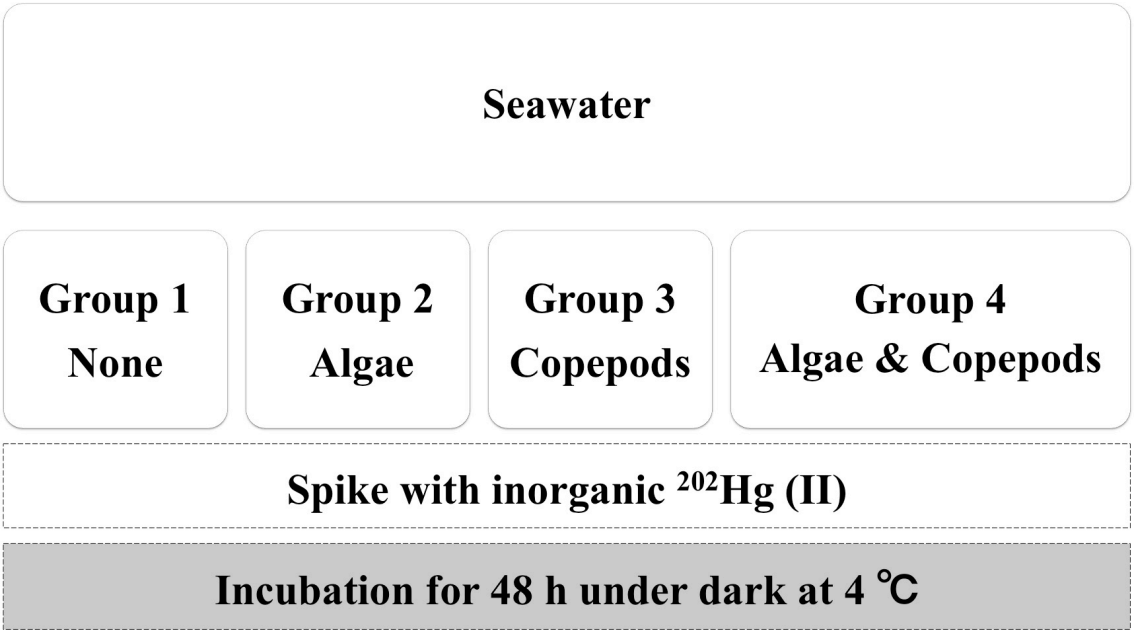

Figure 5-2: Flow chart of the experimental procedures for the incubations.

To start the incubation experiment, the unfiltered seawater was transferred into pre-cleaned, airtight glass bottles (250 mL, with Teflon cap liner, DURAN). The bottles were then spiked with inorganic ^{202}Hg(II) to a concentration of ~1000 ng/L, followed by the addition of starving copepods for Groups 3 and 4 (five individuals in each bottle), and the cryptophyte *R. salina* to a cell density of ~1.1×10^5 cells/mL for Groups 2 and 4 (Figure 5-2). Then, the bottles were filled with the unfiltered seawater and capped

without headspace. Given the small mass of the copepods (~2 mg/individual), the inorganic ^{202}Hg(II) was added to the incubated seawater to a target concentration three orders of magnitude higher than in natural seawater, to ensure that the potential methylation in the presence of copepods would be detectable. The inorganic ^{202}Hg(II) stock solution was prepared following the procedures described in Chapter 3 of this study. Immediately after the additions, all bottles were fixed to a phytoplankton wheel rotating at 1 rpm to keep the system well mixed during incubations. All experiments were performed at 4 °C in the dark to mimic the ambient cold, dark conditions in the Arctic seawater. All copepods were living actively, and those in Group 4 kept grazing algae and producing fecal pellets throughout the incubations. At 0, 24 and 48 h of the incubation, the phytoplankton wheel was stopped for parameter measurements. The seawater DO and temperature were measured with an optical O_2 meter (FireStingO_2, Pyroscience, Germany) and an optode spots (SensorSpot, Pyroscience, Germany) placed on the inside of the incubation bottle, respectively. Less than 1 mL of the incubated seawater was sampled for the measurements of the *R. salina* cell density by counting cells with a hemocytometer under microscopy after Lugol's fixation (Figure 5-S1).

The incubations were stopped 48 h after the inorganic ^{202}Hg(II) addition and different samples were collected from the incubation bottles. Copepods were sampled into 15 mL HDPE bottles with a pair of pre-cleaned Teflon tweezers. For incubations with algae, the seawater was filtered through pre-combusted and weighed GF/F filters (Whatman, nominal pore size of 0.7 μm). The filters were then collected into 50 mm petri dishes for algae (and fecal pellets) samples, and the filtrates were sampled into 50 mL new polypropylene tubes (BD Falcon) and pre-cleaned Teflon bottles for the analysis of

seawater Hg_T and MMHg, respectively. The samples of algae and fecal pellets were not further differentiated in Group 4. Seawater samples were also collected from incubations without algae. The seawater samples for Hg_T were acidified to 0.5% (v/v) with concentrated HCl (CMOS grade, JT Baker), and the MMHg seawater samples were frozen to prevent conversion from DMHg (Black et al., 2009). All samples were kept refrigerated at 4 ºC (seawater Hg_T samples) or frozen at –20 ºC (all other samples) during storage and shipment to the Ultra-Clean Trace Elements Laboratory (UCTEL) at the University of Manitoba for analysis.

5.2.3 Analysis of Mercury Species Isotopes

Seawater Hg_T samples were oxidized using 0.5% BrCl v/v (prepared from KBr and $KBrO_3$ in 95 % concentrated HCl, JT Baker) for at least 6 h before being analyzed. Seawater MMHg was extracted through dichloromethane extraction and back extraction to water by solvent evaporation (Horvat et al., 1993). For the copepod and filter samples, extra preparation was required to measure Hg species and isotopes. The dry weight of algae (and fecal pellets) were determined by: 1) drying the filter with algae (and fecal pellets) in an oven at 60 ºC (VWR symphony Gravity Convection Oven 414004-550) and weighing it on an analytical balance (Mettler Toledo AG204); 2) subtracting the dry weight of filter previously measured following the same procedures (Pućko et al., 2014). Copepods were freeze-dried in freeze dryer (Labconco FreeZone) and weighed on a microbalance (Mettler Toledo XPR6UD5) (Pućko et al., 2014). Copepods were digested in 4 M HNO_3 at 55 ºC for 16 h (Hintelmann and Nguyen, 2005), and filters were digested in aqua regia (volume ratio of H_2SO_4 and HNO_3 at 4:1) at 180 ºC for 4 h (Hendzel and

Jamieson, 1976). The digest of copepods was split for Hg_T and MMHg analysis. MMHg in copepods digest was extracted with dichloromethane following same procedures as for seawater (Horvat et al., 1993). The procedures of filter MMHg extraction were based on acid leaching with $HNO_3/CuSO_4$, dichloromethane extraction and back extraction into water (Carrasco and Vassileva, 2015).

After sample preparation, Hg_T and MMHg were analyzed for their isotope abundances using cold vapor atomic fluorescence spectrometry (CVAFS)-ICPMS. The Hg_T was analyzed on a Tekran 2600 Hg analyzer following U.S. EPA 1631 (EPA, 2002). The MMHg was analyzed on a MERX (the Brooks Rand Automatic Methylmercury System) following U.S. EPA 1630 (EPA, 2001), in which Hg species are ethylated with $NaB(Et)_4$ and separated by gas chromatography column before CVAFS detection. The Hg species from the Tekran 2600 and MERX were then directed to an ICPMS (Perkin Elmer Elan DRC II) by a polyethylene line for the determination of Hg species-specific isotope abundances. Relative counts of different isotopes were integrated using MATLAB scripts to quantify isotopic signals in the peaks of Hg_T and MMHg. Among the seven isotopes of Hg, only isotopes 202 and 200 were quantified for further calculations (see Section 5.2.4 for details). Figure 5-S2 shows example chromatogram for isotopes of Hg_T, MMHg and inorganic Hg(II). Calculated as three times standard deviation of seven laboratory blank replicates, detection limits (DL) were 0.48, 0.33 pg for $MM^{202}Hg$ and $MM^{200}Hg$, and 1.67, 0.97 pg for $^{202}Hg_T$ and $^{200}Hg_T$, respectively. When sampling from incubation bottles, Milli-Q water was also collected to serve as field blanks, and the concentrations were lower than DL for both Hg_T and MMHg. By analyzing certified reference material (CRM), the recoveries were calculated as 91–115%

and 75–93% for Hg_T and MMHg, respectively. In this study, the CRM used for Hg_T and MMHg were BCR-579 (Coastal Seawater, 1.9 ± 0.5 ng/kg, Institute for Reference Materials and Measurements, European Commission - Joint Research Centre) and Tort 3 (Lobster Hepatopancreas Reference Material for Trace Metals, 0.137 ± 0.012 mg/kg, National Research Council Canada), respectively.

5.2.4 Calculation for Mercury Bioaccumulation and Mercury Methylation

The measured Hg isotopes were from two sources: Hg in the ambient environment (e.g., ambient seawater) and that from added inorganic ^{202}Hg(II). For example, ambient $^{200}Hg_T$ and the minor $^{200}Hg_T$ component of the added inorganic ^{202}Hg(II) both contributed to the measured $^{200}Hg_T$; $MM^{202}Hg$ in the ambient environment and that methylated from added inorganic ^{202}Hg(II) formed the measured $MM^{202}Hg$. With a linear matrix inverse approach (Hintelmann and Evans, 1997; Hintelmann and Ogrinc, 2003), in which ^{200}Hg and ^{202}Hg were assigned as tracer isotopes of ambient and added Hg, respectively, we were able to distinguish contributions of spiked Hg from that of ambient Hg in the Hg_T and MMHg isotopes measured for each sample (see Appendix for details).

Although both ambient and added Hg contributed to the Hg bioaccumulation in algae and copepods during the incubation, we quantify only that of added Hg, as much of the ambient Hg in the organisms was accumulated in their life stages prior to the 48-h incubation experiments. By dividing the biotic concentrations of Hg_T and MMHg from added Hg to these concentrations in the incubated marine waters, the BAFs of Hg species in algae and copepods were calculated. We used the different incubation groups to assess the contributions from different pathways to the total bioaccumulation, including

seawater bioconcentration, trophic transfer, and the potential Hg methylation in copepod guts. For algae and starving copepods, the calculated BAFs are essentially bioconcentration factors (BCFs), as seawater bioconcentration is the sole pathway for observed bioaccumulation. For copepods feeding with algae, the contribution of seawater bioconcentration is assumed to be equal to the BAF measured in starving copepods (Hirota et al., 1983), with additional sources from trophic transfer and potential Hg methylation in copepod guts. By dividing the Hg species concentrations in copepods by those in algae and fecal pellets, we calculated the biomagnification factors (BMFs) in Group 4 incubations. The calculated BMFs may also include contribution from the potential Hg methylation in copepod guts and/or fecal pellets.

The isotope ratios of the MMHg peaks allow us to quantify methylation of the $^{202}Hg_T$ substrate. As Hg(0) can be directly methylated (Colombo et al., 2013), our method is of more rational than those in previous studies (Lehnherr et al., 2011; Monperrus et al., 2007), where only inorganic Hg(II) was taken as substrate for Hg methylation. By dividing MMHg methylated from added Hg isotope by the substrate, we calculated the methylation ratios for different sample types in each incubation group (detailed calculations are shown in Appendix). The overall methylation ratio was calculated for each incubation group so comparison can be made among different groups. To calculate the overall methylation ratio, we summed the Hg substrate and methylated MMHg from all sample types in an incubation, and then divided the summed MMHg by the summed Hg substrate.

5.3 Results and Discussion

5.3.1 Bioaccumulation of Mercury Species

Table 5-1 shows the log BAFs for MMHg and Hg_T in algae (and fecal pellets) and copepods from each incubation group. The BAF values were calculated from the concentrations of Hg_T and MMHg sourced from inorganic $^{202}Hg(II)$ additions (Table 5-S1). When calculating BAFs, we used dry weight biotic pollutant concentrations, instead of the typically used wet weight biotic pollutant concentrations (Arnot and Gobas, 2006). Hence, our log BAF values are ~0.7 greater than those expressed on the wet weight basis, assuming an 80% water content in marine phytoplankton (Fisher et al., 1983) and zooplankton (Omori, 1969). In all our samples, MMHg concentrations account for a very small portion (<0.1%) of Hg_T, so the BAFs calculated for Hg_T can be considered as BAFs for inorganic Hg.

Table 5-1: Bioaccumulation factors (BAFs) of total Hg (Hg_T) and monomethylmercury (MMHg) in algae (*Rhodomonas salina*) and fecal pellets, and copepod (*Calanus hyperboreus*) determined from the incubation experiments.

Incubation Groups	log BAF-Algae (and fecal pellets)		log BAF-Copepod	
	Hg_T	MMHg	Hg_T	MMHg
	(Mean ± standard deviation, range)		(Mean ± standard deviation, range)	
Group 2 (Algae)	4.55 ± 0.07, 4.48–4.63	4.34 ± 0.16, 4.19–4.50		
Group 3 (Copepods)			3.80 ± 0.02, 3.78–3.82	4.21 ± 0.11, 4.10–4.32
Group 4 (Algae & Copepods)	4.40 ± 0.05, 4.34–4.44	4.18 ± 0.25, 3.82–4.38	4.40 ± 0.04, 4.34–4.42	4.98 ± 0.20, 4.73–5.23

In this study, all the BAFs for Hg_T and MMHg fall within the wide ranges reported in previous studies when converted to a wet weight basis. Here the samples of algae and fecal pellets in Group 4 were also categorized as phytoplankton, because their

Hg BAFs are not significantly different (t test, $p > 0.05$) from those of algae in Group 2. The plankton BAFs for Hg species are influenced by a series of factors, including the sampling season, dissolved organic carbon concentrations, biota species, sizes and abundances (Gosnell et al., 2017; Lee and Fisher, 2016). Gosnell et al. (2017) measured BAFs for phytoplankton and zooplankton sampled in different seasons and in different size classes in Long Island Sound: phytoplankton log BAFs ranges were 2.4–5.0 and 2.6–5.5 for Hg_T and MMHg, respectively; zooplankton log BAFs ranges were 2.1–4.9 and 2.9–6.4 for Hg_T and MMHg, respectively.

5.3.2 Bioconcentration and Trophic Transfer of Mercury Species

For algae and fecal pellets, all the Hg bioaccumulation observed was from seawater bioconcentration. In both Groups 2 and 4, the algae (and fecal pellets) log BCFs for MMHg are not significantly different (t test, $p > 0.05$) from those for Hg_T (Table 5-1). This is because passive diffusion is the principal pathway for both MMHg and inorganic Hg to phytoplankton (Mason et al., 1996). The *R. salina* log BCFs for MMHg (4.34 ± 0.16) are lower than those recently measured (~4.85, wet weight basis) from incubations with the same species (Lee and Fisher, 2016), probably because the cell density in our incubations ($\sim 1.1 \times 10^5$ cells/ml) was much higher than theirs ($\sim 1.0 \times 10^4$ cells/ml), and because increasing cell density decreases phytoplankton BCFs (Lee and Fisher, 2016).

For copepods, pathways for Hg species bioaccumulation differed between incubation groups. In the absence of algae as food source, copepod BAFs in Group 3 are essentially BCFs. In Group 4, zooplankton also accumulated Hg species from trophic transfer, as they do in natural environments. Additionally, the potential gut Hg

methylation may also contribute to bioaccumulation of MMHg in copepods (Pućko et al., 2014). In the Beaufort Sea and Amundsen Gulf, *C. hyperboreus* Hg_T and MMHg concentrations (dry weight) were 14 ± 4 and 7 ± 1 ng/g (Pućko et al., 2014), respectively. Marine waters in the same regions had Hg_T concentrations of 0.22 ± 0.09 ng/L and MeHg concentrations of 0.04 ± 0.03 ng/L (Wang et al., 2012). Using these concentrations, the *C. hyperboreus* log BAFs for Hg_T and inorganic Hg were calculated as 4.80 and 4.59, respectively. The log BAFs for MMHg are in excess of the calculated value of 5.24, as seawater MMHg comprises only part of the measured MeHg concentrations in seawater. In Group 4, the *C. hyperboreus* log BAFs for both Hg_T (essentially inorganic Hg) (4.40 ± 0.04) and MMHg (4.98 ± 0.20) are lower than those from field observations. Bioaccumulation could have been limited by our short incubation period (48 h) as opposed to the active grazing season (~40 days *per* year) of *C. hyperboreus* in the field (Forest et al., 2011). Meanwhile, the copepod population density in our incubations (1.5×10^4 individuals /m^3) was much higher than in the Arctic Ocean (<1.5×10^3 individuals /m^3) (Dawson, 1978), and could lower the BAFs for MMHg (Hirota et al., 1983).

Table 5-2 shows the estimated contributions from different pathways to Hg_T and MMHg bioaccumulation in copepods fed with *R. salina* in Group 4 incubations. Seawater bioconcentration only accounted for a minor fraction of Hg bioaccumulation, with the contribution percentages at 25.6% ± 2.4% and 21.6% ± 9.3% for Hg_T and MMHg, respectively. Trophic transfer was the major pathway for Hg_T bioaccumulation, and its sum with the potential guts Hg methylation composed the major fraction of MMHg BAFs. Because Hg methylation was not enhanced in copepod guts (Section 5.3.3), trophic transfer was the primary pathway for MMHg bioaccumulation to copepods. This

is consistent with the current understanding that trophic transfer is the predominant pathway for MMHg to zooplankton while direct uptake from waters accounts for a minor fraction (Lee and Fisher, 2017; Schartup et al., 2017). In our calculations, BAFs from seawater bioconcentration in Groups 2 and 4 were assumed to be the same, despite different concentrations of Hg_T and MMHg. This assumption was based on a previous study that measured constant log BAFs at 6.44 ± 0.10 and 3.85 ± 0.10 for MMHg and Hg_T, respectively, in a copepod *Acartia clausi* incubated in the seawater with Hg species concentrations ranging from 50 to 500 ng/L (Hirota et al., 1983).

Table 5-2: Relative contributions of different pathways to bioaccumulation of total Hg (Hg_T) and monomethylmercury (MMHg) in copepods (*Calanus hyperboreus*) from Group 4 incubations.

	Hg_T Bioaccumulation	MMHg Bioaccumulation
Seawater bioconcentration	25.6% ± 2.4%, 23.7%–28.8%	21.6% ± 9.3%, 10.6%–32.9%
Trophic transfer	74.5% ± 2.4%, 71.2%–76.3%	79.5% ± 9.3%, 67.1%–89.4%

In both Groups 3 and 4, copepod log BAFs are significantly higher for MMHg than for Hg_T (t test, $p < 0.05$) (Table 5-1), demonstrating the preferential uptake of MMHg in copepods. The preferential bioaccumulation can either be from seawater bioconcentration or trophic transfer (Lee and Fisher, 2017; Schartup et al., 2017), and the latter is considered the major responsible mechanism (Mason et al., 1995; Wang and Wong, 2003). Direct uptake from seawater does contribute to the preferential bioaccumulation, as BAFs are higher for MMHg than for Hg_T in Group 3, where trophic transfer was absent. In Group 4, the calculated BMFs were only from trophic transfer, due to the absence of Hg methylation enhancement in copepod guts (Section 5.3.3).

Therefore, the higher (t test, $p < 0.01$) log BMFs for MMHg (6.60 ± 1.47, 4.62–8.14) than for Hg_T (0.99 ± 0.02, 0.96–1.01) suggest that trophic transfer has contributed to the preferential uptake of MMHg. The preferential biomagnification of MMHg results from its higher assimilation efficiencies (Lee and Fisher, 2017; Schartup et al., 2017). This might be related to the MMHg and inorganic Hg(II) distribution pattern in phytoplankton cell and the grazing behavior of zooplankton. Mason et al. (1995) found that inorganic Hg(II) was principally bound to phytoplankton cell membrane (91%), and MMHg mainly resided in cytoplasm (63%) (Mason et al., 1995). During the grazing process, zooplankton mainly digests cytoplasm content and simply defecates the membrane material (Reinfelder and Fisher, 1991).

5.3.3 Mercury Methylation Not Enhanced in Copepod Microenvironments

Figure 5-3 shows the overall methylation ratios of the four incubation groups, as well as the methylation ratios for different sample types in each group. According to the hypothesis that copepod guts or fecal pellets are hotspots for Hg methylation, we expected higher overall Hg methylation ratios in Groups 3 and 4 incubations with copepods, compared to seawater incubations (Group 1) controls. However, the overall methylation ratio in Group 1 ($(23.0 \pm 0.6) \times 10^{-5}$) is similar (t test, $p = 0.68$) to that in Group 3 ($(27.2 \pm 8.4) \times 10^{-5}$), and significantly higher (t test, $p < 0.01$) than that in Group 4 ($(8.8 \pm 1.2) \times 10^{-5}$) (Figure 5-3). Because Hg methylation was not enhanced in incubations with copepods, the hypothesis of accelerated Hg methylation in microenvironments is not supported. As anoxic conditions are unlikely to develop in guts of starving copepods, it is not surprising that Hg methylation was not enhanced in Group

3. In copepods feeding on algae, the guts and fecal pellets can become anaerobic to facilitate microbial production of MMHg (Alldredge and Cohen, 1987; Tang et al., 2011). However, Hg methylation in Group 4 was not enhanced as expected. Instead, its overall methylation ratio is even lower than that in Group 3 with starving copepods (t test, $p < 0.05$).

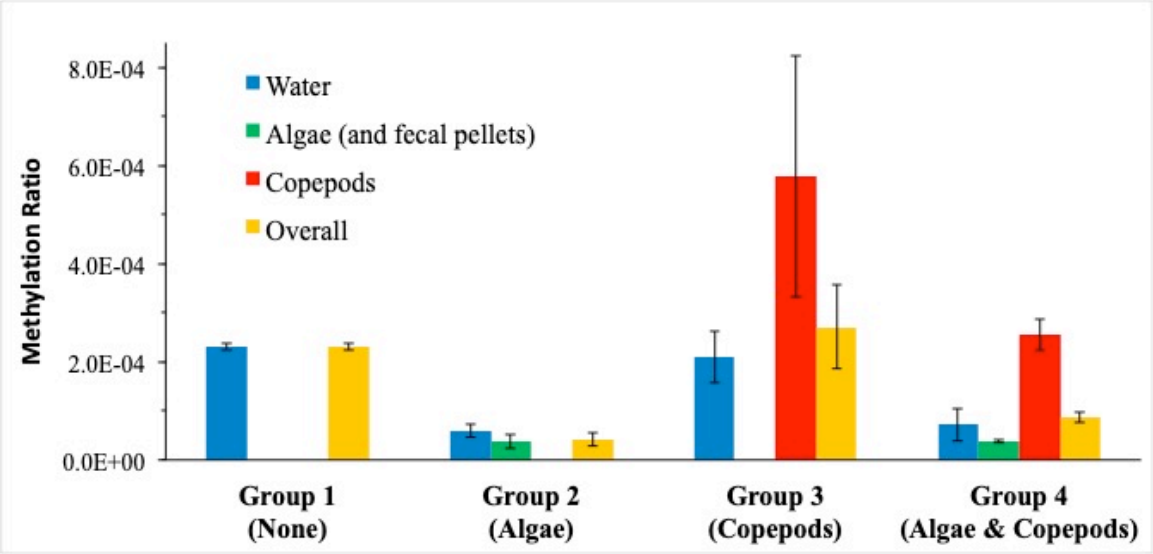

Figure 5-3: Overall and treatment-specific mercury methylation ratios determined from the incubation experiments.

In this study, Hg methylation was not enhanced in copepod guts or fecal pellets, probably because the anoxic conditions developed in these sites were not stable enough for the growth and thriving of Hg methylators. In a previous study, neither methanogenic bacteria nor sulfide were detected in anoxic aggregates composed of phytoplankton detritus and fecal pellets (Ploug et al., 1997). The authors explained that the anoxic conditions in the aggregates were too unstable (anoxia, high gradients of DO and pH did not persist) for methanogenic bacteria and sulfate reducing bacteria. The study also postulated that only microbes capable of tolerating wide range of DO and pH could efficiently exploit these anoxic environments. In copepod guts and fecal pellets, the

observed sharp DO and pH gradients could hardly sustain anaerobic conditions (Alldredge and Cohen, 1987; Tang et al., 2011). Therefore, the instability of the anoxic environment may have limited the anaerobic microbial activities, and the accompanying Hg methylation.

Alternatively, Hg methylation in copepod guts and fecal pellets might be zooplankton species-specific, as was seen in methane production, another anaerobic microbial process (de Angelis and Lee, 1994). Hence, the absence of microsite Hg methylation in our experiments does not necessarily mean that Hg methylation does not occur in microenvironments. However, if copepod methylation dominated seawater MeHg production, we would expect correlations between marine MeHg distribution, copepod abundance, and primary production. As primary production is much lower in the Canada Basin than in Baffin Bay and the eastern Canadian Arctic Archipelago, we would expect lower concentrations of MeHg in the Canada Basin. However, MeHg concentrations are higher in the Canada Basin than in Baffin Bay and the eastern Canadian Arctic Archipelago (Wang—this study, Chapters 2 and 4). Therefore, the MeHg production in microenvironments is unlikely an important MeHg source, even if the mechanism occurs.

5.3.4 Inhibitory Effects of Phytoplankton in Mercury Methylation

A recent study postulated that the presence of marine phytoplankton could enhance Hg methylation (Bratkič et al., 2016). However, this is not supported by our incubation experiments. The lowest overall Hg methylation ratio ($(4.2 \pm 1.4) \times 10^{-5}$) was observed in algae incubations (Group 2) (Figure 5-3). The incubations with algae (Groups

2 and 4) have an overall methylation ratio ($(6.6 \pm 2.2) \times 10^{-5}$) that is significantly lower (t test, $p < 0.05$) than that ($(25.0 \pm 2.0) \times 10^{-5}$) of incubations without algae (Groups 1 and 3). Moreover, the methylation ratio of seawater is significantly lower (t test, $p < 0.01$) in incubations with algae ($(6.6 \pm 0.6) \times 10^{-5}$ d^{-1}) than in incubations without algae ($(22.0 \pm 1.0) \times 10^{-5}$ d^{-1}). The lower overall and seawater methylation ratios in incubations with algae, along with the fact that algae (and fecal pellets) have the lowest methylation ratio of all samples types (Figure 5-3), suggest that algae may inhibit Hg methylation and/or facilitate MMHg demethylation. In a recent study, only about 10% of the added MMHg was lost during the 72-hour incubations with *R. salina* at cell densities of up to 2×10^4 cells/ml, and recoveries of the added MMHg were close to 100% for incubations with most other marine phytoplankton (Lee and Fisher, 2016). Therefore, the low methylation ratios observed in incubations with the same algae species were unlikely due to enhanced MMHg demethylation by marine algae. Although not directly applicable to the largely uncharacterized mechanisms for seawater Hg methylation, a recent study showed that *Skeletonema costatum*, a marine alga, greatly inhibited the methylation of Hg by an iron-reducing bacterium (*Geobacter sulfurreducens* PCA) (Ding et al., 2018). Algal inhibition of Hg methylation is consistent with the MeHg profiles observed in the world's oceans. Except at a few locations (Bowman et al., 2015; Bratkič et al., 2016; Heimbürger et al., 2010), most seawater profiles show low concentrations of MeHg at the depth of subsurface chlorophyll a maximum (SCM) (Cossa et al., 2011; Lehnherr et al., 2011; Munson et al., 2015; Sunderland et al., 2009; Wang et al., 2012). The inhibitory effects of algae may have contributed to the observed low MeHg concentrations at the depth of SCM in addition to photo-demethylation and biological uptake.

If *R. salina* indeed inhibits Hg methylation, it is possible that the low overall methylation ratio of Group 4 was the consequence of the inhibitory effects, while Hg methylation may still be enhanced in copepod guts and/or fecal pellets. If fecal pellets were hotspots of Hg methylation, the methylation ratio measured in algae and fecal pellets from Group 4 would be much higher than in algae from Group 2. However, the methylation ratio in algae and fecal pellets from Group 4 ($(4.0 \pm 0.4) \times 10^{-5}$) is similar (t test, $p = 0.97$) to that of algae from in Group 2 ($(3.8 \pm 1.4) \times 10^{-5}$). Likewise, if Hg methylation were enhanced in anoxic copepod guts, the methylation ratio of feeding copepods in Group 4 would be higher than that of starving copepods in Group 3. Instead, copepods methylation ratio in Group 4 ($(25.4 \pm 3.2) \times 10^{-5}$) is lower than that of starving copepods ($(57.6 \pm 24.6) \times 10^{-5}$) in Group 3 (Figure 5-3), although the difference is not significant (t test, $p = 0.09$). Therefore, our results do not support the hypothesis that Hg methylation is enhanced in copepod guts or fecal pellets. As a result, all the MMHg bioaccumulation in Group 4 was contributed from seawater bioconcentration and trophic transfer (Section 5.3.2, above).

5.4 Conclusions

Our incubation experiments examined the Hg bioaccumulation in *C. hyperboreus*, a key marine zooplankton species in the Arctic. The copepods accumulated Hg_T and MMHg from both seawater uptake and trophic transfer, and the latter was the dominant bioaccumulation mechanism. Comparing to inorganic Hg, MMHg was preferentially bioaccumulated in copepods through both bioconcentration and biomagnification.

Methylation of Hg was not enhanced in guts or fecal pellets in *C. hyperboreus*,

thus not supporting the hypothesis that these microenvironments are hotspots for MMHg production in marine environment. Although the hypothesized methylation mechanism may still occur in other zooplankton species, such MMHg production is unlikely the major source of seawater MeHg in the Arctic, as suggested by the high MeHg concentrations in the Canada Basin where primary production and zooplankton abundance are extremely low. Therefore, the production of marine MeHg in the Arctic must be in other mechanisms, which remain to be identified and elucidated by future studies.

References

Alldredge, A.L., and Cohen, Y. (1987). Can microscale chemical patches persist in the sea? Microelectrode study of marine snow, fecal pellets. Science 235, 689-691.

AMAP (2009). AMAP Assessment 2009: Human health in the Arctic. Arctic Monitoring and Assessment Program: Oslo.

AMAP (2011). AMAP Assessment 2011: Mercury in the Arctic. Arctic Monitoring and Assessment Program: Oslo.

AMAP (2018). AMAP Assessment 2018: Biological effects of contaminants on Arctic wildlife and fish. Mercury in the Arctic. Arctic Monitoring and Assessment Program: Tromsø.

Arnot, J.A., and Gobas, F.A. (2006). A review of bioconcentration factor (BCF) and bioaccumulation factor (BAF) assessments for organic chemicals in aquatic organisms. Environmental Reviews 14, 257-297.

Black, F.J., Conaway, C.H., and Flegal, A.R. (2009). Stability of dimethyl mercury in seawater and its conversion to monomethyl mercury. Environmental Science & Technology 43, 4056-4062.

Bowman, K.L., Hammerschmidt, C.R., Lamborg, C.H., and Swarr, G. (2015). Mercury in the north Atlantic ocean: The US GEOTRACES zonal and meridional sections. Deep Sea Research Part II: Topical Studies in Oceanography 116, 251-261.

Bratkič, A., Vahčič, M., Kotnik, J., Obu Vazner, K., Begu, E., Woodward, E.M.S., and Horvat, M. (2016). Mercury presence and speciation in the South Atlantic Ocean along the 40° S transect. Global Biogeochemical Cycles 30, 105-119.

Carrasco, L., and Vassileva, E. (2015). Determination of methylmercury in marine sediment samples: Method validation and occurrence data. Analytica Chimica Acta 853, 167-178.

Colombo, M.J., Ha, J., Reinfelder, J.R., Barkay, T., and Yee, N. (2013). Anaerobic oxidation of Hg (0) and methylmercury formation by Desulfovibrio desulfuricans ND132. Geochimica et Cosmochimica Acta 112, 166-177.

Cossa, D., Averty, B., and Pirrone, N. (2009). The origin of methylmercury in open Mediterranean waters. Limnology and Oceanography 54, 837-844.

Cossa, D., Heimbuerger, L.-E., Lannuzel, D., Rintoul, S.R., Butler, E.C.V., Bowie, A.R., Averty, B., Watson, R.J., and Remenyi, T. (2011). Mercury in the Southern Ocean. Geochim Cosmochim Acta 75, 4037-4052.

Darnis, G., and Fortier, L. (2012). Zooplankton respiration and the export of carbon at depth in the Amundsen Gulf (Arctic Ocean). Journal of Geophysical Research: Oceans 117(C4).

Dawson, J.K. (1978). Vertical distribution of Calanus hyperboreus in the central Arctic Ocean. Limnology and Oceanography 23, 950-957.

de Angelis, M.A., and Lee, C. (1994). Methane production during zooplankton grazing on marine phytoplankton. Limnology and Oceanography 39, 1298-1308.

Ding, L.-Y., He, N.-N., Yang, S., Zhang, L.-J., Liang, P., Wu, S.-C., Wong, M.H., and Tao, H.-C. (2019). Inhibitory effects of Skeletonema costatum on mercury methylation by Geobacter sulfurreducens PCA. Chemosphere 216, 179-185.

EPA, U. (2001). Method 1630. Methyl Mercury in Water by Distillation, Aqueous Ethylation, Purge and Trap, and CVAFS. United States Environmental Protection Agency: Washington, DC.

EPA, U. (2002). Method 1631: Revision E: Mercury in water by oxidation, purge and trap, and cold vapor atomic fluorescence spectrometry. United States Environmental Protection Agency: Washington, DC.

Fisher, N.S., Bjerregaard, P., and Fowler, S.W. (1983). Interactions of marine plankton with transuranic elements. 1. Biokinetics of neptunium, plutonium, americium, and californium in phytoplankton. Limnology and Oceanography 28, 432-447.

Forest, A., Tremblay, J.-É., Gratton, Y., Martin, J., Gagnon, J., Darnis, G., Sampei, M., Fortier, L., Ardyna, M., and Gosselin, M. (2011). Biogenic carbon flows through the planktonic food web of the Amundsen Gulf (Arctic Ocean): A synthesis of field measurements and inverse modeling analyses. Progress in Oceanography 91, 410-436.

Foster, K.L., Stern, G.A., Pazerniuk, M.A., Hickie, B., Walkusz, W., Wang, F., and Macdonald, R.W. (2012). Mercury biomagnification in marine zooplankton food webs in Hudson Bay. Environmental Science & Technology 46, 12952-12959.

Gosnell, K.J., Balcom, P.H., Tobias, C.R., Gilhooly, W.P., and Mason, R.P. (2017). Spatial and temporal trophic transfer dynamics of mercury and methylmercury into zooplankton and phytoplankton of Long Island Sound. Limnology and Oceanography 62, 1122-1138.

Hammerschmidt, C.R., Finiguerra, M.B., Weller, R.L., and Fitzgerald, W.F. (2013). Methylmercury accumulation in plankton on the continental margin of the Northwest Atlantic Ocean. Environmental Science & Tecnology 47, 3671-3677.

Heimbürger, L.-E., Cossa, D., Marty, J.-C., Migon, C., Averty, B., Dufour, A., and Ras, J. (2010). Methyl mercury distributions in relation to the presence of nano-and picophytoplankton in an oceanic water column (Ligurian Sea, North-western Mediterranean). Geochimica et Cosmochimica Acta 74, 5549-5559.

Heimbürger, L.-E., Sonke, J.E., Cossa, D., Point, D., Lagane, C., Laffont, L., Galfond, B.T., Nicolaus, M., Rabe, B., and van der Loeff, M.R. (2015). Shallow methylmercury production in the marginal sea ice zone of the central Arctic Ocean. Scientific Reports 5, 10318.

Hendzel, M.R., and Jamieson, D.M. (1976). Determination of mercury in fish. Analytical Chemistry 48, 926-928.

Hintelmann, H., and Evans, R. (1997). Application of stable isotopes in environmental tracer studies–Measurement of monomethylmercury (CH3Hg+) by isotope dilution ICP-MS and detection of species transformation. Fresenius' Journal of Analytical Chemistry 358, 378-385.

Hintelmann, H., and Nguyen, H.T. (2005). Extraction of methylmercury from tissue and plant samples by acid leaching. Analytical and Bioanalytical Chemistry 381, 360-365.

Hintelmann, H., and Ogrinc, N. (2003). Determination of stable mercury isotopes by ICP/MS and their application in environmental studies. American Chemical Society Symposium Series 835, 321-338.

Hirche, H.-J. (1997). Life cycle of the copepod Calanus hyperboreus in the Greenland Sea. Marine Biology 128, 607-618.

Hirota, R., Asada, J., Tajima, S., and Fujiki, M. (1983). Accumulation of mercury by the marine copepod Acartia clausi. Nippon Suisan Gakkaishi 49, 1249-1251.

Hop, H., and Gjøsæter, H. (2013). Polar cod (Boreogadus saida) and capelin (Mallotus villosus) as key species in marine food webs of the Arctic and the Barents Sea. Marine Biology Research 9, 878-894.

Horvat, M., Liang, L., and Bloom, N.S. (1993). Comparison of distillation with other current isolation methods for the determination of methyl mercury compounds in low level environmental samples: Part II. Water. Analytica Chimica Acta 282, 153-168.

Lee, C.S., and Fisher, N.S. (2016). Methylmercury uptake by diverse marine phytoplankton. Limnology and Oceanography 61, 1626-1639.

Lee, C.S., and Fisher, N.S. (2017). Bioaccumulation of methylmercury in a marine copepod. Environmental Toxicology and Chemistry 36, 1287-1293.

Lehnherr, I., Louis, V.L.S., Hintelmann, H., and Kirk, J.L. (2011). Methylation of inorganic mercury in polar marine waters. Nature Geoscience 4, 298-302.

Mason, R., Reinfelder, J., and Morel, F. (1995). Bioaccumulation of mercury and methylmercury. Water, Air, & Soil Pollution 80, 915-921.

Mason, R.P., Reinfelder, J.R., and Morel, F.M. (1996). Uptake, toxicity, and trophic transfer of mercury in a coastal diatom. Environmental Science & Technology 30, 1835-1845.

Mason, R.P., Choi, A.L., Fitzgerald, W.F., Hammerschmidt, C.R., Lamborg, C.H., Soerensen, A.L., and Sunderland, E.M. (2012). Mercury biogeochemical cycling in the ocean and policy implications. Environmental Research 119, 101-117.

Monperrus, M., Tessier, E., Amouroux, D., Leynaert, A., Huonnic, P., and Donard, O. (2007). Mercury methylation, demethylation and reduction rates in coastal and marine surface waters of the Mediterranean Sea. Marine Chemistry 107, 49-63.

Munson, K.M., Lamborg, C.H., Swarr, G.J., and Saito, M.A. (2015). Mercury Species Concentrations and Fluxes in the Central Tropical Pacific Ocean. Global Biogeochemical Cycles 29, 656-676.

Nørregaard, R. D., Nielsen, T. G., Møller, E. F., Strand, J., Espersen, L., & Møhl, M. (2014). Evaluating pyrene toxicity on Arctic key copepod species Calanus hyperboreus. Ecotoxicology 23, 163-174.

Omori, M. (1969). Weight and chemical composition of some important oceanic zooplankton in the North Pacific Ocean. Marine Biology 3, 4-10.

Parks, J.M., Johs, A., Podar, M., Bridou, R., Hurt, R.A., Smith, S.D., Tomanicek, S.J., Qian, Y., Brown, S.D., Brandt, C.C., et al. (2013). The genetic basis for bacterial mercury methylation. Science 339, 1332–1335.

Ploug, H., Kühl, M., Buchholz, B., and Jørgensen, B. (1997). Anoxic aggregates an ephemeral phenomenon in the ocean. Aquatic Microbial Ecology 13, 285-294.

Podar, M., Gilmour, C.C., Brandt, C.C., Soren, A., Brown, S.D., Crable, B.R., Palumbo, A.V., Somenahally, A.C., and Elias, D.A. (2015). Global prevalence and distribution of genes and microorganisms involved in mercury methylation. Science Advances 1, e1500675.

Pućko, M., Burt, A., Walkusz, W., Wang, F., Macdonald, R., Rysgaard, S., Barber, D., Tremblay, J.-É., and Stern, G. (2014). Transformation of mercury at the bottom of the Arctic food web: An overlooked puzzle in the mercury exposure narrative. Environmental Science & Technology 48, 7280-7288.

Reinfelder, J.R., and Fisher, N.S. (1991). The assimilation of elements ingested by marine copepods. Science 251, 794-796.

Schartup, A.T., Qureshi, A., Dassuncao, C., Thackray, C.P., Harding, G., and Sunderland, E.M. (2017). A Model for Methylmercury Uptake and Trophic Transfer by Marine Plankton. Environmental Science & Technology 52, 654-662.

Scott, C.L., Kwasniewski, S., Falk-Petersen, S., and Sargent, J.R. (2000). Lipids and life strategies of Calanus finmarchicus, Calanus glacialis and Calanus hyperboreus in late autumn, Kongsfjorden, Svalbard. Polar Biology 23, 510-516.

Sunderland, E.M., Krabbenhoft, D.P., Moreau, J.W., Strode, S.A., and Landing, W.M. (2009). Mercury sources, distribution, and bioavailability in the North Pacific Ocean: Insights from data and models. Global Biogeochemical Cycles 23, 1-14.

Tang, C.C., Ross, C.K., Yao, T., Petrie, B., DeTracey, B.M., and Dunlap, E. (2004). The circulation, water masses and sea-ice of Baffin Bay. Progress in Oceanography 63, 183-228.

Tang, K.W., Glud, R.N., Glud, A., Rysgaard, S., and Nielsen, T.G. (2011). Copepod guts as biogeochemical hotspots in the sea: Evidence from microelectrode profiling of Calanus spp. Limnology and Oceanography 56, 666-672.

Wang, F., Macdonald, R., Armstrong, D., and Stern, G. (2012). Total and methylated mercury in the Beaufort Sea: The role of local and recent organic remineralization. Environmental Science & Technology 46, 11821–11828.

Wang, K., Munson, K.M., Beaupré-Laperrière, A., Mucci, A., Macdonald, R.M., Wang, F. (2018). Subsurface seawater methylmercury maximum explains biotic mercury concentrations in the Canadian Arctic. Scientific Reports, 8(1), 14465. https://doi.org/10.1038/s41598-018-32760-0.

Wang, W.-X., and Wong, R.S. (2003). Bioaccumulation kinetics and exposure pathways of inorganic mercury and methylmercury in a marine fish, the sweetlips Plectorhinchus gibbosus. Marine Ecology Progress Series 261, 257-268.

Supplementary Information

Table 5-S1: Concentrations of total Hg (Hg_T) and monomethylmercury (MMHg) (mean ± standard deviation) from spiked Hg in samples of seawater, algae (and fecal pellets), and copepods from the incubation experiments.

Incubation Groups	Seawater		Algae (and fecal pellets)		Copepods	
	Hg_T (ng/L)	MMHg (ng/L)	Hg_T (ng/g)	MMHg (ng/g)	Hg_T (ng/g)	MMHg (ng/g)
Group 1 (None)	923 ± 75.2	0.212 ± 0.011				
Group 2 (Algae)	207 ± 20.4	0.012 ± 0.001	7400 ± 489	0.293 ± 0.130		
Group 3 (Copepods)	1160 ± 15.9	0.244 ± 0.064			7290 ± 502	4.33 ± 2.08
Group 4 (Algae & Copepods)	265 ± 38.8	0.020 ± 0.012	6620 ± 333	0.259 ± 0.034	6550 ± 315	1.67 ± 0.25

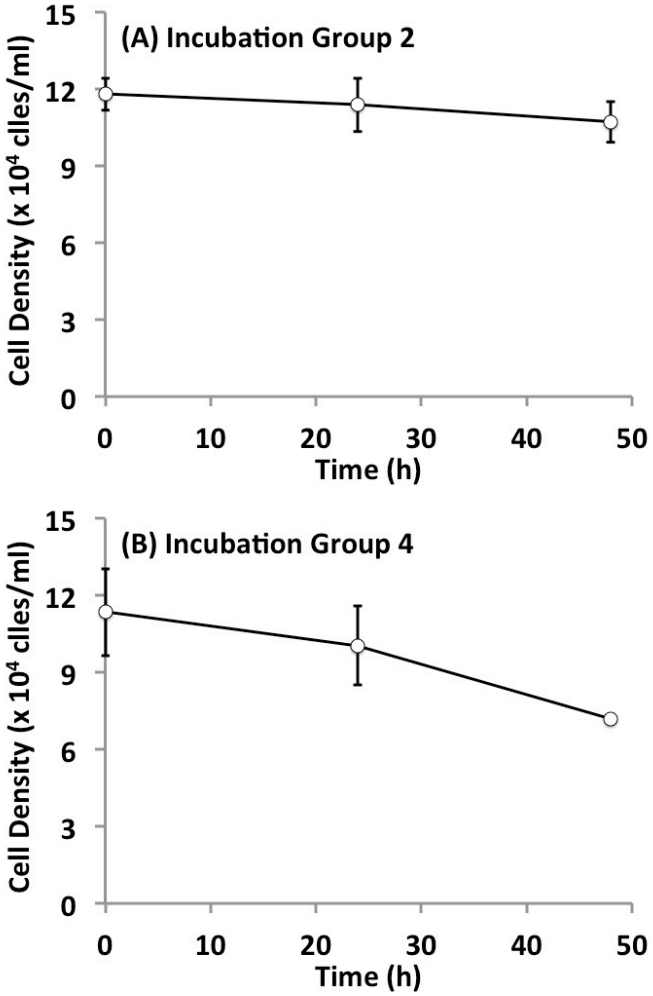

Figure 5-S1: Cell density changes over time in Group 2 and Group 4 incubations.

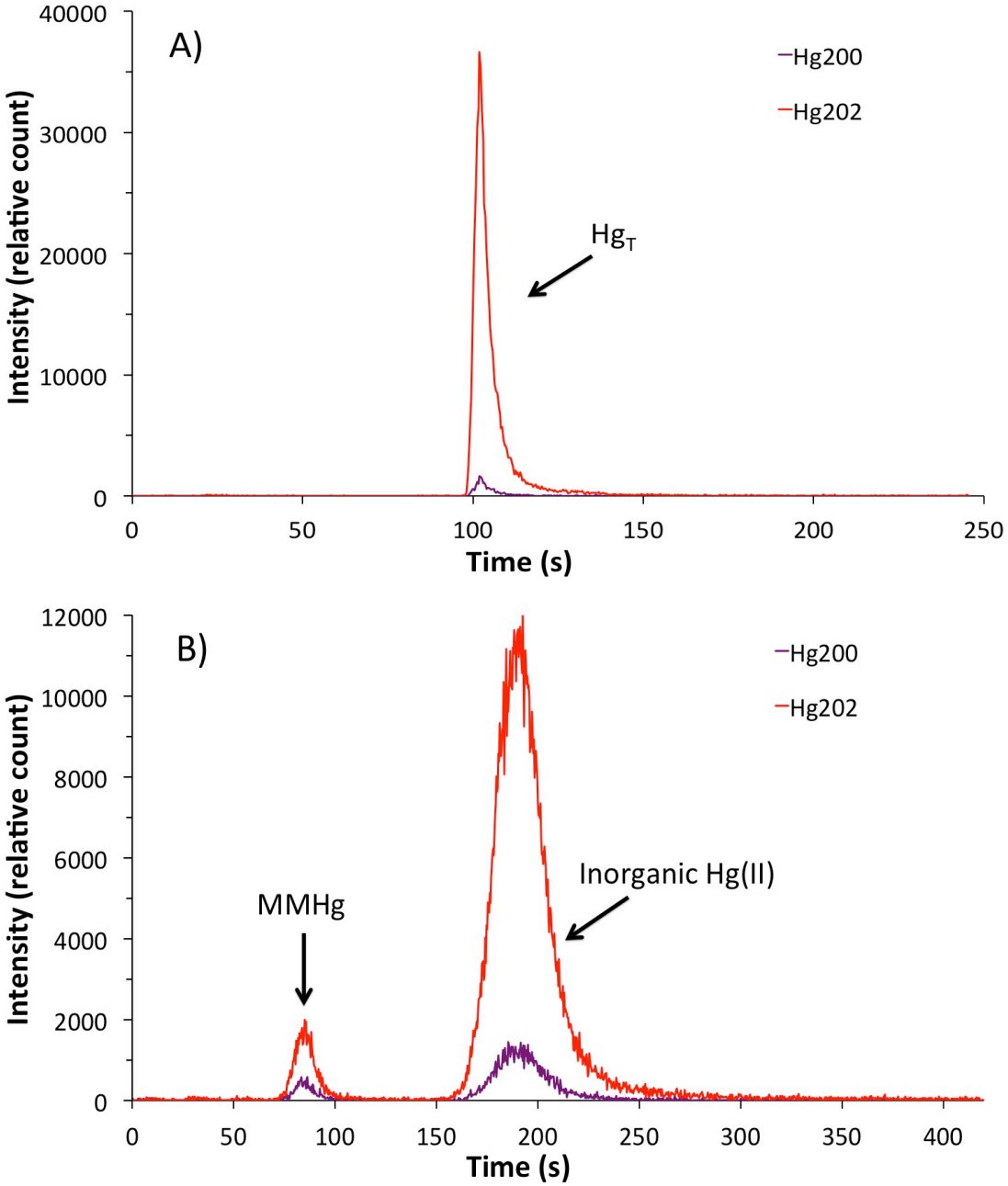

Figure 5-S2: Example chromatogram for isotopes of A) total mercury (Hg_T) and B) monomethylmercury (MMHg) determined by ICP-MS.

Chapter 6: Conclusions and Outlook

6.1 Conclusions and Scientific Contributions

To fill the knowledge gaps in mercury (Hg) biogeochemistry in the Arctic marine system, we proposed a series of research hypotheses and carried out various studies to test them. Major scientific findings from this thesis study, with respect to the original research hypotheses, are summarized below.

Chapter 2 of this dissertation tested the research hypothesis that seawater Hg distribution explains spatial gradients of biotic Hg in the Canadian Arctic. Unlike the elevated biotic Hg levels in the western Canadian Arctic, concentrations of total Hg (Hg_T) in seawater are lower in this region. In contrast, methylated Hg (MeHg, sum of monomethylmercury (MMHg) and dimethylmercury (DMHg)) displays a distinctive subsurface enrichment at shallow depths, and the peak concentrations exhibit a spatial trend mirroring that of biotic Hg. The biological uptake of the subsurface MeHg in seawater and subsequent biomagnification readily explains the longitudinal gradient of biotic Hg concentrations in the Canadian Arctic, which has been a major mystery in Arctic Hg cycle (Brown et al., 2018; Wagemann et al., 1996).

Chapter 3 assessed the validity of seawater incubation approach in determining seawater Hg methylation and demethylation rates. This widely used approach is found to have major deficiencies in determining rates of Hg methylation and demethylation in seawater; as such the reaction rates measured by this approach need to be scrutinized and re-evaluated (Lehnherr et al., 2011; Monperrus et al., 2007; Munson, 2014; Munson et al., 2018; Whalin et al., 2007).

Chapter 4 examined the hypothesis that seawater MeHg in the Canadian Arctic originates from in-situ production in the water column. By linking MeHg distributions with ancillary data, we found that the MeHg in Canadian Arctic seawater is more likely from long-distance advection of MeHg that is produced in the Chukchi Sea sediments, rather than in-situ production in the water column as postulated in previous studies (Lehnherr et al., 2011; Wang et al., 2012). The long-distance transport implies that marine MeHg in Arctic seawater must have a half-life time much longer than previously estimated (Lehnherr et al., 2011).

In Chapter 5, we studied the Hg bioaccumulation in an Arctic marine copepod, *Calanus hyperboreus*, and tested the hypothesis that anoxic microenvironments in copepod gut and/or fecal pellets are hotspots for Hg methylation in oxic ambient seawater (Alldredge & Cohen, 1987; Tang et al., 2011). MMHg was preferentially bioaccumulated over inorganic Hg(II) in *Calanus hyperboreus*, and the dominant bioaccumulation mechanism was trophic transfer. Production of MMHg was not enhanced in the copepod guts or fecal pellets, suggesting that these microenvironments are unlikely hotspots for Hg methylation. In addition, our results suggest that marine algae may inhibit Hg methylation in seawater, and this inhibitory effect may contribute to the low concentrations of MeHg at the depth of the subsurface chlorophyll a maximum in the world's oceans.

6.2 Future Directions

Through this dissertation study, important progresses have been made in filling the knowledge gaps as summarized above. However, future studies are needed to before

we can project how Hg in the Arctic marine system will change in response to a changing climate and to emission controls under the Minamata Convention on Mercury. Below are some perspectives on future research directions that are directly related to this thesis research.

The Hg species measured in this study are Hg_T and MeHg in unfiltered seawater. More Hg speciation measurements are needed in future studies, to better understand the distribution of Hg species and the transformations among these species. For example, measurements of Hg(0) can help us understand its production from Hg (II) reduction, and the Hg exchange between seawater and the atmosphere. It is believed that MMHg and DMHg can be interconverted in seawater (Fitzgerald et al., 2007). To understand the interconversion mechanisms, one first step is to differentiate MMHg and DMHg in seawater. In this study, MeHg was significantly correlated with apparent oxygen utilization, nutrients and N*, which may have distinct relationships to MMHg and/or DMHg. Examining these relationships can help trace the source of MeHg in the Canadian Arctic seawater. For both inorganic Hg(II) and MeHg, scavenging with particles is an important part of their cycle in marine environment (Fitzgerald et al., 2007; Mason et al., 2012). Furthermore, particles play important roles in transporting Hg to the Arctic seawater, in the pathway of atmospheric deposition (Steffen et al., 2008), riverine input (Leitch et al., 2007), and melting from glacier, sea ice and snow (Poulain et al., 2007). Therefore, measuring the particulate Hg species and the particles themselves can help us assess the roles of particles in marine Hg cycle, and better understand the marine Hg cycle itself.

Chapter 4 of this study proposed that the subsurface MeHg enrichment in the Canadian Arctic is likely originated from anaerobic Hg methylation in Chukchi Shelf sediments. However, the process of Hg methylation has not been investigated in the Chukchi Sea sediments, although other anaerobic processes such as denitrification in the Chukchi Shelf have been well documented (Chang and Devol, 2009; McTigue et al., 2016). To test our hypothesis, a series of questions remain to be answered by further studies: 1) Is MeHg produced in the Chukchi Sea sediments? 2) If so, is the MeHg release from this source high enough to maintain the MeHg observed in the water column? 3) Is the loss rate of seawater MeHg slow enough to allow its long-distance transport to the Canadian Arctic? A field research campaign in the Chukchi Sea area would be necessary.

The prevailing view attributes seawater MeHg in other oceans to in-situ Hg methylation in the water column, but the mechanisms are poorly understood (Mason et al., 2012). The hypothesized mechanism of enhanced Hg methylation in anoxic microenvironments is not supported by this study. So far, the known gene cluster (*hgcA-hgcB*) responsible for Hg methylation has been found only in anaerobic microbes (Parks et al., 2013; Podar et al., 2015), which are unlikely to thrive and generate high concentrations of MeHg in oxic seawater. In a recent study, *hgcA-hgcB* like genes were found in *Nitrospina*, an aerobic microbe in sea ice brine (Gionfriddo et al., 2016). The *hgcA-hgcB* or *hgcA-hgcB* like genes may also exist in seawater aerobes, and enable them to methylate Hg in the oxic seawater. Further studies are required to identify these microbes and test whether these species are capable of methylating Hg in oxic seawater. On the other hand, abiotic pathways of Hg methylation also exist in seawater (Celo et al., 2006). For example, mono-, di- and tri-methyltin compounds are potential methylators of

inorganic Hg(II) in seawater (Cerrati et al., 1992), and methyl iodide may contribute to seawater MeHg by methylating Hg(0) (Celo et al., 2006). Future researches should try to identify the chemicals responsible for seawater Hg methylation, and assess its contribution to MeHg in seawater.

This study shows that the incubation approach with stable isotope addition has major deficiencies in determining rates of Hg methylation and demethylation in seawater, including unexplainable reaction kinetics and time zero methylation and demethylation. In addition, the reaction rates measured by this approach (Lehnherr et al., 2011; Monperrus et al., 2007; Munson et al., 2018) are several orders of magnitude higher than those speculated from Hg species distribution in oceans (Mason et al., 1995; Mason and Fitzgerald, 1993). The immediate methylation and demethylation and the higher rates determined by incubation approach likely resulted from two differences between incubation and ambient seawater: 1) the conditions (e.g., pressure, compositions of chemicals like gases) in incubations are different from in-situ environments; 2) the isotope labeled Hg species added behave differently from those in ambient seawater, and might be less stable. To provide more reliable estimates on methylation and demethylation rates, these differences should be addressed in the future studies. For the first limitation, one possible solution is to conduct the incubation experiments in-situ in the water column. For the second limitation, pre-equilibrium should be achieved between ambient Hg species and the newly spiked isotope labeled ones, before starting the incubation experiments.

This study reveals that the shallow enrichment of MeHg in Arctic seawater eventually leads to the elevated biota Hg levels. It is bioaccumulation that enriches

MMHg from extremely low concentrations in seawater (typically < 0.1 ng/L, Mason et al., 2012) to concentration frequently exceeding toxicity thresholds in apex predators (e.g., 500–1800 μg/kg in the muscle of beluga, measured by Gaden and Stern, 2010). Throughout the bioaccumualation in marine food webs, the greatest degree of enrichment occurs from seawater to phytoplankton. Zooplankton also plays an important role in the Hg bioaccumulation process (Lee and Fisher, 2017; Schartup et al., 2017). However, most studies on biotic Hg in the Arctic have focused on top predators (AMAP, 2011), and much less is known on Hg bioaccumulation at the base of marine food webs, although a few studies have been carried out (Foster et al., 2012; Pućko et al., 2014; Pomerleau et al., 2016; Wang—this work, Chapter 5). In the future, more studies are required on the Hg bioaccumulation in marine food webs, especially at the lower trophic levels such as phytoplankton and zooplankton (Hammerschmidt et al., 2013; Schartup et al., 2017).

References

Alldredge, A.L., and Cohen, Y. (1987). Can microscale chemical patches persist in the sea? Microelectrode study of marine snow, fecal pellets. Science 235, 689-691.

AMAP (2011). AMAP Assessment 2011: Mercury in the Arctic. Arctic Monitoring and Assessment Program: Oslo.

Brown, T.M., Macdonald, R.W., Muir, D.C., and Letcher, R.J. (2018). The distribution and trends of persistent organic pollutants and mercury in marine mammals from Canada's Eastern Arctic. Science of The Total Environment 618, 500-517.

Celo, V., Lean, D.R., and Scott, S.L. (2006). Abiotic methylation of mercury in the aquatic environment. Science of the Total Environment 368, 126-137.

Cerrati, G., Bernhard, M., and Weber, J.H. (1992). Model reactions for abiotic mercury (II) methylation: Kinetics of methylation of mercury (II) by mono-, di-, and tri-methyltin in seawater. Applied Organometallic Chemistry 6, 587-595.

Chang, B.X., and Devol, A.H. (2009). Seasonal and spatial patterns of sedimentary denitrification rates in the Chukchi Sea. Deep Sea Research Part II: Topical Studies in Oceanography 56, 1339-1350.

Fitzgerald, W.F., Lamborg, C.H., and Hammerschmidt, C.R. (2007). Marine biogeochemical cycling of mercury. Chemical Reviews 107, 641-662.

Foster, K.L., Stern, G.A., Pazerniuk, M.A., Hickie, B., Walkusz, W., Wang, F., and Macdonald, R.W. (2012). Mercury biomagnification in marine zooplankton food webs in Hudson Bay. Environmental Science & Technology 46, 12952-12959.

Gaden, A., and Stern, G. (2010). Temporal Trends in Beluga, narwhal and walrus mercury levels: links to climate chage. In A Little Less Arctic: Top Predators in the World's Largest Northern Island Sea, Hudson Bay (Springer), pp. 197 - 216.

Gionfriddo, C.M., Tate, M.T., Wick, R.R., Schultz, M.B., Zemla, A., Thelen, M.P., Schofield, R., Krabbenhoft, D.P., Holt, K.E., and Moreau, J.W. (2016). Microbial mercury methylation in Antarctic sea ice. Nature microbiology 1, 16127.

Hammerschmidt, C.R., Finiguerra, M.B., Weller, R.L., and Fitzgerald, W.F. (2013). Methylmercury accumulation in plankton on the continental margin of the Northwest Atlantic Ocean. Environmental Science & Tecnology 47, 3671-3677.

Lee, C.S., and Fisher, N.S. (2017). Bioaccumulation of methylmercury in a marine copepod. Environmental Toxicology and Chemistry 36, 1287-1293.

Lehnherr, I., Louis, V.L.S., Hintelmann, H., and Kirk, J.L. (2011). Methylation of inorganic mercury in polar marine waters. Nature Geoscience 4, 298-302.

Leitch, D.R., Carrie, J., Lean, D., Macdonald, R.W., Stern, G.A., and Wang, F. (2007). The delivery of mercury to the Beaufort Sea of the Arctic Ocean by the Mackenzie River. Science of the Total Environment 373, 178-195.

Mason, R., Rolfhus, K., and Fitzgerald, W. (1995). Methylated and elemental mercury cycling in surface and deep ocean waters of the North Atlantic. In Mercury as a Global Pollutant (Springer), pp. 665-677.

Mason, R.P., Choi, A.L., Fitzgerald, W.F., Hammerschmidt, C.R., Lamborg, C.H., Soerensen, A.L., and Sunderland, E.M. (2012). Mercury biogeochemical cycling in the ocean and policy implications. Environmental research 119, 101-117.

Mason, R.P., and Fitzgerald, W.F. (1993). The distribution and biogeochemical cycling of mercury in the equatorial Pacific Ocean. Deep Sea Research Part I: Oceanographic Research Papers 40, 1897-1924.

McTigue, N., Gardner, W., Dunton, K., and Hardison, A. (2016). Biotic and abiotic controls on co-occurring nitrogen cycling processes in shallow Arctic shelf sediments. Nature Communications 7, 13145.

Monperrus, M., Tessier, E., Amouroux, D., Leynaert, A., Huonnic, P., and Donard, O. (2007). Mercury methylation, demethylation and reduction rates in coastal and marine surface waters of the Mediterranean Sea. Marine Chemistry 107, 49-63.

Munson, K.M. (2014). Transformations of mercury in the marine water column (Massachusetts Institute of Technology).

Munson, K. M., Lamborg, C. H., Boiteau, R. M., and Saito, M. A. (2018) Dynamic mercury methylation and demethylation in oligotrophic marine water, Biogeosciences 15, 6451-6460.

Parks, J.M., Johs, A., Podar, M., Bridou, R., Hurt, R.A., Smith, S.D., Tomanicek, S.J., Qian, Y., Brown, S.D., and Brandt, C.C. (2013). The genetic basis for bacterial mercury methylation. Science 339, 1332-1335.

Podar, M., Gilmour, C.C., Brandt, C.C., Soren, A., Brown, S.D., Crable, B.R., Palumbo, A.V., Somenahally, A.C., and Elias, D.A. (2015). Global prevalence and distribution of genes and microorganisms involved in mercury methylation. Science Advances 1, e1500675.

Pomerleau, C., Stern, G.A., Pućko, M., Foster, K.L., Macdonald, R.W., and Fortier, L. (2016). Pan-Arctic concentrations of mercury and stable isotope ratios of carbon (δ 13 C) and nitrogen (δ 15 N) in marine zooplankton. Science of the Total Environment 551, 92-100.

Poulain, A.J., Garcia, E., Amyot, M., Campbell, P.G., and Ariya, P.A. (2007). Mercury distribution, partitioning and speciation in coastal vs. inland High Arctic snow. Geochimica et Cosmochimica Acta 71, 3419-3431.

Pućko, M., Burt, A., Walkusz, W., Wang, F., Macdonald, R., Rysgaard, S., Barber, D., Tremblay, J.-É., and Stern, G. (2014). Transformation of mercury at the bottom of the Arctic food web: An overlooked puzzle in the mercury exposure narrative. Environmental Science & Technology 48, 7280-7288.

Schartup, A.T., Qureshi, A., Dassuncao, C., Thackray, C.P., Harding, G., and Sunderland, E.M. (2017). A Model for Methylmercury Uptake and Trophic Transfer by Marine Plankton. Environmental Science & Technology 52, 654–662.

Steffen, A., Douglas, T., Amyot, M., Ariya, P., Aspmo, K., Berg, T., Bottenheim, J., Brooks, S., Cobbett, F., and Dastoor, A. (2008). A synthesis of atmospheric mercury depletion event chemistry in the atmosphere and snow. Atmospheric Chemistry and Physics 8, 1445-1482.

Tang, K.W., Glud, R.N., Glud, A., Rysgaard, S., and Nielsen, T.G. (2011). Copepod guts as biogeochemical hotspots in the sea: Evidence from microelectrode profiling of Calanus spp. Limnology and Oceanography 56, 666-672.

Wagemann, R., Innes, S., and Richard, P. (1996). Overview and regional and temporal differences of heavy metals in Arctic whales and ringed seals in the Canadian Arctic. Science of the Total Environment 186, 41-66.

Wang, F., Macdonald, R.W., Armstrong, D.A., and Stern, G.A. (2012). Total and Methylated Mercury in the Beaufort Sea: The Role of Local and Recent Organic Remineralization. Environmental Science & Technology 46, 11821-11828.

Whalin, L., Kim, E.-H., and Mason, R. (2007). Factors influencing the oxidation, reduction, methylation and demethylation of mercury species in coastal waters. Marine Chemistry 107, 278-294.

Appendix: Quantification of Mercury Methylation and Demethylation

In this study, isotopically enriched mercury (Hg) species were used to study the Hg transformation processes. As described in Chapter 3, inorganic ^{202}Hg(II) and ^{198}monomethylmercury (MMHg) were added to trace Hg methylation and demethylation simultaneously. In Chapter 5, inorganic ^{202}Hg(II) was added to track Hg methylation. In these processes, isotopically enriched Hg species were transformed in the following reactions:

$$^{202}Hg^{2+} + CH_3^- \rightarrow CH_3\,^{202}Hg^+ \quad (1)$$

$$CH_3\,^{198}Hg^+ \rightarrow {}^{198}Hg^{2+} + CH_3^- \quad (2)$$

Although demethylation of MMHg can result in Hg(0), its transformation rates are three orders of magnitude lower than that of its conversion to inorganic Hg(II) (Lehnherr et al., 2011). Therefore, we did not include Hg(0) in Equation (2).

Individual isotope abundances in different Hg species were measured by cold vapor atomic fluorescence spectrometry (CVAFS) coupled with ICP-MS as described in the main text. However, the measured isotope abundances included both the Hg from the ambient environment and the added Hg. To accurately quantify the Hg methylation and demethylation processes, we calculated the isotope abundances in different Hg species from the added Hg using a linear matrix inverse approach (Hintelmann and Evans, 1997; Hintelmann and Ogrinc, 2003).

To demonstrate the calculation process, we use the experiments in Chapter 3 of this study as an example. In the experiments, the measured isotope abundances of

inorganic Hg(II) and methylated Hg (MeHg, sum of MMHg and dimethylmercury) were contributed from three different sources: the ambient seawater Hg, the added $CH_3{}^{198}Hg^+$, and the addition of inorganic $^{202}Hg(II)$.

$$\Sigma^{200}Hg = {}^{200}sw + {}^{200}meth + {}^{200}inorg \quad (3)$$

$$\Sigma^{198}Hg = {}^{198}sw + {}^{198}meth + {}^{198}inorg \quad (4)$$

$$\Sigma^{202}Hg = {}^{202}sw + {}^{202}meth + {}^{202}inorg \quad (5)$$

where $\Sigma^{200}Hg$, $\Sigma^{198}Hg$ and $\Sigma^{202}Hg$ are the measured ^{200}Hg, ^{198}Hg and ^{202}Hg of different Hg species, sw denotes the ambient seawater in incubation bottles, meth denotes the $CH_3{}^{198}Hg^+$ addition, and inorg denotes the added inorganic $^{202}Hg^{2+}$. Although ^{202}Hg is the predominant isotope (> 98%) in the added inorganic $^{202}Hg^{2+}$, inorganic $^{198}Hg^{2+}$ accounts for a small percentage. Similarly, a small fraction of the $CH_3{}^{198}Hg^+$ addition is $CH_3{}^{202}Hg^+$.

The ratio sets of isotopes in different Hg sources are:

$^{200}sw/^{200}sw = R_{11} = 1$ $\quad$ $^{200}meth/^{198}meth = R_{12}$ $\quad$ $^{200}inorg/^{202}inorg = R_{13}$

$^{198}sw/^{200}sw = R_{21}$ $\quad$ $^{198}meth/^{198}meth = R_{22} = 1$ $\quad$ $^{198}inorg\ /^{202}inorg = R_{23}$

$^{202}sw/^{200}sw = R_{31}$ $\quad$ $^{202}meth/^{198}meth = R_{32}$ $\quad$ $^{202}inorg/^{202}inorg = R_{33} = 1$

Substituting the ratio sets into Equations (3) to (5) yields the following equations:

$$\Sigma^{200}Hg = {}^{200}sw + R_{12}{}^{198}meth + R_{13}{}^{202}inorg \quad (6)$$

$$\Sigma^{198}Hg = R_{21}{}^{200}sw + {}^{198}meth + R_{23}{}^{202}inorg \quad (7)$$

$$\Sigma^{202}Hg = R_{31}{}^{200}sw + R_{32}{}^{198}meth + {}^{202}inorg \quad (8)$$

Rewrite the system of Equations (6) to (8) in matrix form,

$$\mathbf{AX = B} \quad (9)$$

with

$$\mathbf{A} = \begin{bmatrix} 1 & R_{12} & R_{13} \\ R_{21} & 1 & R_{23} \\ R_{31} & R_{32} & 1 \end{bmatrix}, \mathbf{X} = \begin{bmatrix} {}^{200}\text{sw} \\ {}^{198}\text{meth} \\ {}^{202}\text{inorg} \end{bmatrix}, \text{and } \mathbf{B} = \begin{bmatrix} \Sigma^{200}\text{Hg} \\ \Sigma^{198}\text{Hg} \\ \Sigma^{202}\text{Hg} \end{bmatrix} \quad (10)$$

where both **A** and **B** are known. For ambient seawater Hg species, the isotopic ratios used were IUPAC values as Hg species from this source are with natural isotopic abundance ratios. For the additions of inorganic $^{202}Hg^{2+}$ and $CH_3{}^{198}Hg^{+}$, the isotopic ratios were from direct measurements instead of values certified by manufacturers (Trace Sciences International Corp., and Oak Ridge National Laboratory) to prevent potential isotope changes during preparation of the isotopically enriched Hg stock solutions. The isotopic ratios determined for different Hg sources are shown in Table Appendix-1. The sum of individual Hg isotope abundances was determined by CVAFS-ICPMS measurements. Thus, the contribution of isotopes from different Hg sources (sw, meth and inorg), present as vector **X** in the formula, can be calculated with the matrix inverse approach:

$$\mathbf{X} = \mathbf{A}^{-1}\,\mathbf{B} \quad (11)$$

Table Appendix-1. Isotopic abundances of mercury species from diffferent sources.

Sources of Hg	Abundances of Hg Isotopes		
	^{200}Hg	^{198}Hg	^{202}Hg
Ambient Seawater Hg	23.10%	9.97%	29.86%
Spike of Inorganic $^{202}Hg^{2+}$	0.84%	0.13%	98.44%
Spike of $CH_3{}^{198}Hg^{+}$	1.65%	93.51%	1.00%

Once the amount of MeHg from added inorganic $^{202}Hg^{2+}$ is calculated, potential methylation during incubation can be estimated. In a previous study, the Hg methylation was approximated as a first-order reaction, and its rate constants (k_m) were estimated by fitting the methylated MMHg concentration time series data to the reaction curve

(Lehnherr et al., 2011). In Chapter 3 of this study, no reliable methylation rates can be estimated as the time series data cannot be fit to first-order reaction curves. We only calculated the Hg methylation percentages during incubations with Equation (12). In the calculation the sum of inorganic $^{202}Hg^{2+}$ and methylated $Me^{202}Hg$ was used as substrate for methylation:

$$\text{Methylation } \% = \frac{^{202}\text{inorg(MeHg)}}{^{202}\text{inorg(inorganic Hg}^{2+}) + {}^{202}\text{inorg(MeHg)}} \times 100\% \quad (12)$$

In Chapter 5, the Hg methylation ratios were calculated in a similar manner. Here, the methylated $MM^{202}Hg$ was divided by the total Hg (Hg_T) from the added inorganic $^{202}Hg(II)$:

$$\text{Methylation Ratio} = \frac{^{202}\text{inorg(MMHg)}}{^{202}\text{inorg(Hg}_T)} \quad (13)$$

Demethylation was approximated as a first-order reaction in a previous study, and its rate constants (k_d) were calculated as the slope of the linear best fit line of ln (MMHg added) with time (Lehnherr et al., 2011). In Chapter 3 of our study, however, the decay of added $CH_3{}^{198}Hg^+$ did not follow first-order kinetics. Therefore, reliable k_d cannot be determined, and only demethylation percentages during incubations were calculated:

$$\text{Demethylation } \% = \frac{^{198}\text{meth(inorganic Hg}^{2+})}{^{198}\text{meth(inorganic Hg}^{2+}) + {}^{198}\text{meth(MeHg)}} \times 100\% \quad (14)$$

References

Black, F.J., Conaway, C.H., and Flegal, A.R. (2009). Stability of dimethyl mercury in seawater and its conversion to monomethyl mercury. Environmental Science & Technology 43, 4056-4062.

Hintelmann, H., and Evans, R. (1997). Application of stable isotopes in environmental tracer studies–Measurement of monomethylmercury (CH3Hg+) by isotope dilution ICP-MS and detection of species transformation. Fresenius' Journal of Analytical Chemistry 358, 378-385

Hintelmann, H., and Ogrinc, N. (2003). Determination of stable mercury isotopes by ICP/MS and their application in environmental studies. American Chemical Society Symposium Series 835, 321-338.

Lehnherr, I., Louis, V.L.S., Hintelmann, H., and Kirk, J.L. (2011). Methylation of inorganic mercury in polar marine waters. Nature Geoscience 4, 298-302.

Monperrus, M., Tessier, E., Amouroux, D., Leynaert, A., Huonnic, P., and Donard, O. (2007). Mercury methylation, demethylation and reduction rates in coastal and marine surface waters of the Mediterranean Sea. Marine Chemistry 107, 49-63.